



Cell specific analysis of AMPA receptor complexes in development and disease

Inaugural-dissertation

for attaining the title of Doctor rerum naturalium (Dr. rer. nat.)
at the Faculty of Mathematics and Natural Sciences,
Heinrich Heine University Düsseldorf

presented by

Andrea Mölders

from Geldern

Düsseldorf, April 2018

from the Institute of Neural and Sensory Physiology
Heinrich Heine University Düsseldorf

Published with the permission from the
Faculty of Mathematics and Natural Sciences,
Heinrich Heine University Düsseldorf

Supervisor: Prof. Dr. med. Nikolaj Klöcker, Heinrich Heine University Düsseldorf

Co-supervisor: Prof. Dr. rer. nat. Christine R. Rose, Heinrich Heine University Düsseldorf

Date of the oral examination: 25.06.2018

„No! Try not. Do... or do not. There is no try!”

Yoda, The Empire Strikes Back – Star Wars Episode V

Table of Content

List of Figures	6
Abbreviations	7
Zusammenfassung	9
Summary	11
1. Introduction	13
1.1 The mammalian central nervous system	13
1.2 Neurons and excitatory synaptic transmission	13
1.3 Ionotropic Glutamate Receptors	14
1.3.1 Membrane topology of AMPARs and structural aspects	14
1.3.2 Molecular diversity and heterogeneity of neuronal AMPARs	15
1.3.3 AMPARs in synaptic plasticity	17
1.4. Auxiliary subunits and AMPAR complex composition	18
1.4.1 The TARP Family	19
1.4.2 The Cornichon Proteins	21
1.4.3 The CKAMP Family	22
1.4.4 The GSG1L Protein	23
1.5. AMPARs in disease	24
1.5 Astrocytes	25
1.5.1 AMPARs in astrocytes	27
2. Aims of the study	29
3. Compendium of publications and manuscripts	30
3.1 “Ontogeny repeats the phylogenetic recruitment of the cargo exporter cornichon into AMPA receptor signaling complexes”	30
3.2 “Depletion of the AMPAR reserve pool impairs synaptic plasticity in a model of hepatic encephalopathy”	39
3.3 “Heterogeneity of the Astrocytic AMPA-Receptor Transcriptome”	49
4. Discussion and conclusion	66
4.1 Analysis of developmental expression of CNIH2/3 and AMPARs and the consequence for the AMPA complex	66
4.2 AMPAR function in the disease model of hepatic encephalopathy (HE)	68
4.3 AMPA Receptor heterogeneity in astrocytes	70
4.4 Conclusions and Outlook	74
Bibliography	76
Danksagung	86
Declaration	88

List of Figures

Figure 1.1: Topology and structure of AMPARs	15
Figure 1.2: Regulation of AMPAR trafficking during synaptic plasticity	17
Figure 1.3: Topology of bona fide auxiliary subunits	19
Figure 1.4: Function of astrocytes	26

Abbreviations

AD	Alzheimer's disease
Aldh1L1	aldehyde dehydrogenase 1 family member L1
AMPA	α -amino-3-hydroxy-5-methyl-4-isoxazole-propionic acid
AMPA	AMPA receptor
ATD	amino-terminal domain
C	carboxyl
Ca	Calcium
CaMKII	Ca ²⁺ -calmodulin-dependent protein kinase II
CKAMP	cysteine-knot AMPAR modulating protein
CI-AMPA	Ca ²⁺ impermeable
CNIH	cornichon homolog
CNS	central nervous system
CP-AMPA	Ca ²⁺ permeable
CTD	carboxyl-terminal domain
DG	dentate gyrus
D-AP5	(2R)-amino-5-phosphonovaleric acid
e.g.	for example
EAAT1	excitatory amino acid transporter 1
EGF	epidermal growth factor
EGFP	enhanced green fluorescent protein
EPSP	excitatory postsynaptic potential
EPSC	excitatory postsynaptic current
ER	endoplasmic reticulum
FACS	fluorescence-activated cell sorting
FRRS1I	ferric-chelate reductase 1-like protein
GABA	γ -aminobutyric acid
GFAP	glial fibrillary acidic protein
GFP	green fluorescent protein
GLAST	glutamate/aspartate transporter
GSG1L	germ cell-specific gene 1-like
GS	glutamine synthetase
HE	hepatic encephalopathy
I	current
i.e.	that is
iGluR	ionotropic glutamate receptor
IPSP	inhibitory postsynaptic potential
K	Potassium
KA	kainate
KAR	kainate receptor
KO	knockout
LRRTM	leucine-rich repeat transmembrane protein
LTD	long-term depression
LTP	long-term potentiation
MAPKs	mitogen-activated protein kinases
MAGUK	membrane-associated guanylate kinase

Abbreviations

mEPSC	miniature excitatory postsynaptic current
mGluR	metabotropic glutamate receptor
mRNA	messenger ribonucleic acid
Na	Sodium
NBQX	2,3-dihydroxy-6-nitro-7-sulfamoyl-benzo[f]quinoxaline-2,3-dione
NG2	neural/glial antigen 2
NSC	neural stem cell
NEP	neuroepithelial precursor cell
NMDA	N-methyl-D-aspartate
NMDAR	N-methyl-D-aspartate receptors
NPTX2	neuronal pentraxin 2
NPTXR	neuronal pentraxin receptor
OPC	oligodendrocyte precursor cell
PNS	peripheral nervous system
PORCN	porcupine
PRRT	proline-rich transmembrane protein
PSD	postsynaptic density
PSD95	postsynaptic density protein-95
PDZ	postsynaptic density protein-95, <i>Drosophila</i> disc large tumor suppressor, zonula occludens-1 protein
Q	glutamine
qPCR	real time PCR
R	arginine
RG	radial glial
RNA	messenger ribonucleic acid
RNOS	reactive nitrogen and oxygen species
STP	short-term plasticity
TARP	transmembrane AMPAR regulatory protein
TBI	traumatic brain injury
TMD	transmembrane domain
V	voltage

Zusammenfassung

L-Glutamat ist der wichtigste exzitatorische Neurotransmitter im zentralen Nervensystem der Wirbeltiere. AMPA-Rezeptoren (AMPA-Rs) sind für den Großteil der schnellen exzitatorischen Neurotransmission zuständig, daher spielen sie eine entscheidende Rolle bei der Gehirnfunktion von Säugetieren. Darüber hinaus sind sie an der Gehirnentwicklung, der neuronalen Migration sowie der synaptischen Reifung beteiligt. Es gibt vier verschiedene AMPA-Rezeptor-Untereinheiten, GluA1-GluA4, welche Homotetramere oder Heterotetramere bilden können. Alle Untereinheiten weisen leicht unterschiedliche funktionelle und elektrophysiologische Eigenschaften auf. Weiterhin wurden in den letzten Jahrzehnten mehrere Hilfsuntereinheiten und interagierende Proteine des nativen AMPAR-Komplexes entdeckt. Sie beeinflussen die Oberflächenexpression von AMPARs und/oder deren funktionelle Eigenschaften. Tatsächlich haben native AMPAR-Komplexe eine hohe molekulare Komplexität, ihre Funktionen verändern sich in der Entwicklung und unterscheiden sich zwischen Hirnregionen. Die vorliegende Arbeit befasst sich mit der molekularen und funktionellen Diversität von AMPARs und untersucht die Diversität in Abhängigkeit von verschiedenen Zelltypen, verschiedenen Entwicklungsstadien und Hirnregionen sowie bei Erkrankung.

Zu Beginn wurde die Expression von Cornichon Proteinen (CNIHs) während der Entwicklung sowie deren Zusammenhang mit der AMPAR-Komplexzusammensetzung untersucht. Die Untersuchung zeigte, dass CNIH2 und CNIH3 während der Entwicklung stark reguliert sind und ihre Expression zu den GluA-Untereinheiten reziprok ist. Jedoch fanden wir heraus, dass sich das relative Verhältnis von CNIH2/3, das in AMPARs integriert ist, während der Entwicklung nicht veränderte. Daher ist zu vermuten, dass es in der frühen Entwicklung einen Überschuss an AMPAR-freiem CNIH2/3 gibt. Diese Menge an AMPAR-freiem CNIH2/3 nahm im Laufe der Entwicklung ab, während die absolute Menge an CNIH2/3, die in AMPAR-Komplexe integriert ist, zunahm. Unsere Daten zeigten, dass CNIHs für AMPARs in der Entwicklung an Bedeutung gewinnen und möglicherweise die Oberflächenexpression von AMPARs während der Entwicklung erhöhen. Daher scheinen CNIHs eine entscheidende Rolle bei der Synapsenreifung während der Gehirnentwicklung spielen.

Im Anschluss wurde die AMPAR-Zusammensetzung und Funktion im Krankheitsmodell der hepatischen Enzephalopathie (HE), einer neuropsychiatrischen Komplikation des Leberversagens, die zu kognitiven Defiziten führt, untersucht. Wir haben ein Co-Kultur-Modell von Neuronen und Astrozyten verwendet, um das Zusammenspiel zwischen Neuronen und Astrozyten während der synaptischen Entwicklung sowie während der Ammoniumbehandlung nachzuahmen. Die chronische Ammoniumbehandlung verursachte eine Reduktion der neuronalen AMPAR Expression. Diese betraf hauptsächlich die extrasynaptischen Komplexe, da die spontane glutamaterge Neurotransmission nicht verändert wurde, wohl aber die Induktion von LTP nicht mehr möglich war. Diese Untersuchung unterstützt die Annahme, dass für LTP ein extrasynaptischer Reservepool von Glutamaterezeptoren benötigt wird. Unsere Studie ist die erste pathophysiologische Untersuchung, die diese Hypothese unterstützt und in der diese Veränderung der AMPAR-Funktion ein entscheidender Schritt bei der Entstehung der Krankheit sein könnte.

Im letzten Schritt wurde der native AMPAR-Komplex in Astrozyten analysiert, da AMPARs nicht ausschließlich neuronale Rezeptoren sind und ihre Zusammensetzung und funktionelle Rolle in z. B. Gliazellen nahezu unbekannt ist. Wir entwickelten einen experimentellen Workflow, der es uns ermöglichte, Astrozyten selektiv aufzureinigen sowie die AMPAR Zusammensetzung spezifisch in Astrozyten zu untersuchen. Die Untersuchung zeigte, dass sich das mRNA Expressionsmuster der AMPARs aus Gesamthirn Astrozyten zwischen den ersten zwei Wochen der Entwicklung nicht unterscheidet, anders als während der neuronalen Entwicklung. Stattdessen identifizierten wir eine große Heterogenität in den Expressionsmustern von astrozytären AMPARs aus Kleinhirn, Neocortex und Hippocampus. Unsere Studie gibt einen ersten Einblick in die molekulare Vielfalt astrozytärer AMPARs.

Die Daten, die in dieser Arbeit vorgestellt werden, veranschaulichen die molekulare und funktionelle Vielfalt von AMPARs in Bezug auf Entwicklungsstadien, verschiedene Hirnregionen und Zelltypen sowie in einem Modell einer Erkrankung. Seit der Entdeckung der Hilfsuntereinheiten und interagierende Proteine scheint es, dass es ein hochmodulares System für AMPARs gibt, das zu einer vielfältigen Zusammensetzung sowie verschiedenen AMPAR Funktionen führt. Dieses modulare System von AMPARs ermöglicht es den Zellen, je nach Aufgabenstellung unterschiedliche AMPARs zu bilden. Allerdings sind bis zum heutigen Zeitpunkt weder das Ausmaß noch die Komplexität dieser Heterogenität vollständig geklärt. Wie diese dann in funktionelle Heterogenität umgesetzt wird, ist ebenfalls unklar. Die vorgestellten Ergebnisse können als Grundlage für die zukünftige Erforschung der Diversität von AMPARs in der normalen Hirnfunktion und Krankheit dienen.

Summary

L-Glutamate is the major excitatory neurotransmitter in the vertebrate central nervous system, and the glutamate receptors of the AMPA subtype (AMPA receptors) play a crucial role in mammalian brain function. They mediate most of the fast excitatory neurotransmission and are involved in brain development, neuronal migration, and synaptic maturation. The AMPAR family contains four pore-lining subunits, GluA1-GluA4, and they can assemble in a homomeric or heteromeric fashion into a tetrameric receptor. All subunits exhibit slightly different gating properties. Furthermore, over the last decades, multiple auxiliary subunits, and constituents of the native AMPAR complex have been discovered. They influence the trafficking of AMPARs and/or fine-tune their functional properties. In fact, native AMPAR complexes show a high molecular complexity and their function changes in development and with brain region. The present work addresses the molecular and functional diversity of AMPARs depending on different cell types, different developmental stages, and brain regions as well as in disease.

First, the developmental expression of cornichon homologs (CNIHs) and their relation with the AMPAR pore composition was investigated. The study showed CNIH2 and CNIH3 are highly regulated during development and their expression is reciprocal to the one of GluA subunits. However, we found that the relative ratio of CNIH2/3 integrated into AMPARs did not change during development. Thus, there is most likely an excess amount of AMPAR-free CNIH2/3 in early development. This amount of AMPAR-free CNIH2/3 declined towards adulthood, whereas the absolute amount of CNIH2/3 integrated into AMPAR complexes did increase during development. Our data indicate that CNIHs gain importance for AMPARs in development and suggest that they may increase surface expression of AMPARs during development. Therefore, CNIHs may play a crucial role in synapse maturation during brain development.

Second, the AMPAR composition and function in the disease model of hepatic encephalopathy (HE), a neuropsychiatric complication of liver failure leading to cognitive deficits, was examined. We employed a co-culture model of neurons and astrocytes to mimic the interplay between neurons and astrocytes not only during the following ammonia treatment but also to model synaptic development and maturation before it. We found that chronic ammonia treatment caused a reduction of the neuronal AMPAR expression, mainly affecting the extrasynaptic complexes since basal glutamatergic neurotransmission was not altered, but the induction of LTP was abolished. This study supports the previous assumption that LTP requires a reserve pool of extrasynaptic glutamate receptors. Our study revealed the first pathophysiological setting, which supports this hypothesis and where this alteration in AMPA function seems to be a crucial step in the pathogenesis.

Third, the native AMPAR complex in astrocytes was analyzed, since AMPARs are not exclusively neuronal receptors and their complex composition and functional role in glial cells have remained elusive. We developed an experimental workflow, which allowed us to purify astrocytes selectively and to examine the astrocytic AMPAR composition. The study revealed that the mRNA expression pattern of AMPARs in isolated whole brain astrocytes does not change during the first two weeks of postnatal development, unlike during neuronal development. Instead, we identified significant heterogeneity in the expression of AMPAR constituents in astrocytes from cerebellum, neocortex, and hippocampus. Our study provides a first insight into the molecular diversity of astrocytic AMPARs.

The data presented in this thesis illustrates the molecular and functional diversity of AMPARs with respect to developmental stages, health and disease, and different brain regions as well as cell types. Since the identification of quite a number of AMPAR complex constituents, it seems that a highly modular system exists for AMPARs resulting in diverse AMPAR complex composition and AMPAR function. The modular system of AMPARs with all the constituents enables the cells to build different AMPARs depending on their task. However, up to now, the full extent and complexity of this heterogeneity are not even fully unraveled, and how this is

translated into functional heterogeneity is still elusive. The presented results can serve as a stepping stone for future research of AMPARs diversity in health and disease.

1. Introduction

1.1 The mammalian central nervous system

A nervous system that receives a lot of sensory information from the body and the environment as well as transmits signals to the whole body is found in most animals. These signals generate a perception and eventually determine the animal's behavior. During evolution, the nervous systems became more and more complex and the ability of processing, storing and recalling information, thereby generating a learning and memory behavior, increased. The nervous system can be divided into two parts, the central nervous system (CNS) and the peripheral nervous system (PNS). The mammalian CNS consists of the brain and the spinal cord, with the brain being the central organ of the nervous system. The brain is one of the most complex organs and the question of how its complex anatomical structure and network circuits as well as its multiple electrical signals can lead to so many diverse cognitive abilities fascinates humans since a long time. Therefore, the brain was always an object of scientific interest and a lot of research was done until today.

Studying the brain is challenging due to its immense complexity, which is the result of the dense packing of the nerve cells, the intricacy of their connections and the profusion of cell types. Today, the behavior of single cells is quite well understood, but the way how they interact with each other and how this interaction generates this complex processing of information remains still elusive (Freeman and Rowitch, 2013; Nicholls, 2011). The research of scientists like Camillo Golgi (1844-1926) and Santiago Ramón y Cajal (1852-1934) as well as Gustav Retzius (1842-1919) and Rudolph Virchow (1821-1902) revealed the complex structure and the diversity of brain. The anatomical studies have shown that the brain consists not only of neurons but also of additional cell types. Rudolph Virchow called the additional cells glia cells and proposed their function as glue for the neurons (De Carlos and Borrell, 2007; Freeman and Rowitch, 2013). Today we know that these cells, which the scientists described in the past, are several types of glial cells. They are highly diverse, have unique functions, and they are not only the glue for neurons. Astrocytes represent the largest class of glial cells in the mammalian CNS and they are distributed throughout the whole brain. They show great variety in morphological and physiological properties and fulfill diverse functions like maintaining the blood-brain barrier, providing trophic and metabolic support to neurons, affording neurotransmitter recycling and controlling synaptogenesis as well as synaptic transmission (reviewed by Haim and Rowitch, 2016). Oligodendrocytes are well known for their function of myelinating axons from neurons and this insulation forms the basis of action potential propagation along axons. Until recently, microglia have been viewed as resident immune cells that only become activated by pathological events and hence protecting the brain against damage and infection. But recent evidence shows that microglia are highly dynamic cells. Apart from their well-known immune functions, microglia can influence synaptic transmission and synaptogenesis and contribute to the maturation of neural circuits (reviewed by Reemst et al., 2016).

1.2 Neurons and excitatory synaptic transmission

Neurons transmit information encoded as electrical signals. There exist two ways for exchanging information between neurons, chemical synapses, and electrical synapses via gap junctions. Transmission of information at chemical synapses occurs by means of neurotransmitters, which diffuse through the synaptic cleft and generate a synaptic potential at the postsynapse. This postsynaptic potential may be excitatory (EPSP) or inhibitory (IPSP). One great advantage of chemical neurotransmission is the ability to amplify signals, as it can be observed at the neuromuscular junction, where one motor neuron can activate multiple muscle cells.

Furthermore, neurons are able to integrate the different excitatory and inhibitory signals, which they receive at their multiple chemical synapses and to determine whether or not to generate an action potential. This mechanism offers the opportunity to modulate signal transmission, whereas electrical transmission is less modifiable, more instantaneous and direct. Glutamate is the major excitatory neurotransmitter in the vertebrate central nervous system. At the postsynaptic site, glutamate can act as a ligand for ionotropic glutamate receptors (iGluRs) or metabotropic glutamate receptors (mGluRs). iGluRs are unselective cation channels and they are mostly permeable for K^+ , Na^+ and Ca^{2+} . They mediate the fast, direct part of excitatory neurotransmission and hence play a crucial role in brain function. On the other hand, mGluRs are G-protein coupled receptors and activate an intracellular signaling cascade upon ligand binding, which is part of the slow modulatory neurotransmission also called indirect transmission.

1.3 Ionotropic Glutamate Receptors

Four different subfamilies of iGluRs are known. They are grouped by their sequence homologies and distinct pharmacological properties. The N-methyl-D-aspartate receptors (NMDARs), α -amino-3-hydroxy-5-methyl-4-isoxazole-propionic acid receptors (AMPA), kainate receptors (KARs) and the delta receptors. The AMPARs and KARs are also classified as non-NMDA receptors, because of their sequence identity and ligand cross-reactivity (Hollmann et al., 1989; Hollmann and Heinemann, 1994; Traynelis et al., 2010). Delta receptors belong to the family of the glutamate receptors because they share sequence homologies; however, until now no functional agonist of these receptors has been found (Hansen et al., 2009; Kakegawa et al., 2011; Naur et al., 2007). Each subfamily of iGluRs comprises different subunit isoforms, but they share the same architecture of a tetrameric receptor complex (Greger et al., 2017; Traynelis et al., 2010). The tetramer assembles in a dimer-of-dimers fashion and only subunits from one subfamily are able to build functional receptors (Sobolevsky et al., 2009). The subunits of one subfamily can assemble in a homomeric or heteromeric fashion into a receptor. The AMPA subfamily contains four pore-lining subunits, GluA1-GluA4, and all subunits exhibit slightly different gating properties and characteristics resulting in a molecular diversity of AMPARs (see next Section; reviewed by Greger et al., 2017; Traynelis et al., 2010).

1.3.1 Membrane topology of AMPARs and structural aspects

The GluA subunit is a three-transmembrane-domain (TMD A-C) protein with an extracellular amino-terminal domain (ATD) and an intracellular carboxyl-terminal domain (CTD). Between transmembrane domains A and B, a pore-loop resides, which inserts from the cytoplasm into the plasma membrane (Hollmann and Heinemann, 1994; Sobolevsky et al., 2009). The ion pore of the channel is formed by the four pore-loops of each GluA subunit in the tetrameric complex (Sobolevsky et al., 2009). The ligand binding domain (LBD) is built from two extracellular lobes of the protein (Sobolevsky et al., 2009). One part is the S1 region, which is located between the ATD and TMD A and the other part, the S2 region is an extracellular loop between the TMD B and TMD C. These two regions form the two domains D1 and D2. The interface of these two domains hosts the ligand binding site (Armstrong et al., 1998). Ligand binding induces conformational changes in the LBD and these changes are transferred via linker regions to transmembrane domains A and C and, as a result, the ion channel opens (Armstrong and Gouaux, 2000; Sobolevsky et al., 2009).

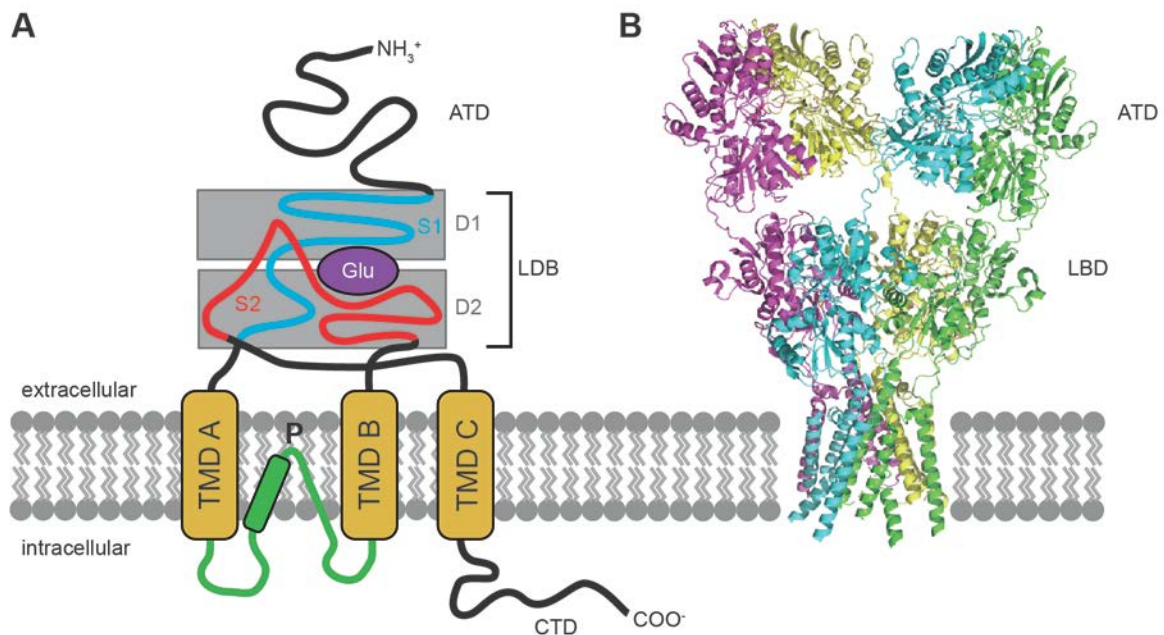


Figure 1.1: Topology and structure of AMPARs. (A) Domain topology of a single AMPA subunit with color-coded domains. The subunit exhibits an amino-terminal domain (ATD), a ligand binding domain (LBD), three transmembrane domains (TMD A-C), one pore-loop and an intracellular carboxyl-terminal domain (CTD). (B) Crystal structure of the AMPAR complex. Each subunit is in a different color. PDB ID 3KG2 (Sobolevsky et al., 2009).

In the endoplasmic reticulum (ER), receptor assembly takes place. In a first step, two subunits form a dimer via the interaction of the ATDs. In a second step, the tetrameric complex is formed by dimerization of the two dimers by interaction of the respective LBDs and TMDs (Greger et al., 2017; Sobolevsky et al., 2009; Traynelis et al., 2010). For localization and anchoring the receptor in the postsynaptic density (PSD), the CTD exhibits binding sites for various scaffolding and cytoskeleton proteins. These binding sites are important for trapping the receptor into the synapse because AMPARs lack a PDZ (postsynaptic density protein-95, *Drosophila* disc large tumor suppressor, zonula occludens-1 protein) binding motif implicating that they cannot interact directly with major PSD scaffolding proteins, i.e. the membrane-associated guanylate kinases (MAGUKs). In addition, CTD has several phosphorylation sites linked to trafficking, especially when involved in synaptic plasticity such as LTP and LTD (Shepherd and Huganir, 2007; Traynelis et al., 2010; see Section 1.3.3.).

1.3.2 Molecular diversity and heterogeneity of neuronal AMPARs

Furthermore, AMPAR subunits are also subject of posttranscriptional modifications, which affect their biophysical properties as well as their subcellular trafficking. One prominent example of posttranscriptional modification is the Q/R RNA editing of the GluA2 subunit. The Q/R editing site is located at the tip of the ion pore; editing leads to an exchange of the amino acid glutamine (Q) for arginine (R). This exchange from an uncharged amino acid to a positively charged one influences dramatically the ion permeability of the channel. Whereas the unedited subunits GluA1/3/4 show Ca^{2+} permeability, Q/R editing of GluA2 abolishes its Ca^{2+} permeability (Burnashev et al., 1992b; Kuner et al., 2001; Sobolevsky et al., 2009). A further effect of Q/R editing is a loss of the voltage-dependent block by intracellular polyamines, which results in a linear current-voltage (I/V) relationship. The positively charged arginine repels polyamines, which are then not able to block the ion pore at positive membrane potentials anymore. Non-edited subunits or tetramers lacking GluA2 show instead an inwardly rectifying I/V relationship (Boulter et al., 1990; Greger et al., 2017; Traynelis et al., 2010). Besides the electrophysiological properties, also trafficking of the GluA2 subunit is affected by Q/R editing. Edited GluA2 subunits

are rather retained in the ER compared to the other AMPA receptor subunits. This retention prevents the assembly of GluA2 homomers as edited subunits will need to co-assemble with other non-edited GluA isoforms for being trafficked to the plasma membrane. This unique trafficking behavior of GluA2 leads to an increased availability of assembling with other subunits and thus to a preferential formation of GluA2 containing heteromeric receptors (Araki et al., 2010; Greger et al., 2017; Greger and Esteban, 2007). GluA2 is the predominant subunit in brain and heterotetramers containing GluA2 are Ca²⁺ impermeable (CI-AMPA receptors). AMPARs without GluA2 are Ca²⁺ permeable receptors (CP-AMPA receptors). AMPAR expression is observed early during brain development and is detected in different cell types like neural stem cells (NSCs), neuroblasts and later in neurons (Jansson and Akerman, 2014; Liu et al., 2006; Martin et al., 1998; Platel et al., 2007). Studies suggest that mRNA is edited as soon as it is expressed. For example, in embryonic mice at E15, most GluA2 subunits were RNA-edited (Jacobs et al., 2009; Wahlstedt et al., 2009). GluA2 mRNA was already edited in neuroepithelial precursor cells (NEPs), which differentiate to NSCs, but no GluA2 protein was found in these cells. Detectable GluA2 protein amounts and functional AMPAR currents appeared only later in more differentiated cells like neurons (Jansson and Akerman, 2014; Pachernegg et al., 2015; Platel et al., 2007).

Different from Q/R editing, alternative splicing is a posttranscriptional modification, which affects all GluA subunits. This modification can generate two alternative flip and flop variants. A short stretch of 115 bp can be alternatively excised resulting in two protein versions of each GluA subunit differing in their gating properties. Thus, the flop variants are less sensitive to the ligand glutamate and desensitize much faster than the respective flip variants (reviewed by Greger et al., 2017; Traynelis et al., 2010).

In general, all four GluA subunits are expressed in the CNS and, at least in neurons, most native AMPAR complexes contain heterotetramers of GluA1/GluA2 or GluA2/GluA3 subunits (Lu et al., 2009; Sans et al., 2003; Wenthold et al., 1996). GluA2 and GluA1 are the most abundant isoforms, whereas GluA3 and GluA4 are less present in the brain (Sans et al., 2003; Schwenk et al., 2012). GluA4 is highly regulated during development; it has a restricted expression in adult brain, with the highest expression being found in cerebellar tissue (Henley and Wilkinson, 2016; Schwenk et al., 2014). In the forebrain, the expression of GluA4 is down-regulated shortly after birth, whereas GluA2 expression in contrast increases (Kumar et al., 2002; Pellegrini-Giampietro et al., 1992; Pickard et al., 2000; Zhu et al., 2000). The GluA4 containing CP-AMPA receptors are important for neonatal synaptic function and are present in silent synapses. This developmental expression profile of GluA isoforms leads to a swap from CP-AMPA receptors to CI-AMPA receptors in silent synapses (Kumar et al., 2002; Pellegrini-Giampietro et al., 1992; Zhu et al., 2000). This change in AMPAR expression profile plays a role in synaptogenesis, synapse maturation, as well as in stabilization of synapses (Hamad et al., 2011; Henley and Wilkinson, 2016). The reduction of GluA4 during the first postnatal weeks and the increase of GluA2 have been confirmed in a proteomic study by Schwenk and colleagues (Schwenk et al., 2014). Also, the postulated decrease of GluA1 and the increase of GluA3 at adolescent stage have been observed (Blair et al., 2013; Schwenk et al., 2014). Furthermore, Schwenk and co-workers demonstrated that the expression of AMPARs differs between brain regions in the adult rat. In the hippocampus, the most abundant subunits are GluA1 and GluA2. In the cortex and striatum, GluA2 is the main subunit, followed by GluA1 and GluA3. As described above, in the adult brain GluA4 expression is found specific brain regions, with the highest expression in cerebellum and brainstem (Schwenk et al., 2014). Furthermore, in the cerebellum AMPARs are mostly GluA1/GluA4 heteromers or GluA4 homomers. The authors concluded that native AMPARs differ largely in their subunit composition with respect to distinct brain regions, neuronal cell types, and circuits (Schwenk et al., 2014). However, one important note on this study is, that whole brain tissue was analyzed without distinguishing between different cell types. Although AMPARs are predominantly expressed by neurons, they are also

present in glial cells. Thus, the observed protein expression pattern represents most likely not only a neuronal one, even though neurons might contribute substantially.

1.3.3 AMPARs in synaptic plasticity

AMPARs mediate the majority of excitatory neurotransmission in the mammalian brain. Moreover, AMPARs define the time course of excitatory postsynaptic currents (EPSCs) by their gating properties, which in turn are influenced by the GluA isoform, their splice variants, RNA editing, and further complex constituents (see Section 1.4). The efficiency of synaptic transmission can change over time resulting in increased or decreased responses to a given stimulus. This process is called synaptic plasticity. By electrophysiological means, two long lasting changes can be observed, long-term potentiation (LTP) and long-term depression (LTD). These changes affect the strength of an excitatory synapse in opposite ways. LTP is an increase of the synaptic response and mostly generated by an increased number of postsynaptic AMPARs. One type of reported LTP is NMDAR-dependent: a repetitive robust stimulation of a synapse leads to a strong depolarization of the plasma membrane and activates NMDARs by removing the voltage-dependent Mg^{2+} block. Due to activation of NMDARs, the intracellular Ca^{2+} concentration increases and Ca^{2+} acts as second messenger activating different downstream calcium pathways. This results in an enhanced synaptic strength, caused by an increased number of AMPARs at the postsynaptic density. LTD, in contrast, is described as a reduction of the synaptic strength and may be generated by a reduced number of postsynaptic AMPARs (Nicholls, 2011). In both processes, AMPAR trafficking is altered compared to the basal conditions. After exit from the Golgi, AMPARs are transported to the dendritic spine and integrated into the plasma membrane. From there they undergo lateral diffusion into the PSD, where AMPARs anchor at scaffolding proteins like PSD-95 (Haering et al., 2014; Henley and Wilkinson, 2016). During LTP, enhanced anchoring of laterally diffusing AMPARs within the PSD can be observed. Furthermore, newly generated AMPARs are incorporated via exocytosis and increase the pool of extrasynaptic AMPARs (Makino and Malinow, 2009; Opazo and Choquet, 2011). LTD, on the other hand, goes along with enhanced endocytosis of AMPARs and a retention of AMPARs in intracellular compartments (Opazo and Choquet, 2011). A study from Granger et al. reported that no specific AMPAR subunits are required to induce LTP and even when all AMPARs are replaced by KARs it is still possible to induce LTP (Granger et al., 2013). LTP was, however, impaired, when the reserve pool of AMPARs and KARs was reduced.

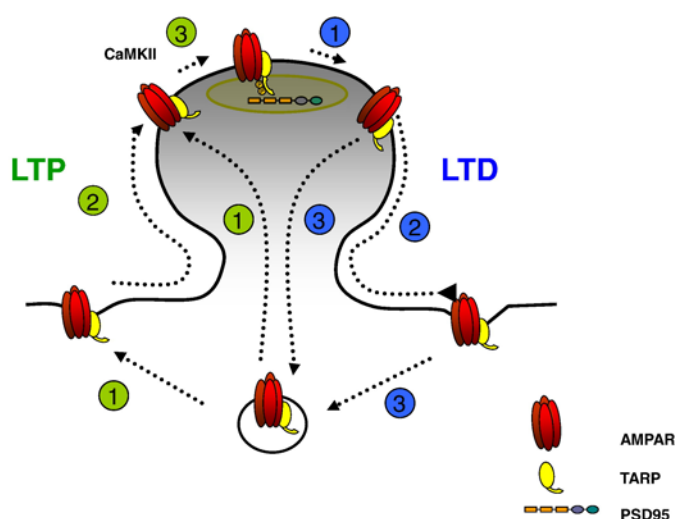


Figure 1.2: Regulation of AMPAR trafficking during synaptic plasticity.

During LTP (in green) AMPARs are inserted either at the dendritic shaft or at the spine lateral to the PSD (1). Newly inserted (or pre-existing) AMPARs rapidly diffuse to synaptic sites (2) where they are trapped by phosphorylation events triggered by CaMKII that presumably increase the affinity to PSD95 (3). During LTD (in blue) the reverse order of events is likely to take place. AMPARs could be destabilized from PSD95 via dephosphorylation (1). AMPARs diffuse out of the synapses (2) where they undergo clathrin-mediated endocytosis (3). Reprinted and reused from Opazo and Choquet, 2011 with permission from Elsevier Inc. © 2010.

This study indicates that recruitment of AMPARs or KARs into the synapse by lateral diffusion or exocytosis is a major factor for LTP (Granger et al., 2013). This finding contradicts with many other studies before, which demonstrated that activity-dependent recruitment of particularly GluA1 was a prerequisite for the initial stage of LTP (Hayashi et al., 2000; Lee et al., 2003; Zamanillo et al., 1999). Enhanced surface expression of GluA1 containing AMPARs is mediated by its phosphorylation by the Ca^{2+} -calmodulin-dependent protein kinase II (CaMKII) (Hayashi et al., 2000; Zamanillo et al., 1999). A possible explanation for the contradictory results may comprise that subunit-specific AMPAR trafficking pathways predominate under physiological circumstances, but that intense LTP protocols, as used in electrophysiological experiments, are able to drive subunit-independent plasticity (Henley and Wilkinson, 2016). This also seems to be the fact for LTD. Again, Granger and colleagues showed that for LTD, AMPARs are not exclusively required. LTD also appears when only KARs are expressed in neurons (Granger and Nicoll, 2014). Given the ability of synapses to anchor a broad range of receptor proteins, these findings suggest that mechanisms of LTP and LTD involve a more general modification of the synapse and that a synapse can modify its composition depending on the activity (Granger et al., 2013; Granger and Nicoll, 2014).

Since most neurons in the adult brain express GluA1/2 or GluA2/3 heteromeric receptors, CP-AMPARs have a very specialized role in the adult brain. Thus, CP-AMPARs play a key part in cerebellar function and in interneurons. A different kind of synaptic plasticity can be observed at the synapse between cerebellar granule cells and inhibitory stellate cells. At the postsynaptic site of stellate cells mainly Ca^{2+} permeable GluA3 homomers are present. High-frequency stimulation induces a switch from synaptic CP-AMPARs to CI-AMPARs, which was determined by a rapid reduction in Ca^{2+} permeability and a change in the rectification index of the AMPAR I/V relationship (Liu and Cull-Candy, 2000). In the hippocampus, parvalbumin-expressing, fast-spiking interneurons express GluA1 and GluA4 subunits, while GluA4 is a key determinant for interneuron function (Fuchs et al., 2007; Pelkey et al., 2015). The GluA4 expression in these interneurons increases during development until p15 and then stays constant, which is different from other neurons (see Section 1.3.2). The knockout (KO) of GluA4, as well as the KO of the AMPAR clustering proteins neuronal pentraxin 2 (NPTX2) and neuronal pentraxin receptor (NPTXR) in these neurons, causes a reduced AMPAR function. This reduced synaptic AMPAR function leads to reduced feedforward inhibition and disrupted network oscillations increasing the susceptibility for epileptiform activity (Fuchs et al., 2007; Pelkey et al., 2015).

1.4. Auxiliary subunits and AMPAR complex composition

Over the last decades, multiple auxiliary subunits and constituents of the native AMPAR complex have been discovered. The transmembrane AMPAR regulatory proteins (TARPs) have been identified first and they are by far the best characterized. The first comprehensive AMPAR proteome study from Schwenk et al., revealed around 30 constituents of AMPAR complexes, with 21 being novel constituents (Schwenk et al., 2012). *Bona fide* AMPA auxiliary subunits are the TARPs, the cornichon homologs 2 and 3 (CNIH2/3; Schwenk et al., 2009), the germ cell-specific gene 1-like (GSG1L) protein (Schwenk et al., 2012; Shanks et al., 2012) and the cysteine-knot AMPAR modulating proteins (CKAMPs) (Klaassen et al., 2016; von Engelhardt et al., 2010). Further constituents of the AMPA complex are the soluble Noelins (Olfactomedins) 1-3 as well as the soluble Brorin and Brorin-like, the Proline-rich transmembrane protein 1 and 2 (PRRT1/2) and Leucine-rich repeat transmembrane protein 4 (LRRTM4) as well as some isoforms of the MAGUKs (Schwenk et al., 2012). The proteins Porcupine (PORCN) and ferric-chelate reductase 1-like protein (FRRS1) play mainly a role during the subcellular processing of AMPARs along the secretory pathway (Brecht et al., 2017; Erlenhardt et al., 2016). Auxiliary subunits and complex constituents associate with AMPARs and modify their trafficking and/or their electrophysiological properties. In fact, interacting proteins play a more prominent role for

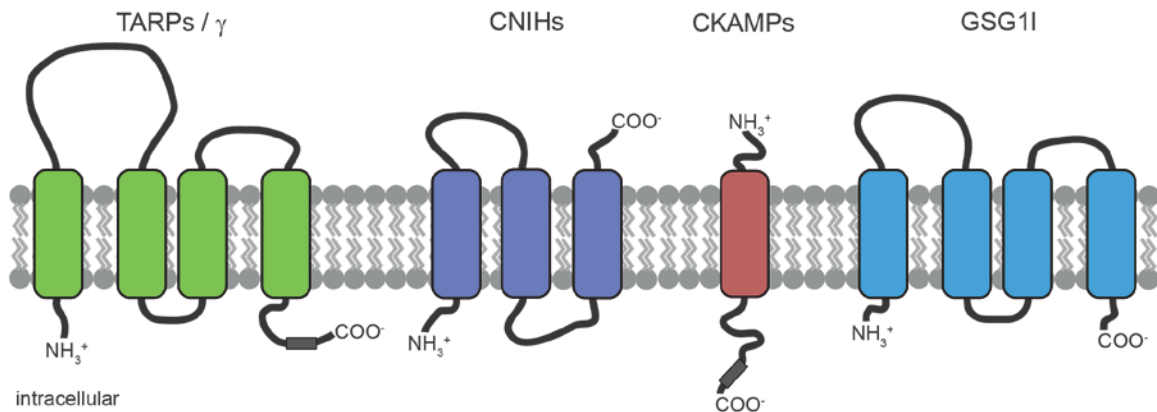


Figure 1.3: Topology of bona fide auxiliary subunits. Modified from Schwenk et al. (Schwenk et al., 2012).

defining the gating kinetics than the different GluA isoforms (Jacobi and von Engelhardt, 2017). AMPAR-interacting proteins differ considerably in the modulation of receptor gating properties and can have opposite effects on one specific property. At the same time, different constituents can affect another gating property similarly (Jacobi and von Engelhardt, 2017). However, not all identified constituents are part of one and the same AMPAR complex. Depending on cell type and brain region, the AMPAR complex composition differs. Even in one cell type, AMPAR complexes with different compositions can coexist as in the postsynapse of stellate cells (see Section 1.3.3). The modular assembly of the pore-lining subunits resulting in diverse properties experiences a second level of diversity by the assembly with further complex constituents. Thus, the interacting proteins offer a highly modular system for AMPARs, in which it is possible to build highly diverse receptors with distinct properties and functions. Due to this modular system, the cells are able to build different AMPARs depending on their particular task. Schwenk et al. postulated a model of how these multi-protein AMPAR complexes are assembling. In this model, the inner core is built from four GluAs and four major auxiliary subunits, like TARPs, CNIHs and GSG1L. The inner core is complemented by “outer core” constituents binding directly to the GluA proteins. But they are interacting with other binding sites of GluA proteins than the inner core auxiliary subunits. At least other peripheral proteins bind proteins from the inner or outer core (Schwenk et al., 2012). The authors also suggest that the GluA subunits have two pairs of binding sites for the four major auxiliary subunits. One pair is a binding site for the TARPs γ -8,4,2,3 and GSG1L. The second binding site harbors CNIH2,3 or TARP γ -2,3 (Schwenk et al., 2012). In their second AMPAR proteome study, Schwenk and co-workers showed that native AMPARs are largely diverse in their subunit composition depending on brain region. In addition, they saw that AMPARs undergo considerable changes in their subunit composition during postnatal development. This finding might underlay the observation that AMPARs are involved in synaptogenesis and synapse maturation (Schwenk et al., 2014). Due to the variety of this modular system, it is possible for cells to react to changes, which occur during diseases or pathophysiological events affecting synaptic homeostasis or homeostatic plasticity. In the next sections, the physiological roles of the *bona fide* auxiliary subunits, the TARPS, CNIHs, CKAMPS and GSG1L s will be discussed in more detail.

1.4.1 The TARP Family

The family of TARPs consists of seven members, which are grouped based on their functional properties and sequence identities in two subfamilies, the type I TARPs (γ -2/stargazin, γ -3, γ -4, γ -8) and type II TARPs (γ -5, γ -7). TARPs are non-pore-forming integral membrane proteins and have four transmembrane domains, with both the N-terminus as well as the C-terminus being located intracellularly (Jackson and Nicoll, 2011). They have a large extracellular loop between

the first two membrane domains and this loop is crucial for the modulation of AMPAR gating (Jackson and Nicoll, 2011; Twomey et al., 2016). The other transmembrane domains are connected with smaller loops. The C-terminus contains phosphorylation sites and a PDZ binding motif, which is essential for synaptic targeting of AMPARs (Jackson and Nicoll, 2011).

The function of γ -2, also called stargazin, have been revealed with the discovery of the stargazer mice, which show an unsteady gait and unusual, repeated head elevations as well as seizures (Letts, 2005). This severe behavior was caused by a mutation in the γ -2 gene leading to an uncompleted translation of the protein and low expression levels of γ -2 in cerebellar granule cells (Letts et al., 1998). As TARPs act as a chaperone for AMPARs and promote their ER export as well as their maturation, surface trafficking of AMPARs to the plasma membrane is disturbed in stargazer mice. As a result of altered trafficking of AMPARs in stargazer mice, cerebellar granule cells exhibit almost no AMPAR currents (Tomita et al., 2003). The enhancement of surface expression is only mediated by type I TARPs but not by type II TARPs (Jackson and Nicoll, 2011). The expression of γ -5 does not affect surface expression of AMPARs and several studies have indicated that γ -7 enhances surface expression of CP-AMPARs, but reduces the surface expression of CI-AMPARs (Bats et al., 2013; Studniarczyk et al., 2013; Yamazaki et al., 2010). This different trafficking behavior explains why the stargazer mouse is the only single-TARP KO mouse that shows a strong phenotype because cerebellar granule cells express only type I TARP γ -2 and the type II TARP γ -7 (Bats et al., 2013). The reduced surface expression of AMPARs may be rescued by the expression of any other type I TARP. In contrast, over-expression of γ -7 in stargazer mouse rescues the surface expression levels of AMPARs only to a small extent (Kato et al., 2007; Tomita et al., 2003). Most other cells express more than one type I TARP (Bats et al., 2013; Fukaya et al., 2005; Menuz et al., 2009) so that they can mutually compensate for each other (Menuz et al., 2008).

The last step of AMPAR trafficking is the transport to synaptic spines and anchoring of AMPARs into the PSD, which is mediated by MAGUKs via their PDZ domains. AMPARs lack a PDZ binding motif and as described above TARPs exhibit one at their end of the C-terminus. Due to the assembling of AMPARs with TARPs and the interaction of TARPs with MAGUKs like PSD-95, the AMPARs get trapped within the synapse (reviewed by Greger et al., 2017; Haering et al., 2014; Henley and Wilkinson, 2016; Jackson and Nicoll, 2011; Kato et al., 2010b). De- and re-phosphorylation of the C-terminal domain of TARPs modulate the interaction with MAGUKs and this mechanism seems to play a significant role for regulation in LTP and LTD (Haering et al., 2014; Jackson and Nicoll, 2011). The type II TARP γ -5 has an atypical PDZ binding motif and is not able to bind on PSD-95 and promote synaptic anchoring of AMPARs (Soto et al., 2009). γ -7 also has an atypical PDZ binding motif, but different from γ -5, it seems to support extrasynaptic anchoring of CP-AMPARs, however not anchoring of CI-AMPARs in the synaptic spine (Studniarczyk et al., 2013).

TARPs do not only influence the maturation and trafficking of AMPARs. They also modulate the channel properties such as agonist efficacy, activation and deactivation rates, and the desensitization rate at the synapse. All type I TARPs enhance the glutamate affinity and kainate efficacy. Whereas γ -7 influence only kainate efficacy and γ -5 reduces glutamate affinity only in GluA2 containing AMPARs (Jackson and Nicoll, 2011; Kato et al., 2010b, 2008). Type I TARPs slow down deactivation and desensitization rates of AMPARs while increasing single-channel conductance and steady-state currents leading to increased current amplitudes (Jackson and Nicoll, 2011; Kato et al., 2010b; Milstein et al., 2007; Soto et al., 2009). For the type II TARPs, the described gating effects of AMPARs are contradictory. In studies by Kato et al., it has been shown that γ -5 modulates gating only of CI-AMPARs, whereas γ -7 affects gating of CP- and CI-AMPARs (Kato et al., 2008, 2007). Soto et al. found instead that γ -5 preferentially regulates the CP-AMPARs in comparison to CI-AMPARs (Soto et al., 2009). Interestingly, both γ -5 and γ -7 are expressed in Bergmann glia cells and the KO of γ -7 in these cells reveals a decrease in GluA1 and GluA4 expression (Yamazaki et al., 2010). Also, the KO of γ -7 in cerebellar stellate

cells affects selectively the CP-AMPA population and leads to a reduction of GluA3 homomers (Bats et al., 2013). These data suggest that both TARPs are important for CP-AMPA function. The binding of TARPs also has an influence on the polyamine block of CP-AMPA. Both types of TARPs lead to a reduced intracellular polyamine block and the I/V curves show reduced rectification (Jackson and Nicoll, 2011; Kato et al., 2010b).

Like for GluAs, the expression of TARPs in the brain is highly heterogeneous (Kato et al., 2007; Tomita et al., 2003). During development, the expression of γ -4 is down-regulated (Fukaya et al., 2005; Tomita et al., 2003), whereas all other TARPs are up-regulated, and highest expression is found in adult brain (Blair et al., 2013; Schwenk et al., 2014; Tomita et al., 2003). Especially, the γ -3 expression peaks in the adult stage and is rather low during development (Schwenk et al., 2014; Tomita et al., 2003). TARP γ -2 seems to be expressed by nearly every type of neuron throughout the brain (Fukaya et al., 2005; Schwenk et al., 2014, 2012). The predominant TARP in hippocampus, cortex, and striatum is γ -8. In the cerebellum, γ -2 and γ -7 are the main expressed subunits and this combination is present in basically all neurons of the cerebellum (Bats et al., 2013; Schwenk et al., 2014; Tomita et al., 2003). TARP γ -5 is not so abundant in the whole brain, but it is particularly found in cerebellar Bergmann glia as well as in the olfactory bulb (Kato et al., 2007; Schwenk et al., 2014, 2012). Bergmann glia expresses also γ -4 and γ -7 (Bats et al., 2013).

1.4.2 The Cornichon Proteins

In contrast to the TARPs, the cornichon homologs (CNIHs) were identified as auxiliary subunits by a proteomic analysis, and it was a surprising finding because cornichons had been described only as ER cargo exporters for soluble growth factors before (Bökel, 2006; Roth et al., 1995; Schwenk et al., 2009). Like the TARPs, the cornichons are non-pore-forming transmembrane proteins. They have three transmembrane domains, with the N-terminus being located intracellularly, and the C-terminus protruding into the extracellular space. They do not exhibit a PDZ binding motif like TARPs.

CNIHs increase the ER export and cycle between ER and Golgi. When they bind to AMPARs, they enhance the export of the receptors from the ER, but also from the Golgi to the plasma membrane. They influence the maturation of AMPARs by promoting traffic along the secretory pathway, thereby changing the glycosylation patterns of AMPARs (Harmel et al., 2012). In heterologous systems, the co-expression of CNIH2/3 and AMPARs leads to an increase of AMPAR surface expression. Several studies showed that CNIHs slow deactivation and desensitization of AMPARs and that CNIH2 enhances the mean channel conductance in heterologous systems (Harmel et al., 2012; Kato et al., 2010a; Schwenk et al., 2009). In hippocampal hilar mossy cells, the KO of CNIH2 leads to accelerated EPSCs indicating that CNIH2 slows EPSCs when integrated into postsynaptic AMPARs (Boudkkazi et al., 2014). In addition, the KO of CNIH2/3 in CA1 neurons reveals that CNIH2/3 is also mandatory for surface expression of AMPARs *in vivo*. Moreover, the KO of CNIH2/3 causes a loss of GluA1/2 heteromers, leading to a reduction of synaptic transmission and impaired LTP. Only a minor portion of Glu2/3 heteromers is left at the synapse of CA1 neurons (Herring et al., 2013). Overexpression of CNIH2 has no effect in hippocampal neurons, however in the stargazer mouse CNIH2 can partially rescue the surface expression of AMPARs in cerebellar granule cells, but cannot take over the synaptic function of γ -2 (Herring et al., 2013; Shi et al., 2010). Only the co-expression of CNIH2 with γ -8 is able to rescue the loss of stargazin (Kato et al., 2010a). Several studies indicate that CNIH2 prefers to interact with GluA1 and γ -8 containing complexes and thus predominantly modulates the properties of GluA1 (Gill et al., 2011; Herring et al., 2013; Kato et al., 2010a). The observed electrophysiological properties of AMPAR currents in hippocampal pyramidal neurons indicate a complex composition with CNIH2 and γ -8 (Herring et al., 2013). In good agreement, the KO of γ -8 reduces CNIH2 expression in

hippocampal neurons (Kato et al., 2010a). The interaction between CNIH2 and GluA1 is probably mediated by TARP γ -8, as γ -8 prevents a functional association of CNIH2 with non-GluA1 subunits (Herring et al., 2013). The proteomic data support this mechanism because CNIH2 and γ -8 seem to bind onto different binding sites (Schwenk et al., 2012). Finally, CNIHs may reduce the TARP stoichiometry in AMPARs when being part of the complex (Schwenk et al., 2009; Shi et al., 2010). CNIH2/3 seems to be also expressed in glia cells and to modulate glial AMPAR complexes. The electrophysiological properties of recorded AMPAR currents in oligodendrocyte precursor cells (OPCs) suggest that CNIHs are present in the complex. Overexpression of CNIH3 in OPCs slows down the desensitization indicating that AMPARs are not fully saturated with CNIHs in these cells (Coombs et al., 2012).

1.4.3 The CKAMP Family

The cysteine-knot AMPAR modulating proteins CKAMP44 and CKAMP52 were also identified in proteomic studies as an AMPAR modulating protein (Schwenk et al., 2012; Shanks et al., 2012; von Engelhardt et al., 2010). Later, the isoforms CKAMP39 and CKAMP59 were identified by bioinformatics (Farrow et al., 2015). Based on sequence similarity the CKAMP genes are grouped to the Shisa protein family (CKAMP44 = Shisa9, CKAMP52 = Shisa6 CKAMP39 = Shisa8, CKAMP52 = Shisa7). The Shisa family is characterized by a cysteine-rich motif in the extracellular domain, one single transmembrane domain, and a proline-rich C-terminal domain. In contrast to the other Shisa proteins, all CKAMP isoforms have a PDZ binding motif at their C-terminus (Farrow et al., 2015; Pei and Grishin, 2012). For CKAMP44 and CKAMP52, it has been shown that they interact via the PDZ binding motif with PSD95 and promote synapse localization of AMPARs (Karataeva et al., 2014; Klaassen et al., 2016).

All CKAMP family members bind to AMPARs and modulate their electrophysiological properties, (Farrow et al., 2015; Khodosevich et al., 2014; von Engelhardt et al., 2010). The co-expression of GluAs and CKAMP44 results in an almost complete loss of functional currents in heterologous systems. Furthermore, CKAMP44 strongly accelerates desensitization rates and delays recovery from desensitization of AMPARs opposite to some TARPs (von Engelhardt et al., 2010). Overexpression and KO experiments of CKAMP44 in neurons revealed that CKAMP44 modulates AMPARs *in vivo* in the same way like in heterologous systems (von Engelhardt et al., 2010). In synapses with a high CKAMP44 abundance like in dentate gyrus (DG), the CKAMP44 mediated increase in AMPAR desensitization leads to a reduced paired-pulse ratio of EPSCs compared to the KO. At CA1 hippocampal synapses, where CKAMP44 is expressed at rather low levels, the paired-pulse ratio is higher when compared to overexpression of CKAMP44. Thus, CKAMP44 play a key role for short-term plasticity (STP) at specific synapses (von Engelhardt et al., 2010). Analysis of AMPARs in DG granule cells revealed that γ -8 and CKAMP44 co-assemble within the same AMPAR complexes. Both subunits are necessary for the efficient targeting of AMPARs to the cell surface within these neurons. With respect to synaptic plasticity in DG granule cells, γ -8 and CKAMP44 have been described to have opposite effects on STP; however, LTP in DG granule cells required only TARP γ -8 but no CKAMP44 (Khodosevich et al., 2014).

The study of Klaassen et al. showed that CKAMP52, different from CKAMP44, reduces the extent of AMPAR desensitization and increases steady-state current amplitudes (Klaassen et al., 2016). In hippocampal CA1 neurons, the KO of CKAMP52 leads to faster rise and decay times of mEPSCs and furthermore to greater depression in STP. The stronger synaptic depression in CKAMP52 KO may be caused by faster AMPAR desensitization. A clear difference between CKAMP44 and CKAMP52 is that CKAMP44 reduces the paired-pulse ratio whereas CKAMP52 reduces synaptic depression (Klaassen et al., 2016).

All CKAMP family members have a brain specific expression and in-situ hybridization data of the CKAMPs revealed distinct expression patterns within the brain. CKAMP44 mRNA is

expressed relative abundantly in most brain regions, especially in the DG of the hippocampus, in the cerebral cortex, olfactory bulb, and cerebellum (von Engelhardt et al., 2010). As CKAMP44, CKAMP59 mRNA shows a more abundant expression in the brain. It is present in the hippocampus, cortex, and olfactory bulb. In contrast, CKAMP52 mRNA can be only found in the cerebellum and olfactory bulb and CKAMP39 mRNA expression is restricted to the hippocampus, cerebellum, and septum (Farrow et al., 2015). The *in-situ* hybridization data from CKAMP52 explains the low abundance of CKAMP52 in the AMPAR complex compared to CKAMP44 observed in proteomic studies (Farrow et al., 2015; Schwenk et al., 2014, 2012). In a regional proteomic analysis, CKAMP44 is found predominantly in the cortex, striatum, and thalamus and only to a lesser extent in the hippocampus and olfactory bulb, whereby the results for some brain regions differ from those of the *in-situ* hybridization (Schwenk et al., 2014; von Engelhardt et al., 2010).

1.4.4 The GSG1L Protein

Like CNIH2/3 and CKAMP44, the protein GSG1L (germ cell-specific gene 1 like) was identified as a complex constituent in a proteomic approach (Schwenk et al., 2012; Shanks et al., 2012). GSG1L shares the membrane topology with TARPs. It has four TMDs with a long extracellular loop between TMD1 and TMD2 and the N- and C-terminus is located intracellularly. Unlike TARPs, it does not have a PDZ binding motif (Haering et al., 2014). Similar to TARPs, the first large extracellular loop plays a key role in the modulation of AMPAR gating as well as the C-terminus (Mao et al., 2017).

It has been shown that GSG1L increases surface expression of GluA2 in heterologous expression systems. Furthermore, GSG1L modifies the gating kinetics of AMPARs by slowing AMPAR deactivation and desensitization as well as decreases the recovery rate from desensitization (Schwenk et al., 2012; Shanks et al., 2012). Contrasting the results in heterologous systems, overexpression of GSG1L reduces surface expression of AMPARs in hippocampal neurons (Gu et al., 2016). In both, hippocampal neurons, and DG granule cells, overexpression of GSG1L leads to faster deactivation and desensitization kinetics of AMPAR currents, and it increases the recovery rate from desensitization (Gu et al., 2016; Mao et al., 2017). These findings strongly suggest that the modulation of AMPARs by GSG1L can differ between heterologous and native systems.

McGee and his colleagues found that in heterologous systems, GSG1L reduces channel conductance and Ca^{2+} permeability of CP-AMPARs as well as increases the block by polyamines, which leads to stronger rectification (McGee et al., 2015). Overexpression of GSG1L in cultured cerebellar stellate cells, which normally do not express GSG1L, results in increased inward rectification of mEPSCs. In hippocampal pyramidal neurons, where GSG1L is present, the KO of GSG1L induces an increase in mEPSC amplitude as well as a higher conductance and shorter decay times revealing that GSG1L acts to suppress current flow through native CP-AMPAR (McGee et al., 2015). In line with the result of McGee et al., it has been found that overexpression of GSG1L in hippocampal neurons as well as in DG granule cells reduces the amplitude and frequency of AMPAR mEPSCs (Gu et al., 2016; Mao et al., 2017). In addition, the KO of GSG1L in hippocampal neurons and DG granule cells leads to a higher frequency of EPSCs and moreover CA1 hippocampal neurons exhibits enhanced LTP (Gu et al., 2016; Mao et al., 2017). But also in the native system, the modulation of AMPARs by GSG1L seems to depend on the cell type, because the KO of GSG1L in DG granule cells does not alter deactivation and desensitization kinetics of AMPARs and also does not lead to increased LTP (Mao et al., 2016).

Furthermore, GSG1L might specifically regulate CNIH2-containing AMPAR complexes and does not alter the gating effects of TARPs on AMPARs (Gu et al., 2016; Schwenk et al., 2012). It is likely that CA1 hippocampal neurons express complexes in which both CNIH2 and GSG1L

participate due to their different AMPA binding sites (Schwenk et al., 2012). These data demonstrate that GSG1L represents a new class of auxiliary subunits endowing the AMPARs with distinct functional properties counteracting the CNIHs (Gu et al., 2016).

In the adult mouse, GSG1L mRNA expression is found mainly in the neocortex, striatum, hippocampus, and olfactory bulb (Lein et al., 2007; Mao et al., 2017). The proteomic analysis reveals that GSG1L does not show high abundance in the brain and that the abundance nearly remains constant during development. But in line with the mRNA data, GSG1L is found in cortex, striatum and also in the thalamus (Schwenk et al., 2014).

1.5. AMPARs in disease

Many neurological and neurodegenerative diseases involve malfunction of excitatory synapses including deficits in LTP and LDP as well as disrupted neuronal circuits, altered synapse structures and abnormal AMPAR function (Chang et al., 2012; Henley and Wilkinson, 2016). Thus, AMPAR dysregulation may be a crucial factor in many neurological diseases, although it may be not the cause of the disorder but a consequence of it (Chang et al., 2012).

Alzheimer's disease (AD), for example, is a neurodegenerative disease characterized by progressive and irreversible memory impairment (Jang and Chung, 2016). It has been shown that amyloid- β oligomers from AD patients inhibit LTP in rats and at the same time enhances LTD affecting the memory of a learned behavior in rats (Shankar et al., 2008). Furthermore, in these rats, a reduced neuronal spine density was observed (Shankar et al., 2008). Additionally, high amyloid- β concentrations induce hyperexcitability in neurons (Jang and Chung, 2016). It has been suggested that an increase in synaptic activity leads to an induction of synaptic downscaling and due to the permanent presence of amyloid- β , synaptic downscaling becomes persistent, eventually resulting in LTD (Jang and Chung, 2016; Liao et al., 2014). Interestingly, amyloid- β is able to bind GluA2 and increase AMPAR-mediated synaptic responses (Henley and Wilkinson, 2016; Jang and Chung, 2016).

Also in hepatic encephalopathy (HE), which is a common neuropsychiatric complication of both acute liver failure and chronic liver disease, synaptic plasticity like LTP and LDP is affected (Wen et al., 2013). Patients suffering from HE show impaired cognitive function (Felipo, 2013). Animal models, from both acute and chronic HE, exhibit dysfunctions in learning and memory function as well as an impaired NMDAR-dependent LTP. Furthermore, these models suggest that altered AMPAR expression and function is involved in the disease of HE (Chepkova et al., 2006; Monfort et al., 2007; Muñoz et al., 2000; Sergeeva et al., 2005).

The expression of CP-AMPARs is highly restricted in the adult brain. However, a switch from CI-AMPARs to CP-AMPARs has been associated with pathologic mechanisms of some diseases (Chang et al., 2012; Henley and Wilkinson, 2016). After an ischemic insult, GluA2 expression is downregulated, but the expression of CP-AMPARs increases leading to higher intracellular Ca^{2+} concentrations and neuronal cell death. Hence, blocking of CP-AMPARs after traumatic brain injury (TBI) reduced neuronal cell death (Chang et al., 2012; Henley and Wilkinson, 2016; Spaethling et al., 2008).

But not only changes in AMPAR expression play a role in disease, also some constituents of AMPARs are directly linked to certain brain diseases. Genetic analyses and genome-wide scans revealed that TARPs, for example, are linked with epilepsy and psychiatric disorders like bipolar disease or schizophrenia (Kato et al., 2010b). In addition, in patients suffering from schizophrenia CNIHs expression is found upregulated (Drummond et al., 2012).

First reports on the still relatively unknown constituent FRRS1I (ferric-chelate reductase 1-like protein, also known as C9orf4) have shown that homozygous FRRS1I mutations in patients cause epileptic encephalopathy and intellectual disability, which are autosomal-recessive inherited disorders (Brechet et al., 2017; Madeo et al., 2016; Shaheen et al., 2016). The study from Brechet and colleagues revealed that FRRS1I exclusively localizes in the ER with

AMPA receptors. FRRS1L operates as a classical catalyst driving the assembly of GluA subunits with TARPs or CNIHs, which is crucial for further biogenesis of AMPARs (Brechet et al., 2017). The KO of FRRS1L causes a dramatic decrease of EPSC amplitudes and a reduction in surface expression at both synaptic and extrasynaptic sites, which can be explained by decreased receptor assembly in the ER. The mutations in FRRS1L, that are found in patients with intellectual disability, disturb the interaction with GluA subunits or completely fail to interact with AMPARs at all (Brechet et al., 2017). The fact that FRRS1L expression increases during development correlating with synapse maturation underlines a crucial role of FRRS1L in AMPAR biogenesis (Schwenk et al., 2014). An alteration of excitatory synapse function during early development may lead to an imbalance between excitatory and inhibitory transmission. Imbalance in transmission is one cause of epilepsy.

1.5 Astrocytes

As mentioned in chapter 1.1, astrocytes are the major part of glia cells in the brain and they are involved in many different functions. Over the last decades, many studies have investigated these distinct functions such as maintaining the blood-brain barrier and neurovascular coupling as well as neurotransmitter recycling. Also, astrocytes play a significant role in ion homeostasis at synapses, like K^+ clearance and regulation. Furthermore, they are involved in the regulation of intra- and extracellular pH and water homeostasis (Allen, 2014; Haim and Rowitch, 2016; Sofroniew and Vinters, 2010). Due to their close proximity to synapses, they serve important functions in regulating neuronal synapse development and modulating synaptic plasticity in the brain. For example, astrocytes secrete factors like thrombospondins, hevin, and glypicans or neurotrophic factors including BDNF and TGF- β , which regulate synaptogenesis. Additionally, they release gliotransmitters like ATP, D-Serine or glutamate (reviewed by Allaman et al., 2011; Allen, 2014; Chung et al., 2015; Haim and Rowitch, 2016).

In the past, astrocytes have been viewed as a homogeneous cellular population. With the recent technical and methodological development, it has become possible to combine genetic labeling and isolation of specific cell types with RNA-Seq. This strategy revealed that astrocytes are extremely heterogeneous reflecting the previously observed variety in their morphological and physiological properties (Bayraktar et al., 2015; Chai et al., 2017; Haim and Rowitch, 2016; Matyash and Kettenmann, 2010). Based on morphological criteria, astrocytes have been subdivided into protoplasmic and fibrous astrocytes. Protoplasmic astrocytes exhibit a radial morphology with a great number of fine processes branched in a complex way. They reside in the CNS grey matter and connect to blood vessels with their perivascular end-feet, by which they take up nutrients from the blood. They also contact neuronal synapses with their fine processes and are part of the so-called tripartite synaptic compartment. In this position, they are active participants in synaptic transmission and influence synaptic development and function (Khakh and Sofroniew, 2015; Molofsky and Deneen, 2015). Fibrous astrocytes, in contrast, are located in the white matter of the CNS. They have far less processes than protoplasmic astrocytes. Their processes are thicker and contain more filaments than grey matter astrocytes. Fibrous astrocytes express high levels of the intermediate filament glial fibrillary acidic protein (GFAP) (Haim and Rowitch, 2016; Khakh and Sofroniew, 2015). A third, rather special type of astrocytes comprises radial glial (RG) cells. RG play an essential role in CNS development by forming elongated filaments to the pial surface, along which developing neurons, as well as other glia cells, migrate to their final destination. At the end of neurogenesis, RG cells transform either directly into astrocytes or can transform in astrocyte progenitors, eventually migrating, proliferating, and differentiating into astrocytes (Bayraktar et al., 2015; Ge and Jia, 2016; Molofsky and Deneen, 2015). Retinal Müller cells and cerebellar Bergmann glia are the only RG cells that persist in the adult CNS and do not vanish during development (Haim and Rowitch, 2016; Molofsky and Deneen, 2015).

Since the protein GFAP was the first marker used for identification of astrocytes, the GFAP+ astrocytes have been most extensively studied. In numerous studies, either GFAP expression or GFAP promoter function have been employed to investigate astrocyte differentiation (Molofsky and Deneen, 2015; Reemst et al., 2016; Sofroniew and Vinters, 2010). However, in the adult brain, not all astrocytes express GFAP and its expression is down-regulated in subpopulations of mature astrocytes. Reactive astrocytes, in contrast, are known to up-regulate GFAP expression after CNS injury (Khakh and Sofroniew, 2015; Sofroniew and Vinters, 2010). In addition, the astrocytic GFAP expression pattern exhibits a regional and local variability in the brain. Most hippocampal astrocytes express GFAP, whereas only a few do so in thalamus. Neocortical astrocytes in superficial and deep layers express detectable GFAP amounts, but in middle layers, only few astrocytes are GFAP+. Finally, cell types like RG and ependymal cells express GFAP in the adult brain. Also, neural stem cells in the SVZ and SGZ are GFAP+ (Khakh and Sofroniew, 2015; Reemst et al., 2016; Sofroniew and Vinters, 2010). In general, astrocytes from the grey matter (protoplasmic astrocytes) express less or non-detectable amounts of GFAP, whereas most white matter astrocytes (fibrous astrocytes) show detectable GFAP levels. The rather variable and diverse expression pattern of GFAP was a first hint at molecular diversity of astrocytes (Sofroniew and Vinters, 2010). In recent years, additional proteins specific for astrocytes have been discovered and used as identification markers including glutamine synthetase (GS), Ca^{2+} -binding protein S100 β , glutamate-aspartate transporter (GLAST or known as excitatory amino acid transporter 1 (EAAT1)) and the aldehyde dehydrogenase 1 family member L1 (Aldh1L1). However, none of them is sufficient to label all types of astrocytes; each of them also shows a distinct expression pattern. For example, EAAT1 expression is higher in the cerebellum than in the hippocampus or neocortex (Khakh and Sofroniew, 2015; Molofsky and Deneen, 2015; Reemst et al., 2016).

Different from neurons, astrocytes do not show active transmission of electrical signals, for which they have been described as electrically passive cells. However, as a compartment of the tripartite synapse, astrocytes respond to neuronal activity with direct depolarization indicating that astrocytes express neurotransmitter receptors. And regarding the heterogeneity of astrocytes, they display within the brain differences in their electrophysiological properties as well as in their calcium signaling (Allen, 2014; Chai et al., 2017; Croft et al., 2015). Indeed, astrocytes exhibit receptors for glutamate, GABA, adenosine, norepinephrine, and acetylcholine. Most of these neurotransmitter receptors are G-protein coupled receptors and their activation leads to the release of calcium from intracellular stores. Due to this increase in

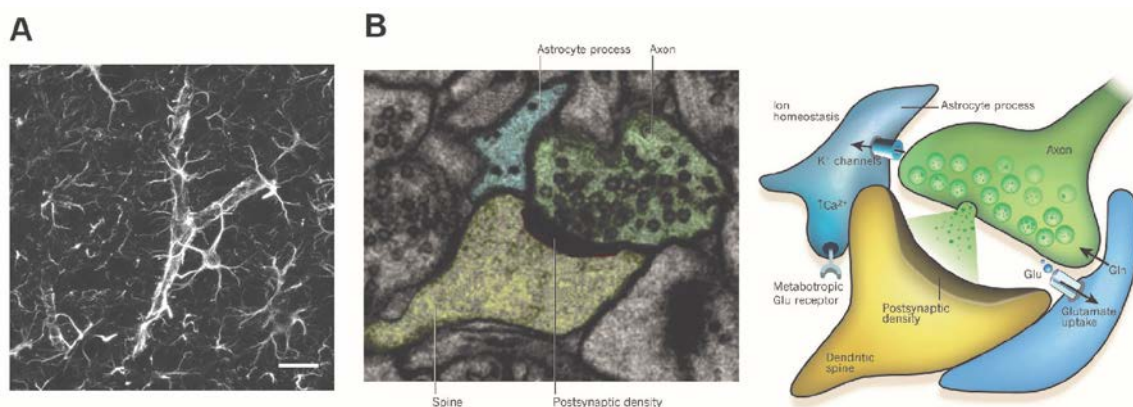


Figure 1.4: Function of astrocytes. (A) Mouse GFAP expressing astrocytes connecting a blood vessel. Scale bar 20 μM . (B) The tripartite synapse. Left: Electron micrograph showing a tripartite synapse in the hippocampus. The astrocyte process is shown in blue, the axon is shown in green and the dendritic spine in yellow with the postsynaptic density. Right: Schematic representation of a tripartite synapse. The processes of astrocytes are intimately associated with synapses. This association is both structural and functional. Reprinted and reused from Eroglu and Barres, 2010 with permission from Elsevier Inc. © 2010.

intracellular calcium, astrocytes may release gliotransmitters and so modulating synaptic functions (Allen, 2014). There is some evidence that astrocytes do not only express metabotropic receptors, but also ionotropic neurotransmitter receptors like AMPARs (Matyash and Kettenmann, 2010). The function and benefit of such expression of ionotropic receptors in an otherwise non-excitabile cell is still elusive, particularly for a protein complex such as AMPARs that play a critical role in modulating fast excitatory neurotransmission. Interestingly, cell specific RNA-Seq data reveal that in cortical astrocytes GluA2 is expressed at higher levels than in neurons (Zhang et al., 2014).

1.5.1 AMPARs in astrocytes

A prominent and well-studied example of astrocytic AMPARs are CP-AMPA receptors in Bergmann glial cells, which are composed of the subunits GluA1 and GluA4 (Burnashev et al., 1992b; Muller et al., 1992). Bergmann glial AMPARs get activated by ectopic vesicular glutamate release of climbing or parallel fibers adjacent to their synapses with Purkinje cells (Matsui, 2005). Ectopic glutamatergic transmission onto Bergmann glia may be subject to both short-term and long-term plasticity, with LTD being predominant in Bergmann glia-specific transmission. The reduction of AMPAR currents in Bergmann glial LTD is explained by depletion of presynaptic vesicle release (Buffo and Rossi, 2013; Croft et al., 2015). In Bergmann glia, the conversion of CP-AMPA receptors into CI-AMPA receptors by introducing the GluA2 gene leads to a retraction of glial processes at synapse as well as to a swelling of synapse boutons. Furthermore, the change from CP-AMPA receptors to CI-AMPA receptors causes a prolonged decay of EPSCs in Purkinje cells and a multiple innervation of Purkinje cells by the climbing fibers (Iino et al., 2001). In line with the result of Iino et al., genetic inactivation of Bergmann glial AMPARs during cerebellar development causes a retraction of their processes, alters Purkinje cell electrophysiological activity, and delays the formation of glutamatergic synapses (Saab et al., 2012). In adult mice, such deletion of Bergmann glial AMPARs is associated with altered fine motor control at the behavioral level (Saab et al., 2012). Beside GluA1 and GluA4, Bergmann glia express the auxiliary subunits TARPs γ -4, γ -5, γ -7 (Bats et al., 2013; Fukaya et al., 2005; Soto et al., 2009; Yamazaki et al., 2010). In Bergmann glia, the KO knockout of γ -7 in leads to a decrease in GluA1 and GluA4 expression. Neither γ -5 nor γ -4 overexpression can compensate the loss of γ -7 in KO animals (Yamazaki et al., 2010).

There is also evidence for the presence of AMPARs in the neocortex (Lalo et al., 2006; Parfenova et al., 2012; Srinivasan et al., 2016; Zhang et al., 2014). A study from Lalo and colleagues (Lalo et al., 2006) revealed that acutely isolated astrocytes from neocortex as well as astrocytes still within the cortical layer II exhibit AMPAR and NMDAR currents. Characteristically, glutamate triggers a biphasic current in those astrocytes. The first, rather fast component is sensitive to the AMPAR and KAR blocker NBQX, the second part of the current is sensitive to D-AP5, which is a specific blocker of NMDARs. The incubation with cyclothiazide, which prevents desensitization of AMPARs, reveals greater AMPAR currents. The authors concluded from their data that NMDARs are typically activated at low levels of transmitter release, due to their higher affinity to glutamate than AMPARs. AMPARs instead are only operative at rather high glutamate concentrations caused by either ectopic release or spill-over of neurotransmitter (Lalo et al., 2006). Furthermore, in cortical astrocytes, AMPARs might act as transducers of glutamatergic transmission in glia-vascular signaling and thereby involved in controlling vasodilation (Parfenova et al., 2012). These functional data are complemented by single cell mRNA expression data of GluA subunits from GFAP/EGFP+ cortical astrocytes (Dzamba et al., 2015; Rusnakova et al., 2013). In those two studies, GluA expression was compared in GFAP/EGFP+ single cells before and after focal cerebral ischemia. The by far highest expression among GluA subunits was observed for GluA2, followed by GluA3, GluA4, and GluA1. After focal cerebral ischemia, the expression of GluA2 decreases slightly, but 14

days post-ischemia it reaches control levels again. In contrast, the other GluA subunits show at least a fourfold increase in expression, especially GluA3 and GluA4, leveling up with GluA2 expression (Dzamba et al., 2015; Rusnakova et al., 2013). The studies showed that the collected single cells can be grouped into different subpopulations and in these subpopulations AMPARs expression is differently regulated during ischemia. However, the gene expression data reveals GluA subunit expression correlates with astrocytic markers as well as some NG2 (Neural/glia antigen 2) cell markers, suggesting that they isolated probably not only astrocytes but also that AMPARs could be regulated differently in glial cells (Dzamba et al., 2015; Rusnakova et al., 2013).

In a study from 1990, in which astrocytes from cerebellum, cortex, and hippocampus were cultured separately, the authors showed that these astrocytes react differently upon an AMPA stimulus (Glaum et al., 1990). A higher percentage of cerebellar cultured astrocytes cells respond to the AMPA stimulus and they exhibit a slight increase in intracellular Ca^{2+} through AMPARs. In contrast, only a few astrocytes from hippocampus and cortex show an increase in Ca^{2+} concentration after AMPA stimuli, but instead, they present higher signals due to NMDAR activation. The authors suggest that hippocampal and cortical astrocyte cultures expressed both NMDARs and AMPARs, whereas cerebellar astrocytes mostly expressed AMPARs.

RNA-Seq data from hippocampal astrocytes indicate AMPAR expression on mRNA level, however, until now, no functional AMPAR currents are observed in hippocampal astrocytes (Chai et al., 2017). Patch-clamp experiments and molecular analyses of hippocampal GFAP/EGFP+ cells revealed AMPAR currents just in a specific subpopulation, but these cells turned out to be NG2 cells instead of astrocytes (Matthias et al., 2003).

In contrast to hippocampal astrocytes, AMPAR currents are more common in brainstem astrocytes and they seem to be involved in the regulation of autonomic reflexes (McDougal et al., 2011).

In summary, AMPARs in astrocytes are related to neuron-glia interaction and seem to be active participants in various brain functions by sensing neuronal activity. Nevertheless, the complex composition AMPARs in astrocytes has remained elusive as well as their functional role and their mechanisms are only unraveled to some extent.

2. Aims of the study

AMPA receptors mediate most of the fast excitatory neurotransmission and play a crucial role in synaptic plasticity. Moreover, they are also involved in brain development, regulation of neuronal migration and synaptic maturation. Native AMPAR complexes show a high molecular complexity: more than 30 complex constituents may co-assemble with the pore-lining subunits GluA1-4 and thereby modulate subcellular trafficking and/or the functional properties of AMPARs. The expression of the pore-lining subunits and complex constituents varies for different types of neurons and brain regions, and also changes during development. The high number of interacting proteins demonstrate that AMPARs are highly diverse and exist as receptors of different molecular compositions, which can differ in their functional properties. Among these proteins, TARPs and CNIHs are the predominant subunits and they have a considerable impact in promoting AMPAR surface transport and in slowing the receptors' gating properties.

In the present work, the following three aims have been pursued:

1. As the expression of AMPAR pore-lining subunits is strictly regulated during development (Henley and Wilkinson, 2016; Schwenk et al., 2014), the present study addressed the question whether other complex constituents may also show developmental expression profiles and thereby give eventually rise to developmentally regulated functional properties of AMPARs. The study was performed with particular emphasis on CNIH2/3.
2. Several neurological and neurodegenerative diseases show deficient synaptic transmission or even disrupted neural circuitry, although it often remains unclear what is cause or consequence of the disease. In these diseases, changes in AMPAR function are often observed (Chang et al., 2012; Henley and Wilkinson, 2016). Here, we sought to study putative changes in AMPAR composition and function involved in a model of hepatic encephalopathy (HE), a neuropsychiatric complication of liver failure leading to cognitive deficits.
3. It has been reported that in the CNS besides neurons, also glial cells can express functional AMPARs. Their molecular composition, however, has been elusive for most cases. Therefore, an experimental workflow had to be developed, which allowed to selectively purify a particular cell type in order to perform cell-type specific analyses of AMPAR composition. In the present study, hGFAP/GFP transgenic mice were employed to analyze astrocytic AMPARs in different brain regions and developmental stages.

3. Compendium of publications and manuscripts

3.1 “Ontogeny repeats the phylogenetic recruitment of the cargo exporter cornichon into AMPA receptor signaling complexes”

Veronika Mauric, **Andrea Mölders**, Nadine Harmel, Bernd Heimrich, Olga A. Sergeeva, Nikolaj Klöcker

Molecular and Cellular Neuroscience, Volume 56, September 2013, Pages 10-17
DOI: 10.1016/j.mcn.2013.02.001

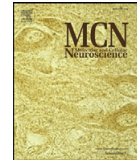
I established, designed, performed, and analyzed the real time PCR (qPCR) experiments as well as prepared the figure of qPCR data and drafted text passages of the manuscript. I contributed to data interpretation and to the writing of the manuscript.

This publication is reprinted and reused with permission from Elsevier Inc. © 2013



Contents lists available at SciVerse ScienceDirect

Molecular and Cellular Neuroscience

journal homepage: www.elsevier.com/locate/ymcne

Ontogeny repeats the phylogenetic recruitment of the cargo exporter cornichon into AMPA receptor signaling complexes

Veronika Mauric^a, Andrea Mölders^a, Nadine Harmel^{a,1}, Bernd Heimrich^b,
Olga A. Sergeeva^a, Nikolaj Klöcker^{a,*}

^a Institute of Neural and Sensory Physiology, Medical Faculty, University of Düsseldorf, 40225 Düsseldorf, Germany

^b Institute of Anatomy and Cell Biology, University of Freiburg, 79104 Freiburg, Germany

ARTICLE INFO

Article history:

Received 28 December 2012

Accepted 1 February 2013

Available online 8 February 2013

Keywords:

GluA

CNIH-2

Developmental expression

Cargo exporter

Auxiliary subunit

ABSTRACT

Besides mediating most of the fast excitatory neurotransmission in the mammalian CNS, ionotropic glutamate receptors of the AMPA subtype (AMPA receptors) serve highly diverse functions in brain development controlling neuronal migration, synaptic growth, and synaptic maturation. Pioneering proteomic studies suggest that this functional diversity is met by a great molecular complexity in native AMPAR composition. Here, we have investigated the expression patterns of two recently identified AMPAR constituents, the cornichon homologues CNIH-2 and CNIH-3, and their assembly with the AMPAR core subunits GluA1–4 in developing rat brain. Unlike GluA1–4 expression, which is up-regulated during postnatal brain development, the two cornichon homologues show maximum mRNA and protein expression early after birth, which then decline towards adulthood. Despite rather reciprocal expression profiles, the overall ratio of CNIH-2/3 complexed with GluAs remains constant throughout development. Our data reveal an excess amount of AMPAR-free CNIH-2/3 early in development, which might serve the evolutionarily conserved role of cornichon as a cargo exporter. With progressing development, however, the amount of AMPAR-free CNIH-2/3 subsides, whereas the one being integrated into AMPAR complexes increases. Hence, the cornichon homologues CNIH-2/3 gain importance in their role as auxiliary subunits of native AMPARs during ontogeny, which reflects their functional evolution in phylogeny.

© 2013 Elsevier Inc. All rights reserved.

Introduction

Ionotropic glutamate receptors of the AMPA subtype (AMPA receptors) mediate most of the fast excitatory neurotransmission in the mammalian CNS. In addition, AMPARs are key determinants of brain development by controlling neuronal migration, synaptogenesis, and synaptic growth (McAllister, 2007; McKinney, 2010). Recent proteomic studies suggest that such highly diverse demands on receptor function might be met by the unforeseen molecular complexity of native AMPARs (Schwenk et al., 2012, 2009; Shanks et al., 2012; von Engelhardt et al., 2010). However, how the molecular composition of native AMPARs varies over brain development and how these variations translate into receptor function remain elusive.

The AMPAR core is formed by a heterotetramer of GluA1–4 subunits (Collingridge et al., 2009; Hollmann and Heinemann, 1994). Differential expression of GluA1–4 in space and time, their combinatorial assembly,

and their modification at both posttranscriptional and posttranslational levels yield a spectrum of different channel properties with respect to gating and trafficking (Coleman et al., 2006; Greger et al., 2002; Lomeli et al., 1994; Sommer et al., 1990; Verdoorn et al., 1991). In native tissue, GluA subunits co-assemble with other proteins that amplify their functional diversity. Besides GluA1–4, the most abundant AMPAR constituents are the transmembrane AMPAR regulatory proteins (TARPs) and the two cornichon homologues CNIH-2 and CNIH-3 (Díaz, 2010; Jackson and Nicoll, 2011). Both TARPs and the two cornichon proteins promote surface expression of AMPARs and increase charge transfer through them by modulating channel gating (Schwenk et al., 2009; Soto et al., 2007; Tomita et al., 2005).

The cornichon gene product was originally identified in *Drosophila* to be required for correct growth factor signaling in oogenesis (Roth et al., 1995). Follow-up studies revealed that cornichon proteins comprise an ancient family of endoplasmic reticulum (ER) cargo exporters, regulating the early anterograde transport not only of members of the epidermal growth factor (EGF) family but also of integral membrane proteins (Bökel et al., 2006; Castro et al., 2007; Hoshino et al., 2007; Powers and Barlowe, 2002, 1998). In agreement with those studies, Shi and co-workers postulated a chaperone-like function also for the rat orthologue CNIH-2 in facilitating ER export of AMPARs (Shi et al., 2010). Other studies suggested a role of CNIH-2 and CNIH-3 in amplifying glutamatergic

* Corresponding author at: Institute of Neural and Sensory Physiology, Medical Faculty, University of Düsseldorf, Universitätsstr. 1, 40225 Düsseldorf, Germany. Fax: +49 211 81 14231.

E-mail address: nikolaj.kloecker@uni-duesseldorf.de (N. Klöcker).

¹ Present address: Janssen Pharmaceutical Research & Development, L.L.C., San Diego, CA 92130, USA.

signaling in both neurons and glial cells by modifying the biophysical properties of AMPARs (Coombs et al., 2012; Gill et al., 2011; Kato et al., 2010). Recently, our lab has demonstrated that GluAs wrest CNIH-2 from its cycle between ER and Golgi and integrate it into complexes, which are trafficked to the cell surface of neurons (Harmel et al., 2012). While still exploiting their evolutionarily conserved role as cargo exporters, GluAs have assigned a phylogenetically novel function to cornichon proteins, and that is to modify AMPAR signaling on the neuronal cell surface.

In the present study, we have investigated the expression profiles of CNIH-2 and CNIH-3 and their assembly into native AMPARs during rat brain development. Early in ontogeny, there is a large excess of CNIH-2, which is not in complex with AMPARs and hence free to serve its ancestral role as a cargo exporter cycling in the early secretory pathway. With progressing development, CNIH-2 expression decreases while the expression of GluAs (and also TARPs) increases. As the overall ratio of CNIH-2 in native AMPARs, however, remains constant, our data show that the excess of AMPAR-free CNIH-2 – and thus presumably its function in general cargo export – subsides during ontogeny.

Results

CNIH-2 gene expression peaks early in development

We analyzed the developmental gene expression patterns of CNIH-2 and CNIH-3 in rat brain from late embryonic stage E18 to adult stage (>P42) by non-radioactive in situ hybridization. For these experiments, three brain areas were selected, in which glutamatergic neurotransmission has been studied in great detail: the hippocampus, the neocortex, and the cerebellum. For in situ hybridization, tissue sections from all developmental stages were processed in parallel to allow for comparison of signal intensities.

As displayed in Fig. 1, both CNIH-2 and CNIH-3 mRNAs are expressed in the hippocampal formation and in the neocortex. In the cerebellum, only CNIH-2 mRNA could be detected by non-radioactive in situ hybridization. Gene expression of CNIH-2 peaked during the first two postnatal weeks and then declined to lowest levels in adult brain. CNIH-3 showed a similar time course of expression in the neocortex, whereas in the hippocampus, it was induced in granule cells of the dentate gyrus (DG) and

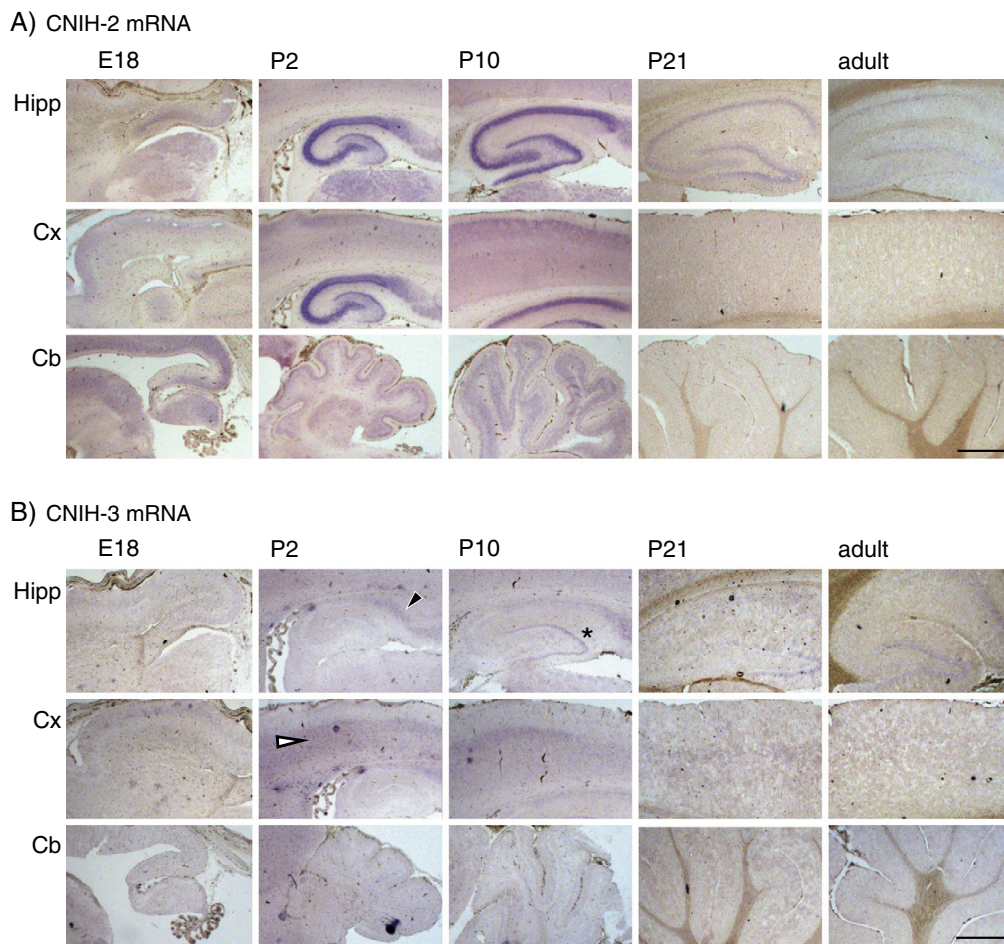


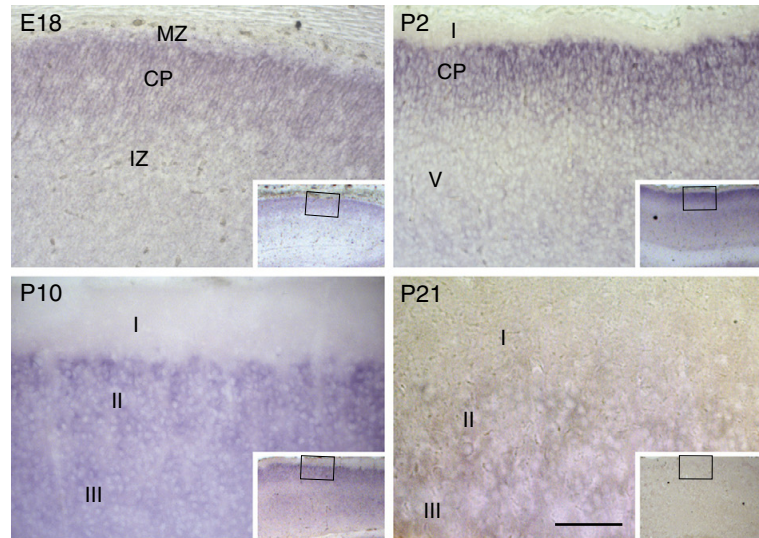
Fig. 1. Spatiotemporal expression patterns of CNIH-2 and CNIH-3 mRNAs in the developing rat brain. Representative images of CNIH-2 (A) and CNIH-3 (B) mRNA distributions in sagittal cryosections at indicated time points, detected by non-radioactive in situ hybridization (CNIH-2: $n=4$; CNIH-3: $n=2$). Each panel represents one experimental run. (A) In hippocampus (Hipp), neocortex (Cx) and cerebellum (Cb), CNIH-2 mRNA expression peaks in early postnatal development. (B) In Hipp and Cx, CNIH-3 mRNA expression is restricted to granule cells (black asterisk), the subiculum (black arrow head) and the cortical plate (white arrow head). No signal was detected in tissue hybridized with the respective sense probes. Anterior end is oriented to the left, scale bars: 500 μm .

in the subiculum during early postnatal stages and then remained constant until adulthood. Irrespective of developmental stage, CNIH-2 mRNA was the predominant isoform expressed in the three selected brain areas as judged by non-radioactive in situ hybridization.

In the hippocampal formation, CNIH-2 mRNA was strongly expressed in granule cells of the DG and in the pyramidal cell layer of the

hippocampus proper. While its hippocampal expression pattern changed only in overall intensity during development, we observed a cellular redistribution of CNIH-2 mRNA within the neocortex and cerebellum over time (Fig. 2). In the neocortex of animals at postnatal day 2 (P2), CNIH-2 mRNA was strongly expressed in the outermost layer of the cortical plate with a gradient fading rostrally. In the third postnatal week, this distinct

A) Neocortex



B) Cerebellum

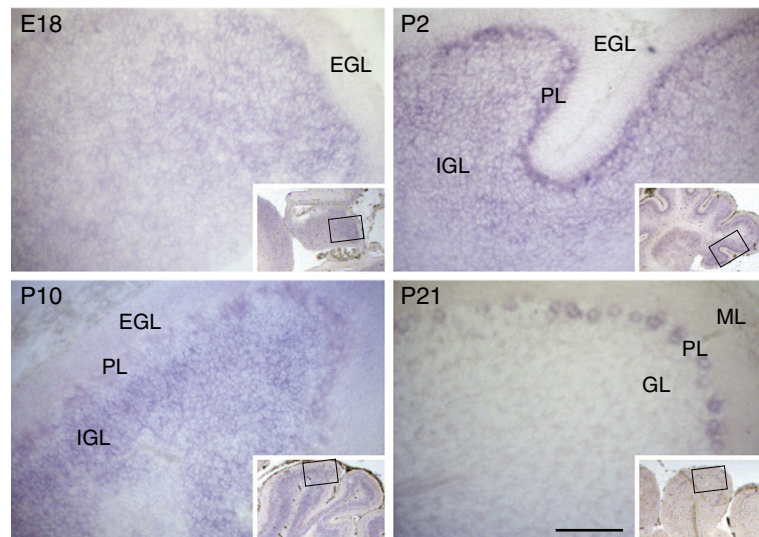


Fig. 2. Developmental redistribution of CNIH-2 mRNA. Representative images of CNIH-2 mRNA expression in the neocortex (A) and cerebellum (B), detected by non-radioactive in situ hybridization. Higher magnification of insets revealed a distinct signal within the cortical plate (CP), which evenly redistributes into all neocortical layers with ongoing maturation, except for the molecular zone (MZ)/neocortical layer I. CNIH-2 mRNA is expressed in the cerebellar anlage at E18 and is detectable in the internal granular layer (IGL) in early postnatal period, besides expression in the presumptive Purkinje cell layer (PL). At late postnatal phases, aligned Purkinje cells express CNIH-2 mRNA, while in granule cells the signal faded. All signal was absent in tissue hybridized with sense probe. MZ: molecular zone; I–V: neocortical layers; IZ: intermediate zone; EGL: external granular layer. Scale bars: 100 μ m.

localization of CNIH-2 mRNA dispersed into all neocortical layers except for layer I, which was devoid of a hybridization signal throughout development. In late embryonic and early postnatal cerebellum, we observed CNIH-2 mRNA in the cerebellar anlage and the presumptive Purkinje cell and internal granule cell layer, respectively, with a complete redistribution into Purkinje neurons by P21.

Reciprocal regulation of CNIH-2 and GluA expression during development

In a second set of experiments, we compared the developmental protein expression pattern of CNIH-2 and CNIH-3 in whole brain membrane fractions with the expression of the four GluA subunits. As β -actin expression is developmentally regulated (Bond and Farmer, 1983), we refrained from using it as a loading control in our Western blot experiments. Instead, CNIH-2/3 expression was quantified relative to one of the four GluA subunits in the same samples and on the same blot membranes.

As shown in Fig. 3A, CNIH-2/3 protein correlated inversely with GluA1–4 protein during development. While the expression of each type of GluA subunit increased postnatally, CNIH-2/3 protein dropped to lowest levels in adult animals. Densitometric quantification revealed a strong decrease in the relative protein expression ratio of CNIH-2/3 to GluA1–4 subunits to $10.9 \pm 4.8\%$ in adulthood ($n = 4$). This was in sharp contrast to the expression patterns of the analyzed TARP isoforms. Both anti- γ -2/3 and anti- γ -8 signals increased during postnatal development, in parallel with the increase in GluA subunit expression. As had been shown before, there was a peak of expression in late postnatal

stages from which the expression of all GluA isoforms and also one of the TARP isoforms tested here slightly declined again towards adulthood (Pellegrini-Giampietro et al., 1991).

The reciprocal regulation of CNIH-2/3 and GluA1–4 protein expression patterns in development reflected respective changes in gene transcription as confirmed by real time PCR experiments (Fig. 3C). At E18, CNIH-2 mRNA expression was 2.08 ± 0.22 fold higher than the one at adult stage, whereas GluA1–4 mRNA expression at E18 was only 0.47 ± 0.1 , 0.55 ± 0.05 , 0.36 ± 0.04 , and 0.6 ± 0.05 fold their expression levels at adult stage, respectively ($n = 3$).

Excess CNIH-2/3 in early development does not co-assemble with GluA subunits

Finally, we performed co-immunoprecipitation experiments to investigate whether the overall ratio of CNIH-2/3 assembled in native AMPAR complexes changes during brain development, as might be inferred from the observed reciprocal expression patterns. To this end, AMPAR complexes were depleted from whole brain membrane fractions at E18 and adult stage using a mixture of antibodies directed against all four GluA subunits (Fig. S2). By means of densitometric Western blot analysis, both the amounts of precipitated GluAs and co-precipitated CNIH-2/3 were then quantified at E18 and adult stage. As shown in Fig. 4, the E18/adult ratios of anti-CNIH-2/3 and anti-GluA signals differed significantly in whole brain membranes (*load*) reflecting the reciprocal expression patterns of CNIH-2/3 and GluA proteins during

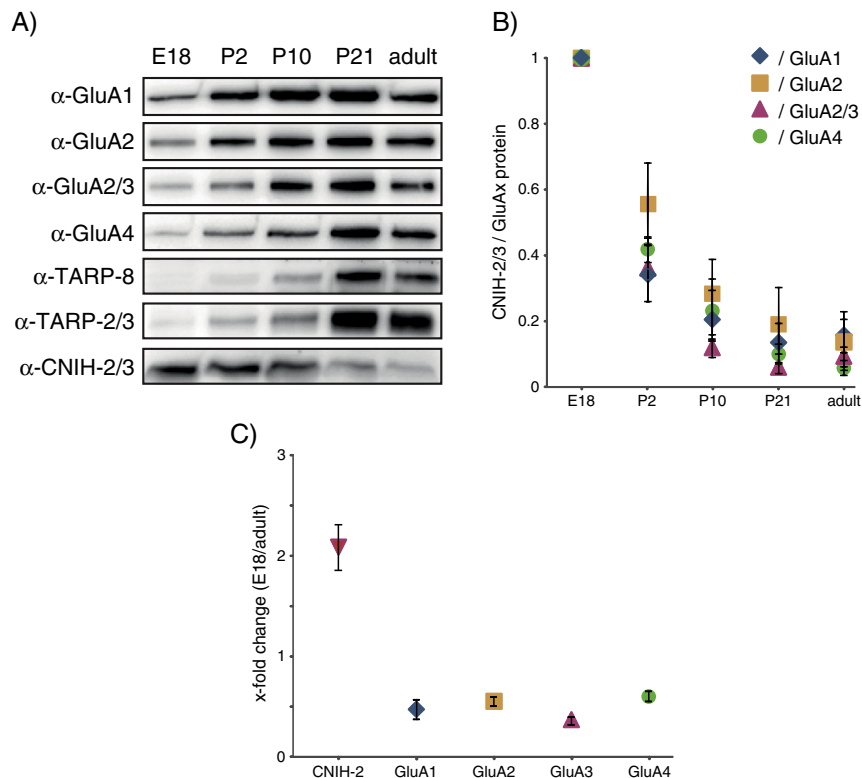


Fig. 3. Developmental protein expression profile of AMPARs. (A) Representative Western blots of whole brain lysates isolated at indicated time points show reciprocal expression patterns of GluAs and TARPs on one side compared to CNIH-2/3 on the other side. (B) Densitometric quantification of Western blot results ($n = 4$). Depicted are relative CNIH-2/3 to GluAx ratios as indicated. (C) Quantification of CNIH-2 and GluA1–4 mRNA expression in whole rat brains at E18 and adult stage by quantitative real time PCR ($n = 3$ animals). The differences in mRNA expression levels in E18 and adult rat brain were calculated directly from Ct values in equal amounts of cDNA, reverse-transcribed from E18 and adult rat brain mRNA, with $\Delta C_t = C_{t, \text{gene}, E18} - C_{t, \text{gene}, \text{adult}}$. Developmental changes in mRNA expression are displayed as multiples (x-fold change) of gene expression at E18 relative to adult stage ($2^{-\Delta C_t}$).

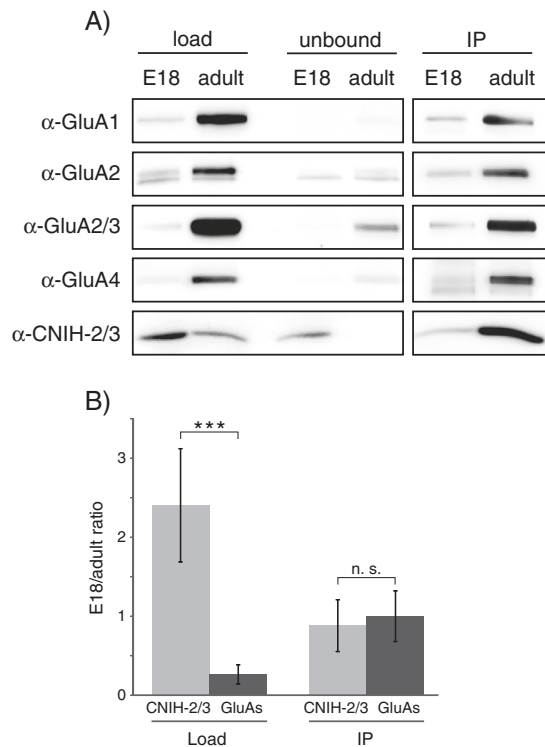


Fig. 4. AMPAR-free CNIH-2/3 protein declines in development. (A) Representative Western blots of immunoprecipitated GluA1–4 subunits and co-precipitated CNIH-2/3 protein. Horizontal lanes probed with indicated antibodies were taken from the same blot membranes; same exposure times are boxed. (B) Quantification of Western blots ($n=3$) from (A) shows densitometrically calculated E18/adult ratios for CNIH-2/3 and all GluAs in load and IP eluate (load = lysate; unbound = supernatant after anti-GluA1–4 affinity purification; IP = immunoprecipitated eluate, concentrated 10 fold). Asterisks mark the significant difference of E18/adult ratios in loads, ($p<0.001$). Note that the relative amount of co-precipitated AMPAR-bound CNIH-2/3 does not change from embryonic E18 to adult stage (CNIH-2/3 IP: 0.87 ± 0.32 ; not significant (n.s.) from GluA1–4 IP: 1 ± 0.31 , $p=0.61$).

development. Thus, at E18 anti-CNIH-2/3 signal intensity was twice the one in adult brain (E18/adult: 2.4 ± 0.72 ; $n=3$), while late embryonic anti-GluA signals were only 25% of the ones detected at adult stage (E18/adult: 0.26 ± 0.12 ; $n=3$). In AMPAR complexes, however, the relative amounts of co-precipitated CNIH-2/3 did not change over time. The E18/adult ratio of co-precipitated CNIH-2/3 (0.87 ± 0.32 ; $n=3$) did not significantly differ from the one of depleted GluAs (1 ± 0.31 ; $n=3$) indicating that the overall stoichiometry of CNIH-2/3 in whole brain AMPAR complexes did not change during development. Accordingly, excess CNIH-2/3 at the early developmental stage segregated into the remaining unbound fraction after depletion of AMPAR complexes (Fig. 4A).

Discussion

In this study, we show that the expression of the two mammalian cornichon homologues CNIH-2 and CNIH-3 in the brain is regulated during development. However, unlike exclusive AMPAR constituents, i.e. the TARP proteins γ -2/3 and γ -8, whose expression profile is directly proportional to the expression of the AMPAR core subunits, CNIH-2/3 display a profile reciprocal to the one of GluA1–4. As the overall ratio of CNIH-2/3 integrated into native AMPARs remains constant over time, there is an excess amount of AMPAR-free CNIH-2/3, which declines during development. Hence, the cornichon homologues gain

importance in their role as auxiliary subunits of native AMPARs during ontogeny, which reflects their functional evolution in phylogeny.

The developmental expression of CNIH-2 and CNIH-3 in brain was studied at mRNA and protein levels from late embryonic stage E18 to adulthood. Both in situ hybridization and whole brain protein data indicate a peak of expression for both homologues early in development with a subsequent decrease towards adult stage. Of the two isoforms investigated, CNIH-2 is the predominant one in the selected brain regions of the neocortex, hippocampus, and cerebellum, in which CNIH-3 mRNA is barely detectable by in situ hybridization. These results are in line with our finding that the cellular localization of CNIH-2 is sufficient to explain the pattern of immunoreactivity in respective brain regions detected by an antibody recognizing both isoforms (Schwenk et al., 2009).

The temporal expression profile of CNIH-2 correlates inversely with the ones of the AMPAR core subunits GluA1–4 (Martin et al., 1998; Pellegrini-Giampietro et al., 1991). This seems rather atypical for an auxiliary β -subunit of an ion channel, also contrasting the developmental expression profiles of the TARPs γ -2/3 and γ -8 (Tomita et al., 2003; Yan and Tomita, 2012). One might infer from these findings that there is a gross developmental change in the ratio, by which CNIH-2 assembles into AMPARs. However, our co-immunoprecipitation experiments depleting the AMPAR core subunits GluA1–4 at embryonic and adult stage demonstrate that the overall ratio of CNIH-2 integrated into AMPARs does not change. The relative amounts of CNIH-2 co-purifying with the four AMPAR core subunits remain constant throughout development. Indeed, local but balancing differences in their stoichiometry with respect to brain region, cell type and subcellular compartment, cannot be excluded, as the co-immunoprecipitations were performed in whole brain tissue. Nevertheless, we detected a large excess of AMPAR-free CNIH-2 early in development, which diminishes until adulthood and readily explains the reciprocal expression profiles of CNIH-2 and GluA subunits. From this, we conclude that the cornichon proteins are not exclusive AMPAR constituents but serve an additional role, particularly in the developing CNS.

What might be the physiological significance of the large excess of AMPAR-free CNIH-2 at late embryonic and early postnatal development? At this stage, CNIH-2 is most strongly expressed in regions, where postmitotic neurons arrive after radial migration and start differentiating, i.e. the superficial layers of the cortical plate, of the hippocampal pyramidal cells, and of the dentate gyrus. Such temporospatial expression profile is reminiscent of the one of EGF-related growth factors, which are known to be exported by cornichon orthologues in other species (Bökel et al., 2006; Castro et al., 2007; Hoshino et al., 2007). Among them, the heparin-binding epidermal growth factor-like growth factor (HB-EGF) has a very similar expression pattern compared with CNIH-2 (Hayase et al., 1998; Kornblum et al., 1999; Nakagawa et al., 1998; Opanashuk et al., 1999; Oyagi and Hara, 2012). HB-EGF expression peaks in the first two postnatal weeks with a predominance in the outer layers of the developing cortical plate, in the pyramidal cell layers and dentate granule cells of the hippocampus, as well as in the cerebellar Purkinje neurons. Intriguingly, the chicken orthologue of CNIH-2 has been shown to export HB-EGF in vitro and to confine the site of HB-EGF action to specific hindbrain neuromeres in vivo by facilitating its secretion (Hoshino et al., 2007). From these reports, one may speculate that the large excess of AMPAR-free CNIH-2 in late embryonic and early postnatal rat brain development may serve to promote cargo export of EGF-like growth factors, i.e. HB-EGF. During this period of brain development, gliogenesis, neuronal and glial cell migration, and neuronal maturation take place, matching the reported mitogenic, chemoattractant, and neurotrophic properties of HB-EGF (Kornblum et al., 1999; Oyagi and Hara, 2012). Furthermore, as growth factors of the EGF-like family are also able to control AMPAR expression and function (Nagano et al., 2007; Namba et al., 2009, 2006), it is worth to mention that GluA1–4 expression gains momentum right after CNIH-2/3 expression have peaked (Martin et al., 1998; Pellegrini-Giampietro et al., 1991).

Recent bioinformatic studies have provided strong support for a close correlation between phylogeny and ontogeny (Domazet-Lošo and Tautz, 2010; Kalinka et al., 2010). As shown in *Drosophila* and zebrafish, there is a phylotypic phase in early development, which is characterized by the expression of an evolutionarily old and highly conserved transcriptome. Ionotropic glutamate receptors (iGluRs) and the prototypic TARP γ -2, are significantly younger in phylogenetic age than the ancient cargo exporter cornichon (Ryan and Grant, 2009; Sakarya et al., 2007; Srivastava et al., 2010). Thus, yeast belonging to the eukaryotic taxon of opisthokonta (average divergence time ca. 1400 million years ago), expresses the cornichon orthologue Erv14p, whereas iGluRs have evolved 200 million years later when eumetazoans diverged from poriferans (amphimedon). TARP γ -2 evolved even later than iGluRs, when bilaterians diverged from cnidarians within the taxon of eumetazoans. Intriguingly, our results show that not only the ontogenic expression profiles of CNIH-2/3, GluA1–4, and the TARPs γ -2/3 and γ -8 reflect their phylogeny, but also the functional diversification of the ER cargo exporter cornichon to become a signaling constituent of AMPARs is repeated in brain development.

Experimental methods

cDNAs

CNIH-2 and CNIH-3 were cloned from rat brain and were verified by sequencing; gene bank accession numbers of the clones used are NM_001025132 (CNIH-2) and NM_001166578 (CNIH-3).

In situ hybridization

Brain tissue from E18, P2, and P10 Wistar rats was subjected to immersion fixation in 4% paraformaldehyde in phosphate buffer (PB) at 4 °C overnight (ON). P21 and adult (>P42) rats were anesthetized and perfused transcardially with 0.9% saline followed by fixative solution. P21 and adult brains were post-fixed at 4 °C for 6 h. All brain tissue was dehydrated in PB containing 20% sucrose at 4 °C ON and stored at –80 °C. Cryosections of 20–25 μ m were cut in sagittal orientation.

Full length CNIH-2 and CNIH-3 cDNAs were subcloned into pBluescript SK– (Stratagene). Sense and antisense riboprobes were synthesized by in vitro transcription with T7 or T3 RNA polymerases and were labeled with DIG (Roche) according to the manufacturer's manual. Labeling efficiencies were determined using DIG quantification and control test strips (Roche). Iso-specificity of the riboprobes was confirmed by in situ hybridization in HeLa cells transduced with the four cornichon rat homologues (Fig. S1).

For detection of CNIH-2 and CNIH-3 mRNAs in brain slices, a standard protocol for non-radioactive in situ hybridization was used. Brain tissue sections from all examined developmental stages were assayed in parallel to allow for comparison of signal intensities. Briefly, the tissue sections were pretreated with 0.2 M HCl for 10 min, digested with proteinase K (Roche) at 37 °C for 5 min and acetylated (0.1 M triethanolamine, 0.25% acetic anhydride, pH 8) before ON incubation with 0.5 ng/ml riboprobes in hybridization buffer (50% formamide, 5 \times SSC, 5 \times Denhardt's solution, 250 μ g/ml yeast tRNA) at 57 °C and 60 °C for CNIH-2 and CNIH-3, respectively. Sections were then washed twice with 50% formamide and 2 \times SSC at hybridization temperatures for 1 h, before re-buffering in maleic acid buffer (MAB; 0.1 M maleic acid, 0.15 M NaCl, pH 7.5) for 30 min at room temperature (RT). After blocking with Roche blocking reagent (1% in MAB) for 1 h at RT, they were finally incubated with an anti-DIG Fab fragments antibody conjugated to alkaline phosphatase (AP) (1:2000 in blocking solution; Roche) at 4 °C ON. Sections were washed 3 \times for 20 min with 1 \times MAB and 2 \times for 10 min with AP buffer (0.1 M Tris pH 9.5, 0.1 M NaCl, 0.05 M MgCl₂). DIG-labeling was visualized by chromogenic detection of AP-activity using ready-to-use 5-bromo-4-chloro-3-indolyl-phosphate and nitro blue tetrazolium solution (Roche; 1:50 in AP buffer).

RNA isolation and cDNA synthesis

Total RNA was isolated from whole brain of Wistar rats at E18 (n=3) and adult (n=3) stage using the RNeasy mini kit (Qiagen). For reverse transcription, 300 μ g RNA were reverse-transcribed with the QuantiTect Reverse Transcription kit (Qiagen), which includes a genomic DNA elimination step. All kits were used according to manufacturer's instructions.

Quantitative real-time PCR

Quantitative real time PCR was performed in an Applied Biosystems StepOne real time PCR System using SYBR green PCR Master mix (Applied Biosystems). Assays were run in a total volume of 10 μ l comprising with the final concentration of SYBR green PCR Master mix, 12 pM forward and reverse primers and 1 μ l of 1:4 diluted cDNA (400 ng). The reactions were performed in MicroAmp optical 96-well reaction plates and the real time PCR parameters were set as follows: initial incubation at 50 °C for 2 min to activate uracil N-glycosylase, 10 min at 95 °C to inactivate the uracil N-glycosylase and activate the AmpliTaq Gold Polymerase, and finally 40 cycles of 15 s at 95 °C, 2 min at 50 °C, and 1 min at 60 °C. Reactions were subjected to a heat dissociation protocol after the final PCR cycle. Each PCR product showed a single peak in the denaturation curve and a single band on a 2% agarose gel at the expected amplicon size. All reactions were carried out in duplicates. Standard curves for real-time PCR protocols with all primer pairs obtained with sequential dilutions up to 1:128 of one cDNA sample were found optimal with linear regression coefficients >0.95. In agreement with previously reported developmental changes in gene expression of conventional house-keeping genes (Bond and Farmer, 1983; Kratzer et al., 2012), we found strong down-regulation (ca. 4 \times) of β -actin expression from E18 to adult stage ($\bar{x}_{C_t, E18, actb} = 16.86 \pm 0.21$ and $\bar{x}_{C_t, adult, actb} = 18.97 \pm 0.13$; n=3 animals, respectively). We therefore refrained from normalizing our data to β -actin gene expression for comparing gene expression levels between E18 and adult stage. Given equal amounts of cDNA used for the PCR reaction, we instead calculated ΔC_t directly from the C_t values at the two developmental stages. Changes in mRNA expression are hence displayed as multiples (x-fold change) of gene expression at E18 relative to adult stage: $E^{\Delta C_t}$, with E being the efficiency of the PCR reaction and $\Delta C_t = C_{t, gene, E18} - C_{t, gene, adult}$.

The following primers were used (sequence in 5'–3' direction):

Gene	Gene name	Primer sequence	Amplicon size	Efficiency
β -Actin	Actb	F CGTGAAGATGACCCAGATCATGTT R GCTCATTGCCGATAGTGATGACCTG	450 bp	1.65
CNIH-2	Cnih2	F TGGCACATCATAGCCTTTGA R GGACGGTGGAGTACCTCC	251 bp	1.85
CNIH-3	Cnih3	F GAGGAACATCGAACCGATCT R GGCATTTCATGACAACCTGGTG	214 bp	1.95
GluA1	Gria1	F GACCATAACCTTGGTCCGGG R CTGGTTGTCTGCTCTCGTCC	258 bp	1.95
GluA2	Gria2	F GAGGACTACCGCAGAAGGAGTAGC R TCGTACCACCAITTTGTTTTCA	251 bp	1.76
GluA3	Gria3	F GCCAGGCGTCTTTTCATTCC R TGCGCCAGAAAAGTGATCTT	272 bp	1.87
GluA4	Gria4	F TCTTGGCAAATGACACAGCAG R TCGCTCCCTGTCTCATATTT	220 bp	1.73

Preparation of membrane proteins

Isolated brains from E18, P2, P10, P21, and adult rats were homogenized with potters in ice-cold homogenization buffer (0.320 M sucrose, 0.01 M Tris pH 7.4, 0.01 M EDTA, 0.01 M iodoacetamide). All buffers used contained freshly added protease inhibitors (aprotinin, pepstatin A and leupeptin, at 0.1 mg/ml each). Cell debris and nuclei were removed by centrifugation at 1000 g for 4 min at 4 °C. The

supernatant was ultra-centrifuged at 125,000 g for 30 min at 4 °C, the resulting pellet containing the crude membrane fraction was re-suspended in 0.02 M Tris (pH 7.4), 0.01 M EDTA and 0.01 M iodoacetamide. Protein concentration was determined by the BCA protein assay reagent using bovine serum albumin as a standard (Pierce). Membrane fractions used for developmental expression analysis of AMPAR constituents were solubilized with ComplexioLyte buffer CL-82 (LogoPharm GmbH) at 1 mg/ml for 30 min at 4 °C before denaturation in Laemmli buffer.

Immunoprecipitation

For immunoprecipitation experiments, crude membrane fractions were solubilized in ComplexioLyte buffer CL-48 (LogoPharm, GmbH) at 1 mg/ml for 30 min at 4 °C. Solubilisates (1.5 mg) were then incubated with 15–30 µg immobilized antibodies at 4 °C for 3 h. The following mixture of antibodies was used: 30% of anti-GluA1 (AB1504, Millipore), 40% of anti-GluA2 (AB1768, Millipore; 75-002, Neuromab), 25% of anti-GluA2/3 (07-598, Millipore) and 5% of anti-GluA4 (AB1508, Millipore). After brief washing with 0.1% ComplexioLyte buffer CL-48, bound proteins were eluted with 1× Laemmli buffer at 37 °C for 10 min. 0.1 M DTT was added after elution.

SDS-PAGE and Western blotting

Protein samples (24 µg each) were run on 12% SDS-PAGE and electroblotted on PVDF membrane (Millipore). Then the blot membrane was cut horizontally at different molecular weight ranges, blocked with Tris-buffered saline containing 1% Tween-20 (TBS-T) and 5% nonfat powdered milk at RT for 1 h before ON incubation at 4 °C with the following antibodies: 0.5 µg/ml of anti-TARP-γ2/3/8 (07-577, Upstate), anti-GluA1 (AB1504, Millipore), anti-GluA2 (75-002, Neuromab; detection of IP blots: MAB397, Millipore), anti-GluA2/3 (07-598, Millipore), 1 µg/ml of anti-GluA4 (AB1508, Millipore), and anti-CNIH-2/3 (1:1000; (Hoshino et al., 2007)) in TBS-T and 2% nonfat powdered milk. Primary antibodies were recognized by goat anti-mouse or goat anti-rabbit secondary antibodies, respectively, conjugated to horseradish peroxidase (Santa Cruz, 1:15000 in TBS-T with 5% nonfat powdered milk). Proteins were visualized with ECL plus reagent (GE Healthcare) using a Fusion Fx luminometer (Vilber). Densitometric analysis was performed using ImageJ software.

Statistical analysis

Data are given as mean ± standard error of mean (SEM) unless otherwise stated. For assessing statistically significant differences, a two-tailed unpaired Student's *t*-test was used.

Supplementary data related to this article can be found online at <http://dx.doi.org/10.1016/j.mcn.2013.02.001>.

Acknowledgment

The work was supported by grants of the Deutsche Forschungsgemeinschaft (SFB974 TP B05) and of the Anton-Betz-Stiftung to N.K. A.M. is an associate member of the iBrain graduate school in Düsseldorf. We also thank Dr. O. Chisaka for a sample of the anti-CNIH-2 antibody.

References

Bökel, C., Dass, S., Wilsch-Bräuninger, M., Roth, S., 2006. *Drosophila* cornichon acts as cargo receptor for ER export of the TGFα-like growth factor Gurken. *Dev. (Camb.)* 133, 459–470.

Bond, J.F., Farmer, S.R., 1983. Regulation of tubulin and actin mRNA production in rat brain: expression of a new beta-tubulin mRNA with development. *Mol. Cell. Biol.* 3, 1333–1342.

Castro, C.P., Piscopo, D., Nakagawa, T., Derynck, R., 2007. Cornichon regulates transport and secretion of TGFα-related proteins in metazoan cells. *J. Cell Sci.* 120, 2454–2466.

Coleman, S.K., Möykkynen, T., Cai, C., von Ossowski, L., Kuismanen, E., Korpi, E.R., Keinänen, K., 2006. Isoform-specific early trafficking of AMPA receptor flip and flop variants. *J. Neurosci. Off. J. Soc. Neurosci.* 26, 11220–11229.

Collingridge, G.L., Olsen, R.W., Peters, J., Spedding, M., 2009. A nomenclature for ligand-gated ion channels. *Neuropharmacology* 56, 2–5.

Coombs, I.D., Soto, D., Zonouzi, M., Renzi, M., Shelley, C., Farrant, M., Cull-Candy, S.G., 2012. Cornichons modify channel properties of recombinant and glial AMPA receptors. *J. Neurosci. Off. J. Soc. Neurosci.* 32, 9796–9804.

Díaz, E., 2010. Regulation of AMPA receptors by transmembrane accessory proteins. *Eur. J. Neurosci.* 32, 261–268.

Domazet-Lošo, T., Tautz, D., 2010. A phylogenetically based transcriptome age index mirrors ontogenetic divergence patterns. *Nature* 468, 815–818.

Gill, M.B., Kato, A.S., Roberts, M.F., Yu, H., Wang, H., Tomita, S., Brecht, D.S., 2011. Cornichon-2 modulates AMPA receptor-transmembrane AMPA receptor regulatory protein assembly to dictate gating and pharmacology. *J. Neurosci. Off. J. Soc. Neurosci.* 31, 6928–6938.

Greger, I.H., Khatri, L., Ziff, E.B., 2002. RNA editing at arg607 controls AMPA receptor exit from the endoplasmic reticulum. *Neuron* 34, 759–772.

Harmel, N., Cokic, B., Zolles, G., Berkefeld, H., Mauric, V., Fakler, B., Stein, V., Klöcker, N., 2012. AMPA receptors commandeering an ancient cargo exporter for use as an auxiliary subunit for signaling. *PLoS One* 7, e30681.

Hayase, Y., Higashiyama, S., Sasahara, M., Amano, S., Nakagawa, T., Taniguchi, N., Hazama, F., 1998. Expression of heparin-binding epidermal growth factor-like growth factor in rat brain. *Brain Res.* 784, 163–178.

Hollmann, M., Heinemann, S., 1994. Cloned glutamate receptors. *Annu. Rev. Neurosci.* 17, 31–108.

Hoshino, H., Uchida, T., Otsuki, T., Kawamoto, S., Okubo, K., Takeichi, M., Chisaka, O., 2007. Cornichon-like protein facilitates secretion of HB-EGF and regulates proper development of cranial nerves. *Mol. Biol. Cell* 18, 1143–1152.

Jackson, A.C., Nicoll, R.A., 2011. The expanding social network of ionotropic glutamate receptors: TARPs and other transmembrane auxiliary subunits. *Neuron* 70, 178–199.

Kalinka, A.T., Varga, K.M., Gerrard, D.T., Preibisch, S., Corcoran, D.L., Jarrells, J., Ohler, U., Bergman, C.M., Tomancak, P., 2010. Gene expression divergence recapitulates the developmental hourglass model. *Nature* 468, 811–814.

Kato, A.S., Gill, M.B., Ho, M.T., Yu, H., Tu, Y., Siuda, E.R., Wang, H., Qian, Y.-W., Nisenbaum, E.S., Tomita, S., Brecht, D.S., 2010. Hippocampal AMPA receptor gating controlled by both TARP and cornichon proteins. *Neuron* 68, 1082–1096.

Kornblum, H.L., Zurcher, S.D., Werb, Z., Derynck, R., Serogy, K.B., 1999. Multiple trophic actions of heparin-binding epidermal growth factor (HB-EGF) in the central nervous system. *Eur. J. Neurosci.* 11, 3236–3246.

Kratzer, I., Vasiljevic, A., Rey, C., Fevre-Montange, M., Saunders, N., Strazielle, N., Ghersi-Egea, J.F., 2012. Complexity and developmental changes in the expression pattern of claudins at the blood-CSF barrier. *Histochem. Cell Biol.* 138, 861–879.

Lomeli, H., Mosbacher, J., Melcher, T., Höger, T., Geiger, J.R., Kuner, T., Monyer, H., Higuchi, M., Bach, a., Seeburg, P.H., 1994. Control of kinetic properties of AMPA receptor channels by nuclear RNA editing. *Science (New York, N.Y.)* 266.

Martin, L.J., Furuta, a., Blackstone, C.D., 1998. AMPA receptor protein in developing rat brain: glutamate receptor-1 expression and localization change at regional, cellular, and subcellular levels with maturation. *Neuroscience* 83.

McAllister, K., 2007. Dynamic aspects of CNS synapse formation. *Annu. Rev. Neurosci.* 30, 425–450.

McKinney, R.A., 2010. Excitatory amino acid involvement in dendritic spine formation, maintenance and remodeling. *J. Physiol.* 588, 107–116.

Nagano, T., Namba, H., Abe, Y., Aoki, H., Takei, N., Nawa, H., 2007. In vivo administration of epidermal growth factor and its homologue attenuates developmental maturation of functional excitatory synapses in cortical GABAergic neurons. *Eur. J. Neurosci.* 25, 380–390.

Nakagawa, T., Sasahara, M., Hayase, Y., Haneda, M., Yasuda, H., Kikkawa, R., Higashiyama, S., Hazama, F., 1998. Neuronal and glial expression of heparin-binding EGF-like growth factor in central nervous system of prenatal and early-postnatal rat. *Brain Res. Dev. Brain Res.* 108, 263–272.

Namba, H., Nagano, T., Iwakura, Y., Xiong, H., Jourdi, H., Takei, N., Nawa, H., 2006. Transforming growth factor alpha attenuates the functional expression of AMPA receptors in cortical GABAergic neurons. *Mol. Cell. Neurosci.* 31, 628–641.

Namba, H., Zheng, Y., Abe, Y., Nawa, H., 2009. Epidermal growth factor administered in the periphery influences excitatory synaptic inputs onto midbrain dopaminergic neurons in postnatal mice. *Neuroscience* 158, 1731–1741.

Opanashuk, L. a, Mark, R.J., Porter, J., Damm, D., Mattson, M.P., Serogy, K.B., 1999. Heparin-binding epidermal growth factor-like growth factor in hippocampus: modulation of expression by seizures and anti-excitotoxic action. *J. Neurosci. Off. J. Soc. Neurosci.* 19.

Oyagi, A., Hara, H., 2012. Essential roles of heparin-binding epidermal growth factor-like growth factor in the brain. *CNS Neurosci. Ther.* 18, 803–810.

Pellegrini-Giampietro, D.E., Bennett, M.V., Zukin, R.S., 1991. Differential expression of three glutamate receptor genes in developing rat brain: an in situ hybridization study. *Proc. Natl. Acad. Sci. U. S. A.* 88, 4157–4161.

Powers, J., Barlowe, C., 1998. Transport of Axl2p depends on Erv14p, an ER-vesicle protein related to the *Drosophila* cornichon gene product. *J. Cell Biol.* 142, 1209–1222.

Powers, J., Barlowe, C., 2002. Erv14p directs a transmembrane secretory protein into COPII-coated transport vesicles. *Mol. Biol. Cell* 13, 880–891.

Roth, S., Neuman-Silberberg, F.S., Barcelo, G., Schüpbach, T., 1995. Cornichon and the EGF receptor signaling process are necessary for both anterior–posterior and dorsal–ventral pattern formation in *Drosophila*. *Cell* 81, 967–978.

Ryan, T.J., Grant, S.G.N., 2009. The origin and evolution of synapses. *Nat. Rev. Neurosci.* 10, 701–712.

- Sakarya, O., Armstrong, K.A., Adamska, M., Adamski, M., Wang, I.F., Tidor, B., Degnan, B.M., Oakley, T.H., Kosik, K.S., 2007. A post-synaptic scaffold at the origin of the animal kingdom. *PLoS One* 2, e506.
- Schwenk, J., Harmel, N., Zolles, G., Bildl, W., Kulik, A., Heimrich, B., Chisaka, O., Jonas, P., Schulte, U., Fakler, B., Klöcker, N., 2009. Functional proteomics identify cornichon proteins as auxiliary subunits of AMPA receptors. *Science* 323, 1313–1319.
- Schwenk, J., Harmel, N., Brechet, A., Zolles, G., Berkefeld, H., Müller, C.S., Bildl, W., Baehrens, D., Hüber, B., Kulik, A., Klöcker, N., Schulte, U., Fakler, B., 2012. High-resolution proteomics unravel architecture and molecular diversity of native AMPA receptor complexes. *Neuron* 74, 621–633.
- Shanks, N.F., Savas, J.N., Maruo, T., Cais, O., Hirao, A., Oe, S., Ghosh, A., Noda, Y., Greger, I.H., Yates, J.R., Nakagawa, T., 2012. Differences in AMPA and kainate receptor interactomes facilitate identification of AMPA receptor auxiliary subunit GSG1L. *Cell Rep.* 1, 590–598.
- Shi, Y., Suh, Y.H., Milstein, A.D., Isozaki, K., Schmid, S.M., Roche, K.W., Nicoll, R.A., 2010. Functional comparison of the effects of TARPs and cornichons on AMPA receptor trafficking and gating. *Proc. Natl. Acad. Sci. U. S. A.* 107.
- Sommer, B., Keinänen, K., Verdoorn, T. a, Wisden, W., Burnashev, N., Herb, a, Köhler, M., Takagi, T., Sakmann, B., Seeburg, P.H., 1990. Flip and flop: a cell-specific functional switch in glutamate-operated channels of the CNS. *Science (New York, N.Y.)* 249.
- Soto, D., Coombs, I.D., Kelly, L., Farrant, M., Cull-Candy, S.G., 2007. Stargazin attenuates intracellular polyamine block of calcium-permeable AMPA receptors. *Nat. Neurosci.* 10, 1260–1267.
- Srivastava, M., Simakov, O., Chapman, J., Fahey, B., Gauthier, M.E. a, Mitros, T., Richards, G.S., Conaco, C., Dacre, M., Hellsten, U., Larroux, C., Putnam, N.H., Stanke, M., Adamska, M., Darling, A., Degnan, S.M., Oakley, T.H., Plachetzki, D.C., Zhai, Y., Adamski, M., Calcino, A., Cummins, S.F., Goodstein, D.M., Harris, C., Jackson, D.J., Leys, S.P., Shu, S., Woodcroft, B.J., Vervoort, M., Kosik, K.S., Manning, G., Degnan, B.M., Rokhsar, D.S., 2010. The *Amphimedon queenslandica* genome and the evolution of animal complexity. *Nature* 466, 720–726.
- Tomita, S., Chen, L., Kawasaki, Y., Petralia, R.S., Wenthold, R.J., Nicoll, R. a, Bredt, D.S., 2003. Functional studies and distribution define a family of transmembrane AMPA receptor regulatory proteins. *J. Cell Biol.* 161.
- Tomita, S., Adesnik, H., Sekiguchi, M., Zhang, W., Wada, K., Howe, J.R., Nicoll, R. a, Bredt, D.S., 2005. Stargazin modulates AMPA receptor gating and trafficking by distinct domains. *Nature* 435.
- Verdoorn, T.A., Burnashev, N., Monyer, H., Seeburg, P.H., Sakmann, B., 1991. Structural determinants of ion flow through recombinant glutamate receptor channels. *Science* 252, 1715–1718.
- von Engelhardt, J., Mack, V., Sprengel, R., Kavenstock, N., Li, K.W., Stern-Bach, Y., Smit, A.B., Seeburg, P.H., Monyer, H., 2010. CKAMP44: a brain-specific protein attenuating short-term synaptic plasticity in the dentate gyrus. *Science* 327, 1518–1522.
- Yan, D., Tomita, S., 2012. Defined criteria for auxiliary subunits of glutamate receptors. *J. Physiol.* 590, 21–31.

3.2 “Depletion of the AMPAR reserve pool impairs synaptic plasticity in a model of hepatic encephalopathy”

Annett Schroeter¹, Shuping Wen¹, **Andrea Mölders**, Nadine Erlenhardt, Valentin Stein, Nikolaj Klöcker; (1 Authors contributed equally)

Molecular and Cellular Neuroscience, Volume 68, September 2015, Pages 331-339
DOI: 10.1016/j.mcn.2015.09.001

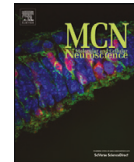
I contributed to the establishing and performing of the cell culture and the *in vitro* HE model. I designed, performed, and analyzed the mRNA expression experiments as well as prepared the figure of mRNA data. I contributed to data interpretation and preparation of figures and drafted text passages of the manuscript. Furthermore, I contributed to the writing and revision of the manuscript including further experiments for the revision.

This publication is reprinted and reused with permission from Elsevier Inc. © 2015



Contents lists available at ScienceDirect

Molecular and Cellular Neuroscience

journal homepage: www.elsevier.com/locate/ymcne

Depletion of the AMPAR reserve pool impairs synaptic plasticity in a model of hepatic encephalopathy

Annett Schroeter^{a,1}, Shuping Wen^{a,1}, Andrea Mölders^a, Nadine Erlenhardt^a,
Valentin Stein^b, Nikolaj Klöcker^{a,*}^a Institute of Neural and Sensory Physiology, Medical Faculty, University of Düsseldorf, Düsseldorf, Germany^b Institute of Physiology II, University of Bonn, Bonn, Germany

ARTICLE INFO

Article history:

Received 18 March 2015

Revised 22 July 2015

Accepted 6 September 2015

Available online 9 September 2015

Keywords:

Hepatic encephalopathy

Ammonia

Glutamatergic neurotransmission

AMPA receptor

NMDA receptor

LTP

LTD

Neuroglial co-culture

ABSTRACT

Hepatic encephalopathy (HE) is the most common neuropsychiatric complication of acute or chronic liver failure. Clinical symptoms include cognitive and intellectual dysfunction as well as impaired motor activity and coordination. There is general consensus that increased levels of ammonia play a central role in the pathogenesis of HE. However, it is still elusive how cognitive performance including the ability to learn and memorize information is affected by ammonia at molecular levels. In the present study, we have employed a neuroglial co-culture model, which preserves neuroglial interplay but allows for cell-type specific molecular and functional analyses, to investigate glutamatergic neurotransmission under conditions of high ammonia. Chronic exposure to ammonia significantly reduced neuronal mRNA and protein expression of AMPA-subtype glutamate receptors (AMPA), which mediate most fast excitatory neurotransmission in the brain. Surprisingly, neurons were able to fully maintain basal glutamatergic neurotransmission as recorded by AMPAR-mediated miniature excitatory postsynaptic currents (mEPSCs) even when >50% of total AMPARs were lost. However, long-lasting, activity-dependent changes in the efficacy of synaptic communication, which model the capability of the brain to learn and store information, were severely constrained. Whereas synaptic efficacy could still be depressed, an increase in synaptic strength was abolished. We conclude that neurons retain basal glutamatergic transmission at the expense of the extrasynaptic population of AMPARs, which is revealed when the extrasynaptic reserve pool is recruited in vain for synaptic potentiation. Our findings thus offer a molecular model, which might not only explain impaired synaptic plasticity in HE but also in other neurological diseases accompanied by a decrease in extrasynaptic AMPAR expression.

© 2015 Elsevier Inc. All rights reserved.

1. Introduction

Hepatic encephalopathy (HE) is the most common neuropsychiatric complication of liver failure. The pathophysiology of HE appears just as complex as its spectrum of clinical symptoms and signs (Aldridge et al., 2015; Butterworth, 2015; Häussinger and Schliess, 2008). Therefore, HE is no longer viewed as a single syndrome: different types of liver disease, i. e. acute versus chronic liver failure, result in different alterations of brain function that seem to be mediated by different mechanisms and might also require different treatment regimens (Felipo, 2013). There is general consensus, however, that hyperammonemia and inflammation play a central and synergistic role among other associated pathogenic factors (Albrecht et al., 2010; Coltart et al., 2013; Desjardins et al., 2012; Rose,

2012). Ammonia forms as a general waste product of protein metabolism. It accumulates when liver function deteriorates, readily crosses the blood–brain-barrier into brain tissue, where it rapidly exceeds the capacity of astrocytes to remove it by synthesizing glutamine, and finally becomes neurotoxic. Animal models of hyperammonemia reproduce many of the clinically observed symptoms including cognitive dysfunctions (Butterworth et al., 2009). Models of portocaval shunting and toxic liver cirrhosis, for instance, exhibited impairments in associative learning and spatial memory (Mendez et al., 2009; Mendez et al., 2011; Mendez et al., 2008; Wesierska et al., 2006), and dietary hyperammonemia constrained learning of avoidance and conditional discrimination behavior (Aguilar et al., 2000).

Long-lasting, activity-dependent changes in the efficacy of synaptic neurotransmission are the leading experimental models for the capability of the brain to learn and memorize information (Bliss and Collingridge, 1993). Multiple forms of synaptic plasticity exist in the brain, with the electrophysiological phenomena of associative long-term potentiation (LTP) and long-term depression (LTD) being

* Corresponding author at: Institute of Neural and Sensory Physiology, Medical Faculty, University of Düsseldorf, Universitätsstr. 1, D-40225 Düsseldorf, Germany.

E-mail address: nikolaj.kloecker@uni-duesseldorf.de (N. Klöcker).

¹ Authors contributed equally.

among the best studied (Lee and Kirkwood, 2011; Malenka and Bear, 2004). Irrespective of the great number of signal transduction pathways being activated in LTP and LTD, the strength of a glutamatergic synapse is eventually determined and varied by the number and the biophysical properties of AMPA-type glutamate receptors (AMPA) in the postsynaptic membrane (Kessels and Malinow, 2009; Malenka and Nicoll, 1999; Malinow and Malenka, 2002; Shepherd and Huganir, 2007). Native AMPARs are formed as complexes of the pore-lining GluA1–4 subunits and accessory proteins shaping the receptors' gating properties and subcellular trafficking (Jackson and Nicoll, 2011). Co-assembly with members of the transmembrane AMPAR regulatory protein (TARP) family enhances surface expression and synaptic targeting of the receptors by direct interaction with the postsynaptic scaffolding protein PSD-95 (Tomita et al., 2003). In addition, most TARPs augment charge transfer through AMPARs as they slow channel deactivation and desensitization, increase ligand affinity, and reduce current rectification (Kato et al., 2010; Milstein and Nicoll, 2008). Besides the TARPs, also the cornichon homologs, CNIH2 and CNIH3, promote cell surface expression of AMPARs and slow their deactivation and desensitization kinetics (Schwenk et al., 2009). Several other complex constituents of native AMPARs have recently been identified in sophisticated proteomic analyses (Schwenk et al., 2012); however, TARPs and CNIHs appear to be the predominant auxiliary subunits interacting with the majority of AMPARs in the mammalian brain. Whereas their significance in shaping the gating properties of native AMPARs is indisputable, a specific role and mode of action of both TARPs and CNIHs in synaptic plasticity is still uncertain (Herring et al., 2013; Rouach et al., 2005; Sumioka et al., 2011).

How do increased levels of ammonia as observed in clinical HE constrain synaptic plasticity? Numerous studies have investigated the modulation of signal transduction pathways activated in LTP or LTD irrespective of being necessary or sufficient for changes in synaptic efficacy (Wen et al., 2013). Yet, the final common pathway of plastic changes in glutamatergic neurotransmission, i.e. the regulation of the number and gating properties of AMPARs, which eventually determine synaptic strength, has rather been neglected. Here, we have employed a co-culture system of neurons and astroglial cells, which preserves part of their interplay during synaptic development and maturation but also allows for cell type-specific molecular and functional analysis, to investigate glutamatergic neurotransmission in conditions that model hyperammonemia in HE. We conclude from our data that chronically high concentrations of ammonia limit synaptic plasticity by compromising the number of extrasynaptic AMPARs, which are required as reserve for enhancing synaptic efficiency.

2. Materials and methods

2.1. Primary cell culture

Acutely dissociated hippocampal neurons were co-cultured with astroglial cells in a neuron–astrocyte co-culture system (Kaech and Banker, 2006). Hippocampi were dissected from E18 embryonic rat brains in dissociation buffer (HBSS supplemented with 1 mM HEPES, pH7.3), and further digested with 0.05% trypsin to isolate hippocampal neurons. Cells were gently triturated with glass Pasteur pipettes and plated in 6-well plates at a density of 4.25×10^5 cells/well or in 24-well plates at a density of 0.68×10^5 cells/well on poly-D-lysine coated coverslips and cultured in neuronal culture medium (Neurobasal medium supplemented with 2% B27@Serum-Free Supplement, 1% Na-pyruvate, 1% Fungizone and 1% penicillin/streptomycin). After incubation at 37 °C and 5% CO₂ for 2 h, coverslips with the attached neurons were transferred into 6-well plates growing astroglia feeder cells at the bottom in an upside down manner. After 24 h, cytosine arabinoside (1-β-D-arabinofuranosylcytosine) was added to these neuron–astrocyte co-cultures to a final

concentration of 5 μM to inhibit glial proliferation. At days 14–16 in vitro (DIV14–16), co-cultures were stressed with 1–5 mM NH₄Cl for 36 h before further experiments.

For preparation of astroglial feeder cells, neocortices of E18 rat embryos were dissociated by cutting them into small pieces, digesting them with 0.05% Trypsin and 1% DNase I (wt/vol) in HBSS buffer at 37 °C before gently triturating them with 10 ml pipettes. The cell suspensions were filtered through a cell strainer (70 μm) to remove undissociated tissue chunks and collected in glia medium (DMEM + Glutamax, supplemented with 10% horse serum, 1% Na-pyruvate, 1% Fungizone and 1% penicillin/streptomycin). Cells were pelleted by centrifugation at 120 g for 10 min, re-suspended in glia medium and plated in 75-cm² flasks. When cells were near confluence (normally after 2–3 weeks), the astroglia cells were harvested and seeded into 6-well plates as feeder layers. 72 h before the preparation of primary hippocampal neurons, the glia medium of the feeder cultures was changed to neuronal culture medium for preconditioning. All culture media and additives were from Life Technologies.

Cell viability was checked by assaying lactate dehydrogenase (LDH) release and by Hoechst 34580/propidium iodide (PI) double staining of neurons. For LDH release assays, the Cytotoxicity Detection Kit^{PLUS} (LDH) was used according to the manufacturer's manual (Roche Applied Science). For Hoechst 34580/propidium iodide (PI) double staining, neurons were incubated with Hoechst 34580 dye (1:1000; Sigma) and 50 μM PI (Sigma) for 20 min at 37 °C. Staining was quantified by wide-field fluorescence microscopy at 360/460 nm and 544/620 nm (excitation/emission) for Hoechst34580 and PI stain, respectively. Experiments were always performed in triplicates. Cell viability did not differ between experimental conditions.

2.2. Quantitative real-time PCR

Total RNA was isolated from primary hippocampal neurons stratified into the respective experimental groups (DIV16–18) using the RNeasy mini kit (Qiagen). For reverse transcription, 500 μg RNA was first spiked with 150 pg of *Escherichia coli* AraB RNA (Applied Microarray, Tempe USA) as external standard and reverse-transcribed with the QuantiTect Reverse Transcription kit (Qiagen) including a genomic DNA elimination step. All kits were used according to manufacturer's instructions. The external bacterial RNA spike was used for improved normalization of gene expression, because several conventional house-keeping genes were regulated under our experimental conditions (Bond and Farmer, 1983; Kratzer et al., 2012).

Quantitative real time PCR was performed in an Applied Biosystems StepOne real time PCR System using SYBR green PCR Mastermix (Applied Biosystems). Assays were run in a total volume of 10 μl of 250 ng cDNA and 100 nM forward and reverse primers in 1× SYBR green PCR Master mix. The reactions were performed in MicroAmp optical 96-well reaction plates. Real time PCR parameters were as follows: 10 min at 95 °C, 40 cycles of 15 s at 95 °C, 55 s at 55 °C, and 60 s at 60 °C each. Reactions were subjected to a heat dissociation protocol after the final PCR cycle. Each PCR product showed a single peak in the denaturation curve and a single band on a 2% agarose gel at the expected amplicon size. All reactions were carried out in triplicates. Standard curves for real-time PCR protocols with all primer pairs obtained with sequential dilutions up to 1:128 of one cDNA sample were found optimal with linear regression coefficients >0.95. The relative expression levels of the GluA and auxiliary subunit mRNAs were normalized to the geometric mean of the bacterial AraB RNA amounts and neuronal hprt1 mRNA expression and analyzed using the Relative Expression Software Tool (REST©, Version 2009; (Pfaffl et al., 2002)).

The following primers were used (sequence in 5'–3' direction):

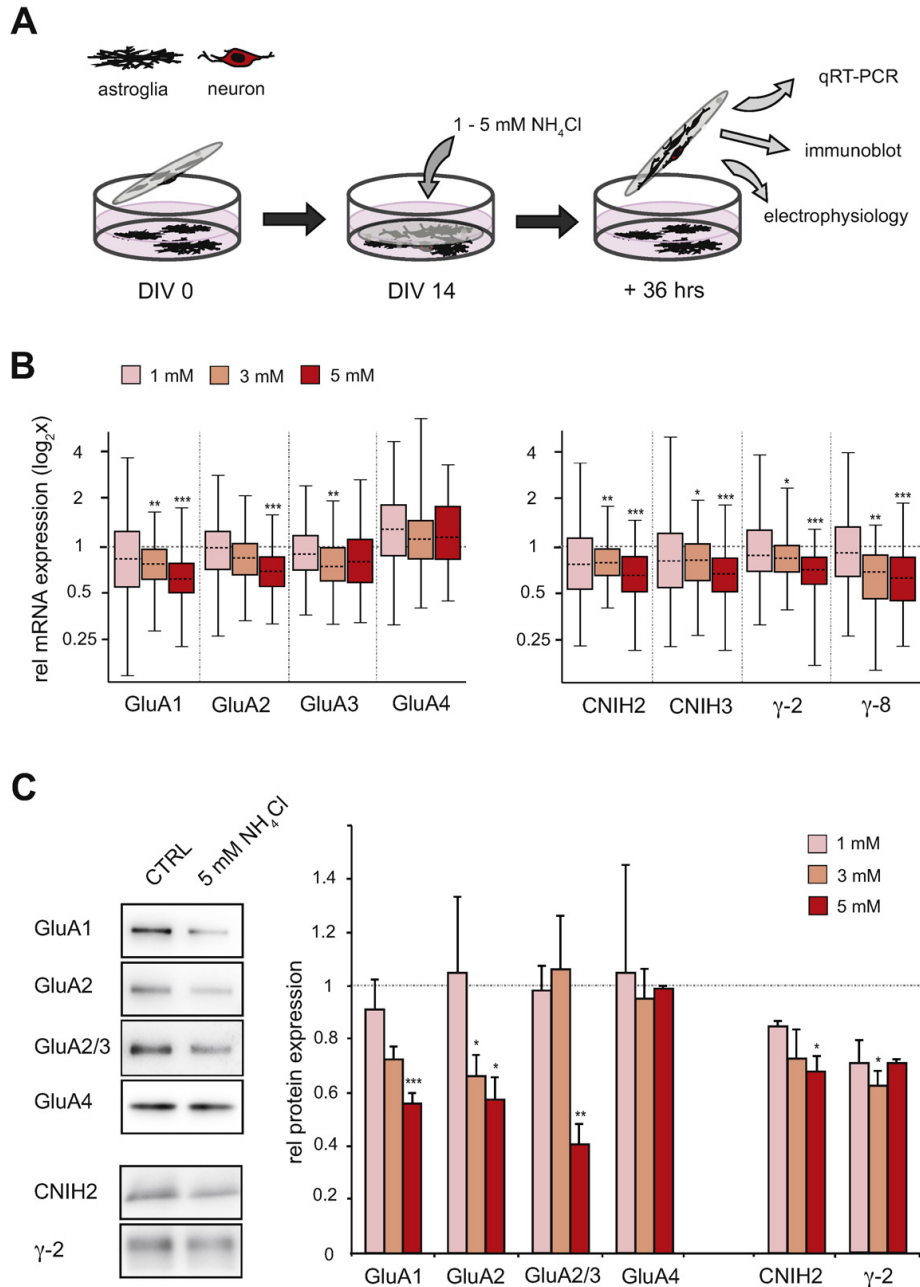


Fig. 1. Neuronal AMPAR expression is decreased in a model of HE. (A) Schematic representation of the neuroglial co-culture system and working sequence. Dissociated embryonic hippocampal neurons were co-cultured with astroglial feeder cells on distinct support plates. After 14 days in vitro (DIV14), cells were incubated with NH_4Cl for another 36 h before analysis. (B) Quantification of mRNA expression of indicated AMPAR constituents in neurons after incubation with indicated concentrations of NH_4Cl . Whisker plot of mRNA expression ratios ($\text{NH}_4\text{Cl}/\text{control}$) compiled with REST© software (see Materials and methods section). Asterisks indicate statistically significant differences from control ($n = 6$ experiments): * $p < 0.05$; ** $p < 0.01$; *** $p < 0.001$. (C) Quantification of protein expression by immunoblot densitometry of indicated AMPAR constituents in neurons after incubation with indicated concentrations of NH_4Cl . Representative Western blots for AMPAR expression in control neurons and after incubation with 5 mM NH_4Cl and a bar graph of mean expression ratios ($\text{NH}_4\text{Cl}/\text{control}$) \pm SEM for n (GluA1) = 7–10, n (GluA2) = 4–5, n (GluA2/3) = 3–5, n (GluA4) = 3–5, n (CNIH2) = 4–9, n (γ -2) = 3–4 independent experiments. Asterisks indicate statistically significant differences from control (* $p < 0.05$; ** $p < 0.01$; *** $p < 0.001$).

	Primer sequence	Amplicon size	Efficiency
AraB	F: ATCCCCTGATCGGTAAGCA R: ACGCCTGAAAGGGTGATTA	126	1.93
Hprt1	F: TACTGGCCACATCAACAGGACTCT R: TCGAAGTGTGGATACAGGCCAGA	200	1.86
Gria1	F: GACCATAACCTTGGTCCGGG R: CTGGTTGTCTGGTCTCGTCC	258	2.00
Gria2	F: GAGGACTACCGCAGAAGGAGTAGC R: TCGTACCACCATTTGTTTTTCA	251	1.88
Gria3	F: GCCAGGCGCTTTTCATCC R: TGGCCCAAGAAAGTATCTT	272	2.00
Gria4	F: TCTTGGCAATGACACAGCAG R: TGCGTCCCTTGCTCCATATT	220	1.99
Cnih2	F: TGGCACAATAGCCCTTGA R: GGACGGTGAAGTACCTCC	150	1.97
Cnih3	F: GAGGAACATCGAACCATCT R: GCATTATGACAACTGGTG	214	2.00
Cacng2	F: GGCTGACACCCGAGAGTATT R: ACTTAGACTCGCAGACACGA	175	1.99
Cacng8	F: GCTGCTGGAAGGGTTGAA R: TTTGTAGACCCGAGAGCCAG	188	1.89

3. SDS-PAGE and immunoblotting

Crude membrane fractions were prepared from primary hippocampal neurons stratified into the respective experimental groups (DIV16–18). Cells were lysed by sonication in 20 mM Tris-HCl pH 7.5, 1 mM iodoacetamide, 1 mM EDTA, 150 mM NaCl supplemented with fresh proteinase inhibitors (aprotinin, leupeptin and pepstatin A, at 100 µg/ml each) and centrifuged at 1000 g for 5 min at 4 °C. The supernatant was ultra-centrifuged at 125,000 g for 30 min at 4 °C. Pellets containing the crude membrane fraction were re-suspended in 1 × Laemmli buffer and incubated for 10 min at 37 °C. Protein samples were resolved by 12% SDS-PAGE, electro-blotted on PVDF membrane (Millipore), and detected by immunoblot analysis. The following antibodies were used: rabbit anti-GluA1 (1:1000, AB1504, Millipore), mouse anti-GluA2 (1:1000, MAB397, Millipore), rabbit anti-GluA2/3 (1:1000, 07–598, Millipore), rabbit anti-GluA4 (1:1000, AB1508, Millipore), rabbit anti-stargazin (1:1000, 07–577, Millipore) and custom-made guinea pig anti-CNIH2 (1:1000, peptide epitope: DELRTDFKNPIDQGNPARARERLKNIERIC), goat anti-rabbit, anti-mouse, or anti-guinea pig secondary antibodies conjugated to horseradish peroxidase (1:15,000, Santa Cruz). Blots were developed with ECL plus reagent (GE Healthcare). Densitometric analysis was performed using ImageJ software. Data are given as mean expression level ± standard error of the mean (SEM) in arbitrary units normalized to untreated control. For assessing statistically significant differences between experimental groups, the non-parametric Kruskal Wallis and Dunn's posthoc analysis were performed.

3.1. Electrophysiological recordings

Miniature excitatory postsynaptic currents (mEPSCs) were recorded from dissociated hippocampal neurons (DIV16–18) at room temperature clamping cells at –60 mV using an EPC-10 amplifier (HEKA). Signals were low-pass filtered at 2.9 kHz and sampled at 20 kHz. mEPSC data were analyzed offline using a custom-written software. Glass electrodes of 3–5 MΩ were filled with (in mM): 90 KCl, 40 KOH, 20 HEPES, 10 EGTA, 0.25 CaCl₂ (pH = 7.3). Extracellular solution contained (in mM): 130 NaCl, 20 HEPES, 5 KCl, 1 MgCl₂, 2.5 CaCl₂, 0.001 TTX, 0.01 gabazine, 0.001 strychnine (pH = 7.3). NMDAR-dependent chemical long-term potentiation (cLTP) and chemical long-term depression (cLTD) were induced by established protocols (Lee et al., 1998; Lu et al., 2001). Briefly, cLTP was elicited by incubation of neurons in 200 µM glycine in Mg²⁺-free extracellular solution for 5 min. Recordings were performed 30 min after induction. cLTD was induced by incubation of neurons in 20 µM NMDA in Mg²⁺-free extracellular solution for 3 min. Recordings were performed 20 min after induction.

Recordings from somatic outside-out patches were performed with glass electrodes of 2–3 MΩ at a holding potential of –70 mV. AMPAR currents were evoked by local application of 10 mM glutamate for 8 s in the presence of 250 µM trichlormethiazide (TCM) to block receptor desensitization.

Electrophysiological data were analyzed with Origin 9 software. All population data is given as mean ± standard error of the mean (SEM) with n = number of neurons and N = number of independent culture preparations. Experiments in control and test groups were always performed in parallel to minimize systematic errors related to culture preparations. The non-parametric Kolmogorow–Smirnow test was used to examine statistical significance of the differences between two samples. For comparing more than two samples, the non-parametric Kruskal–Wallis test and Dunn's posthoc test were applied.

4. Results

4.1. The expression of neuronal AMPARs is decreased in a model of hepatic encephalopathy

We cultured dissociated hippocampal neurons prepared from embryonic rats (E18) on astrocytic feeder cells following established protocols (Kaech and Banker, 2006). This co-culture model offers the advantage of yielding a homogenous population of pyramidal neurons, which grow well-characterized synaptic connections with each other in a glial cell-derived microenvironment within 2–3 weeks (Fig. 1A). Molecular and functional analysis of the cultured cell types, however, can then be performed separately, as neurons and glial cells are cultured on opposed support plates.

At DIV14, cultures were incubated with ammonium chloride (NH₄Cl) at concentrations of 1, 3, and 5 mM for 36 h to model CNS concentrations of ammonia known to occur in animal models of HE (Butterworth et al., 2009; Felipo and Butterworth, 2002; Swain et al., 1992) before neurons were submitted to a molecular analysis of AMPAR expression by qPCR and immunoblotting. Cell viability checked by assaying LDH release and Hoechst 34580/propidium iodide double staining was not affected by the treatment (data not shown). As depicted in Fig. 1B, incubation with NH₄Cl reduced neuronal mRNA expression of the main pore-lining AMPAR subunits GluA1 and GluA2 in a dose-dependent manner. In cultures treated with 5 mM NH₄Cl, neuronal GluA1 mRNA decreased to 62% (p < 0.001; n = 6) and GluA2 mRNA decreased to 69% of control (p < 0.001; n = 6). By contrast, GluA3 and GluA4 mRNA expression did not change after incubation with up to 5 mM NH₄Cl. In parallel with the ion channel pore-forming GluA subunits, also mRNA expression of selected auxiliary subunits known to be important determinants of AMPAR trafficking and gating, i. e. the two cornichon homologs, CNIH2 and CNIH3, and two TARPs, γ-2 and γ-8, decreased with rising concentrations of NH₄Cl to levels between 62 and 66% of control (p < 0.001; n = 6) at 5 mM NH₄Cl. We also tested whether the observed changes in mRNA expression would translate into significant decreases in protein expression after 36 h of NH₄Cl incubation. Fig. 1C shows that protein expression indeed reflected the decrease in mRNA expression of both the pore-forming and the auxiliary AMPAR subunits. At a maximum concentration of 5 mM NH₄Cl, GluA1 and GluA2 protein expression was diminished to 56 ± 4% (p < 0.001; n = 10) and 58 ± 8% of control (p < 0.001; n = 4), respectively. GluA4 protein expression remained unaffected. The protein expression of the two auxiliary subunits, which could be detected unequivocally by available antibodies, CNIH2 and TARP γ-2, were decreased to 68 ± 6% (p < 0.001; n = 9) and to 71 ± 2% of control (p < 0.05; n = 3), respectively.

Thus, incubation of a neuro-glial co-culture system with NH₄Cl to model pivotal aspects of HE leads to a dose-dependent decrease in the expression of neuronal AMPARs.

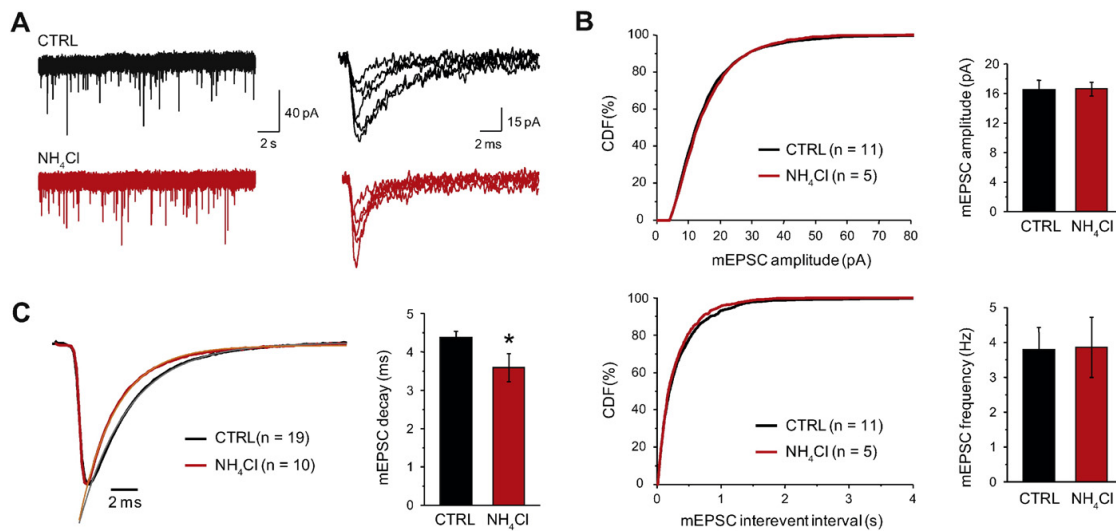


Fig. 2. AMPAR-mediated synaptic neurotransmission is retained in the model of HE. (A) Sample recordings of AMPAR-mediated mEPSCs from non-treated (CTRL) and NH₄Cl-treated hippocampal neurons (NH₄Cl, 5 mM). Five individual mEPSCs from each experimental group are superimposed to appreciate their time courses (right). (B) Amplitudes and frequencies of AMPAR-mediated mEPSCs are plotted cumulatively (cumulative distribution function, CDF) and as mean \pm SEM (bar graphs) for non-treated control and NH₄Cl-treated neurons. Note that there is no difference between the two experimental groups. (C) mEPSCs from control (n = 19) and NH₄Cl-treated (n = 10) neurons were averaged and scaled. Note the small but significant decrease in the mEPSC decay time constant in NH₄Cl-treated neurons. Asterisk marks a statistically significant difference from control (* $p < 0.05$).

4.2. Basal glutamatergic synaptic transmission is retained

Given the observed reduction in neuronal AMPAR expression after incubation with NH₄Cl, we sought to investigate the functional consequences. Unexpectedly, spontaneous glutamatergic synaptic transmission was maintained between neurons despite incubation with up to 5 mM NH₄Cl for 36 h. As shown in Fig. 2, both amplitude and frequency of AMPAR mediated mEPSCs did not change and yielded 16.5 ± 1.3 pA and 3.8 ± 0.6 Hz in untreated control (n = 11, N = 4) and 16.6 ± 0.9 pA and 3.9 ± 0.9 Hz in treated neurons (n = 5, N = 4), respectively. There was, however, a moderate reduction in the average mEPSC decay time constant from 4.4 ± 0.2 ms in control neurons to 3.6 ± 0.4 ms in neurons incubated with 5 mM NH₄Cl for 36 h (Fig. 2C). In contrast to synaptic AMPAR currents, extrasynaptic AMPAR currents recorded in somatic outside-out patches did indeed decrease in a dose-dependent manner (Fig. 3). A saturating glutamate concentration of 10 mM charged with 250 μ M TCM to block receptor desensitization elicited steady-state currents of 153 ± 33 pA (n = 6, N = 3) at a holding potential of -70 mV, which decreased to 101 ± 22 pA (n.s.; n = 9, N = 3) and 62 ± 12 pA ($p < 0.05$; n = 6, N = 3) in somatic patches from hippocampal neurons incubated with 3 mM and 5 mM NH₄Cl, respectively.

Thus, the reduction in total AMPAR expression in high ammonia conditions leads to a distinct reduction of functional extrasynaptic AMPARs, whereas the number of functional synaptic AMPARs was retained.

4.3. Selective impairment of synaptic plasticity

Next, we challenged dissociated hippocampal neurons by eliciting synaptic plasticity with and without prior incubation with NH₄Cl. To this end, established protocols for inducing NMDAR-dependent chemical long-term potentiation (cLTP) and chemical long-term depression (cLTD) were used (Lee et al., 1998; Lu et al., 2001). As depicted in Fig. 4A, short incubation of neurons with 200 μ M glycine in Mg²⁺-free extracellular solution for 5 min to briefly activate NMDARs significantly increased AMPAR-mediated mEPSCs in amplitude from 17.9 ± 1 pA

(n = 10, N = 3) to 24 ± 1.1 pA ($p < 0.001$; n = 14, N = 3), but left their frequency rather unchanged (3.2 ± 0.6 Hz and 3.7 ± 0.7 Hz in untreated and glycine-treated neurons, respectively). Prior incubation of neurons with NH₄Cl for 36 h, however, prevented the increase in mEPSC amplitude after glycine-mediated NMDAR activation (Fig. 4B). AMPAR mEPSC amplitudes were 18.4 ± 2.3 pA (n = 6, N = 3) and 16.9 ± 1.3 pA (n = 10, N = 3) for untreated and glycine-treated neurons after prior incubation with 5 mM NH₄Cl, respectively. mEPSC frequencies were again unchanged (4.2 ± 1.3 Hz and 4.1 ± 0.9 Hz for untreated and glycine-treated neurons, respectively). Finally, we tested whether also NMDAR-dependent induction of cLTD was compromised in neurons pre-treated with NH₄Cl (Fig. 5). A brief pulse of 20 μ M NMDA for 3 min in Mg²⁺-free extracellular solution known to induce robust cLTD reduced mEPSC amplitudes from 18.9 ± 2.4 pA to 10.2 ± 0.7 pA in control (n = 7, N = 2) and NMDA stimulated neurons ($p < 0.001$; n = 6, N = 2), respectively. The frequencies of mEPSCs remained within the same range (3.8 ± 0.7 Hz and 3.7 ± 0.7 Hz before and after NMDA stimulation, respectively).

Thus, NMDAR-dependent synaptic plasticity was selectively targeted: pretreatment with 5 mM NH₄Cl abolished cLTP while leaving cLTD unaffected.

5. Discussion

In the present study, we have used a co-culture system of neurons and astroglial feeder cells to model the effects of hyperammonemia as in HE, a common neuropsychiatric complication of acute and chronic liver disease, on the brain. Our data show that chronic stress of ammonia reduces the neuronal expression of AMPAR complexes, the main mediators of fast excitatory neurotransmission in the brain. Intriguingly, neurons are able to preserve basal glutamatergic transmission even when about half of the total AMPAR population is lost. However, synaptic plasticity is severely constrained under high ammonia conditions: Whereas synaptic efficacy can still be downregulated, an increase in synaptic strength is no longer possible. We conclude that neurons retain basal synaptic transmission at the expense of extrasynaptic

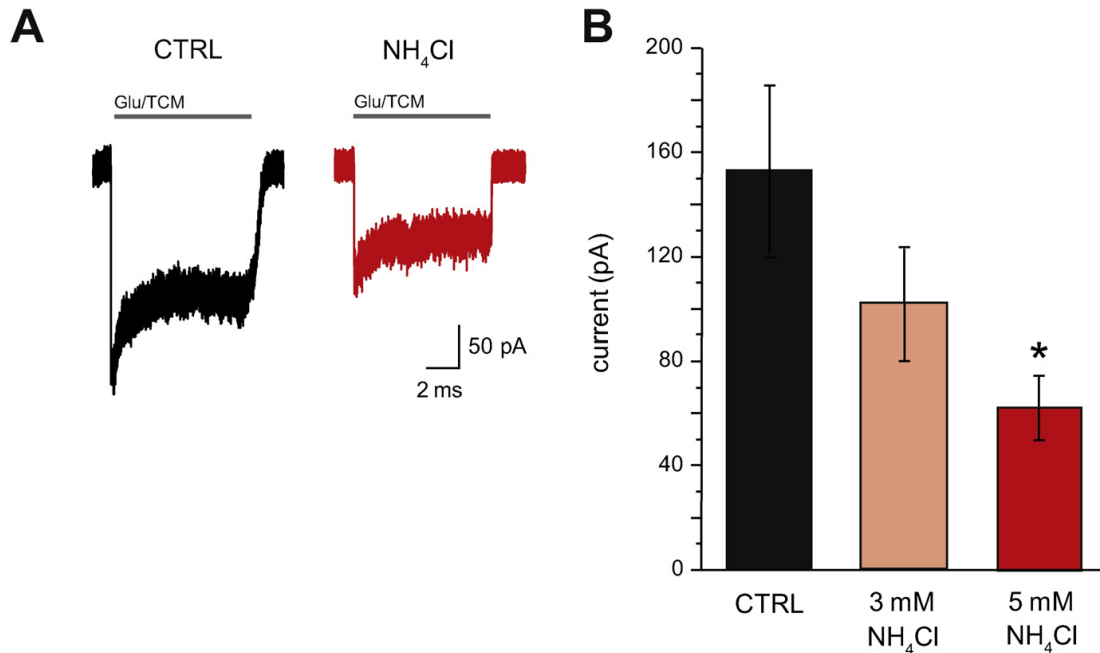


Fig. 3. High ammonia reduces the pool of extrasynaptic AMPARs. (A) Representative recordings of AMPAR currents from somatic outside-out patches from non-treated (CTRL) and NH_4Cl -treated hippocampal neurons (NH_4Cl , 5 mM) elicited by 10 mM glutamate and 250 μM TCM to block receptor desensitization. (B) Steady-state AMPAR current amplitudes in non-treated control neurons ($n = 6$, CTRL) and in neurons treated with 3 mM ($n = 9$) and 5 mM NH_4Cl ($n = 6$) are given as mean \pm SEM. Note the dose-dependent decrease in extrasynaptic AMPAR current amplitudes with increasing concentrations of NH_4Cl . Asterisk marks a statistically significant difference from control (* $p < 0.05$).

AMPARs, which is uncovered when the reserve pool is recruited in vain to potentiate synaptic strength.

In the brain, ammonia is predominantly detoxified in astrocytes by glutamine synthesis. In good agreement, astrocytes have been reported to protect neurons against ammonia toxicity (Rao et al., 2005). With increasing ammonia concentrations, glutamine will accumulate resulting in cell swelling and eventually in cytotoxic edema (Häussinger and Görg, 2010). However, it is still under debate whether glial edema is the central cause for HE symptoms, particularly in chronic HE; in contrast, there is evidence that direct alteration of neurotransmission is critically involved in the pathogenesis of cognitive and motor impairments (Felipo, 2013). For our study, we have therefore chosen a co-culture model of hippocampal neurons and astroglial cells in order to maintain neuro-glia interplay to a certain extent (Kaech and Banker, 2006). Cells were grown in sandwich orientation on different support plates holding the advantage over organotypic slice culture or in vivo models that both electrophysiological and comprehensive molecular analyses can be performed in a cell-type specific manner. Our results show that neurons stressed with relevant concentrations of ammonia in co-culture with astroglia showed a dose-dependent decrease in the expression of AMPAR mRNAs and proteins. Both the main pore-lining subunits, GluA1 and GluA2, and the most abundant auxiliary subunits of the TARP and CNIH protein families in hippocampus were affected (Monyer et al., 1991; Schwenk et al., 2012). With respect to molecular mechanisms being involved in AMPAR downregulation, we can only speculate at this point. Ammonia is a rather broadly acting pathogen. It is known that ammonia increases oxidative and nitrosative stress (Görg et al., 2013). Reactive oxygen species may oxidize RNA as has been demonstrated in astrocytes and even more pronounced in neurons in an animal model of HE (Görg et al., 2008). Oxidation of RNA could result in accelerated degradation and impair translation into protein. Also,

direct effects of ammonia on gene transcription should not be excluded (Norenberg et al., 2009), which might explain the decrease in AMPAR expression.

Most intriguingly, however, there was no change in basal glutamatergic neurotransmission despite a loss of about half of the neuronal AMPAR population. Highest levels of ammonia did neither affect the amplitude nor the frequency of AMPAR mediated mEPSCs. As revealed by our recordings from somatic outside-out patches, the severe loss of neuronal AMPARs induced by high ammonia translated into their selective reduction within the extrasynaptic plasma membrane domain. Thus, neurons suffering a loss of half of their AMPARs due to a rather unspecific disease stimulus maintained synaptic transmission at the expense of extrasynaptic receptors. Current models of postsynaptic receptor localization assume lateral surface traffic between synaptic and extrasynaptic membranes as an important link between internal recycling and receptor trapping at the postsynaptic density (PSD) via interaction with scaffold proteins (Choquet and Triller, 2013; Opazo et al., 2012). Applied to our data, we expect receptor diffusion rates into or out of the synapse to change significantly in response to the dramatic loss of AMPARs in order to maintain basal neurotransmission. Given a loss of 60% AMPARs, their synaptic dwell time should increase by 2.5-fold to ensure stable mEPSC amplitudes (Czöndör et al., 2012), which reflect postsynaptic receptor numbers. How could synaptic dwell time of AMPARs increase? Most likely, receptor trapping at the PSD may be enhanced. Auxiliary TARP proteins are thought to link GluA subunits to the scaffold protein PSD-95, a process that can be bi-directionally regulated by posttranslational modification of the TARP C-terminal tail (Sumioka et al., 2010; Tomita et al., 2005). Whereas phosphorylation of a cluster of serine residues in TARPs mobilizes its C-terminus for interaction with PSD-95 by interfering with an otherwise inhibiting TARP-membrane phospholipid interaction (Sumioka et al., 2010),

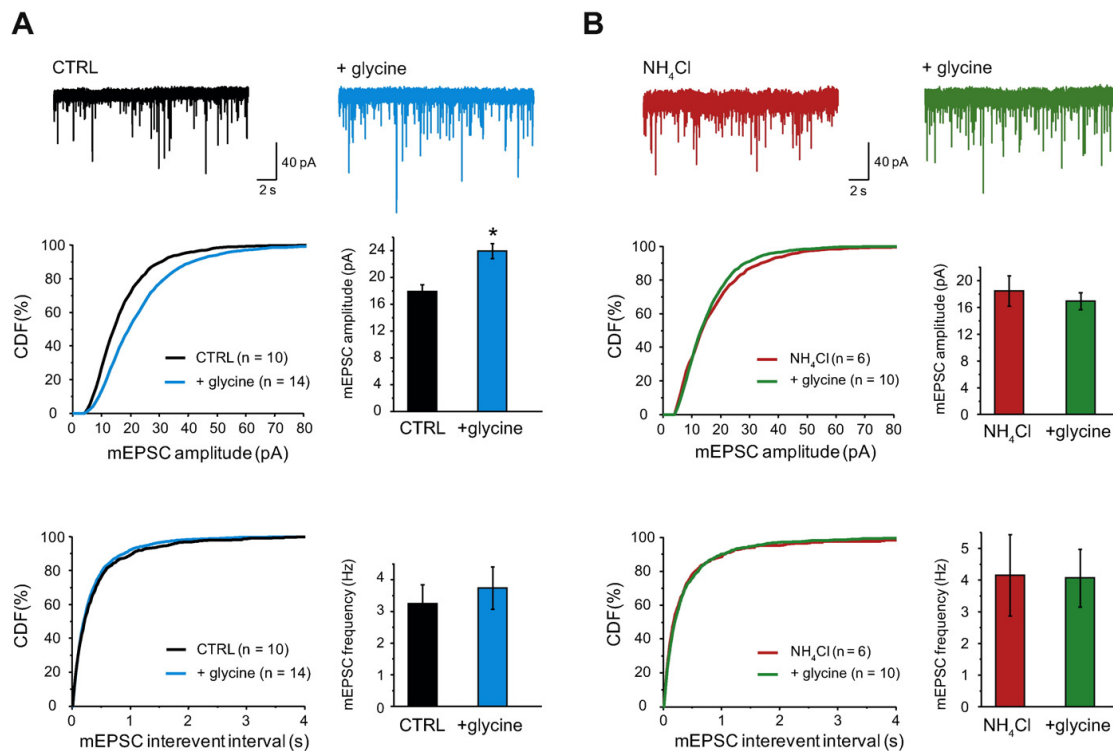


Fig. 4. Synaptic potentiation is abolished in the model of HE. (A) Induction of chemical long-term potentiation (cLTP) in dissociated hippocampal neurons by a brief pulse of 200 μ M glycine for 5 min in Mg^{2+} -free extracellular solution. Sample recordings of AMPAR-mediated mEPSCs from non-treated control neurons before (CTRL) and 30 min after induction of cLTP (+ glycine). Amplitudes and frequencies of mEPSCs are plotted cumulatively (cumulative distribution function, CDF) and as mean \pm SEM (bar graphs) for non-treated control (CTRL) and glycine-treated neurons (+ glycine). Note the significant increase in AMPAR-mediated mEPSC amplitude. Asterisk marks a statistically significant difference from control (* $p < 0.05$). (B) Prior treatment of neurons with 5 mM NH_4Cl prevented the induction of cLTP. Shown are again sample recordings, cumulative plots of mEPSC amplitudes and frequencies, and bar graphs of their means \pm SEM. Note that AMPAR-mediated mEPSCs are indistinguishable in both experimental groups after prior incubation with NH_4Cl .

phosphorylation of their very C-terminal PDZ-ligand motif has been reported to disrupt PSD-95 binding (Chetkovich et al., 2002; Stein and Chetkovich, 2010). Indeed, significant changes in the brain phosphoproteome have been described in animal models of HE (Brunelli et al., 2012). Changes in the molecular composition of AMPARs towards a higher TARP/GluA ratio, which could also improve receptor trapping at the PSD by increasing multi-valence of TARP-PSD-95 interactions (Sainlos et al., 2011), are rather unlikely, as we found the predominant hippocampal TARPs γ -8 and γ -2 to be reduced to similar extent as the main pore-lining GluA subunits. Moreover, mEPSC kinetics were accelerated after ammonia treatment exhibiting shorter decay time constants, which argues against an increase in the TARP/GluA ratio that would be expected to slow receptor gating (Milstein and Nicoll, 2008). The faster mEPSC decay times in ammonia treated neurons might be due to a different stoichiometry of GluA subunits with a bias for the fast gating GluA3 and GluA4 subunits; in contrast to GluA1 and GluA2, GluA3 and GluA4 expression remained grossly unaffected in our model. Finally, we cannot exclude ammonia-induced morphological changes in synapse geometry also known to be a determinant of synaptic strength and hence maybe at least supportive in maintaining mEPSC amplitudes (Freche et al., 2011).

Despite the ability of neurons to maintain basal neurotransmission under high ammonia conditions, synaptic plasticity was severely impaired. Whereas a brief activation of NMDARs by their co-agonist glycine elicited an increase in mEPSC amplitude in control neurons, this form of cLTP was completely abolished by prior ammonia treatment. Similar to AMPAR expression, also NMDAR expression might

have been significantly affected in ammonia treated neurons explaining the lack of plasticity. However, application of the selective agonist NMDA readily induced cLTD in ammonia treated neurons indicating functional NMDAR expression. Such selective impairment of plasticity with synaptic potentiation being abolished and depression being preserved is highly reminiscent of the electrophysiological GluA1 knock out phenotype (Granger and Nicoll, 2014; Granger et al., 2013; Selcher et al., 2012; Zamanillo et al., 1999). The common characteristic of the genetic deletion of GluA1 and our disease model is the severe reduction in the size of the extrasynaptic population of AMPARs, whereas the size of the synaptic population quantified by AMPAR mediated EPSC amplitudes remains stable. In line with the previous interpretations of GluA1 deletion (Granger and Nicoll, 2014; Granger et al., 2013), we therefore conclude from our data that ammonia treatment constrains synaptic plasticity by reducing the number of extrasynaptic AMPARs. Our study represents the first pathophysiological setting strongly supporting the hypothesis that a sufficiently large reserve pool of extrasynaptic receptors is a prerequisite for LTP induction.

In summary, our study shows that chronically high concentrations of ammonia as can arise in clinical HE reduce neuronal expression of AMPARs, which mediate most of the fast excitatory neurotransmission in the brain. Neurons are, however, capable of maintaining basal glutamatergic transmission by keeping the numbers of synaptic AMPARs constant at the expense of the extrasynaptic reserve pool of receptors. When it comes to synaptic plasticity requiring surpassing amounts of AMPARs, the diminished extrasynaptic pool fails to fulfill synaptic needs and potentiation fails. We hypothesize that our findings might

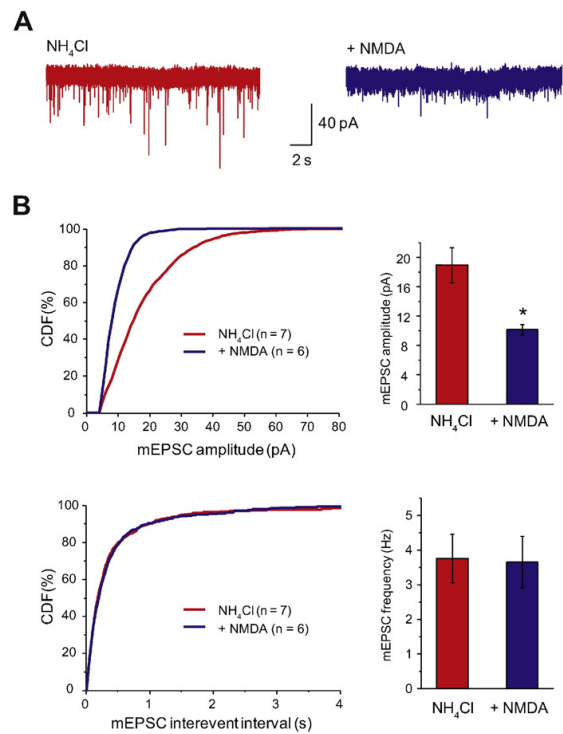


Fig. 5. Synaptic depression is preserved in the model of HE. Induction of chemical long-term depression (cLTD) in dissociated hippocampal neurons by a brief pulse of 20 μ M N-methyl-D-aspartate (NMDA) for 3 min in Mg^{2+} -free extracellular solution. (A) Sample recordings of AMPAR-mediated mEPSCs from NH_4Cl -treated hippocampal neurons (NH_4Cl , 5 mM) before and 20 min after induction of cLTD (+ NMDA). (B) Amplitudes and frequencies of mEPSCs are plotted cumulatively (cumulative distribution function, CDF) and as mean \pm SEM (bar graphs). Note the significant decrease in mEPSC amplitude after NMDA stimulation. Asterisk marks a statistically significant difference from control (* $p < 0.05$).

model impaired synaptic plasticity not only in hyperammonemia but also in other disease states including neurodegenerative disorders, which show decreases in extrasynaptic AMPAR expression.

Acknowledgments

The authors thank Claudia Wittrock for her excellent technical assistance. The work was supported by grants of the Deutsche Forschungsgemeinschaft (SFB974 TP B05) and of the Anton-Betz-Stiftung to N.K. A.M. is an associate member of the iBrain graduate school at the University of Düsseldorf.

References

- Aguilar, M.A., et al., 2000. Chronic moderate hyperammonemia impairs active and passive avoidance behavior and conditional discrimination learning in rats. *Exp. Neurol.* 161, 704–713.
- Albrecht, J., et al., 2010. Glutamine as a mediator of ammonia neurotoxicity: a critical appraisal. *Biochem. Pharmacol.* 80, 1303–1308.
- Aldridge, D.R., et al., 2015. Pathogenesis of hepatic encephalopathy: role of ammonia and systemic inflammation. *J. Clin. Exp. Hepatol.* 5, S7–S20.
- Bliss, T.V.P., Collingridge, G.L., 1993. A synaptic model of memory: long-term potentiation in the hippocampus. *Nature* 361, 31–39.
- Bond, J.F., Farmer, S.R., 1983. Regulation of tubulin and actin mRNA production in rat brain: expression of a new, β -tubulin mRNA with development. *Mol. Cell. Biol.* 3, 1333–1342.

- Brunelli, L., et al., 2012. Exploratory investigation on nitro- and phospho-proteome cerebellum changes in hyperammonemia and hepatic encephalopathy rat models. *Metab. Brain Dis.* 27, 37–49.
- Butterworth, R.F., 2015. Pathogenesis of hepatic encephalopathy and brain edema in acute liver failure. *J. Clin. Exp. Hepatol.* 5, S96–S103.
- Butterworth, R.F., et al., 2009. Experimental models of hepatic encephalopathy: ISHEN guidelines. *Liver Int.* 29, 783–788.
- Chetkovich, D.M., et al., 2002. Phosphorylation of the postsynaptic density-95 (PSD-95)/discs large/zona occludens-1 binding site of stargazin regulates binding to PSD-95 and synaptic targeting of AMPA receptors. *J. Neurosci.* 22, 5791–5796.
- Choquet, D., Triller, A., 2013. The dynamic synapse. *Neuron* 80, 691–703.
- Coltart, I., et al., 2013. Inflammation and hepatic encephalopathy. *Arch. Biochem. Biophys.* 536, 189–196.
- Czöndör, K., et al., 2012. Unified quantitative model of AMPA receptor trafficking at synapses. *Proc. Natl. Acad. Sci. U. S. A.* 109, 3522–3527.
- Desjardins, P., et al., 2012. Pathogenesis of hepatic encephalopathy and brain edema in acute liver failure: role of glutamine redefined. *Neurochem. Int.* 60, 690–696.
- Felipo, V., 2013. Hepatic encephalopathy: effects of liver failure on brain function. *Nat. Rev. Neurosci.* 14, 851–858.
- Felipo, V., Butterworth, R.F., 2002. Neurobiology of ammonia. *Prog. Neurobiol.* 67, 259–279.
- Freche, D., et al., 2011. Synapse geometry and receptor dynamics modulate synaptic strength. *PLoS One* 6, e25122.
- Görg, B., et al., 2008. Ammonia induces RNA oxidation in cultured astrocytes and brain in vivo. *Hepatology* 48, 567–579.
- Görg, B., et al., 2013. Osmotic and oxidative/nitrosative stress in ammonia toxicity and hepatic encephalopathy. *Arch. Biochem. Biophys.* 536, 158–163.
- Granger, A.J., Nicoll, R.A., 2014. LTD expression is independent of glutamate receptor subtype. *Front. Synaptic Neurosci.* 6, 15.
- Granger, A.J., et al., 2013. LTP requires a reserve pool of glutamate receptors independent of subunit type. *Nature* 493, 495–500.
- Häussinger, D., Görg, B., 2010. Interaction of oxidative stress, astrocyte swelling and cerebral ammonia toxicity. *Curr. Opin. Clin. Nutr. Metab. Care* 13, 87–92.
- Häussinger, D., Schliess, F., 2008. Pathogenetic mechanisms of hepatic encephalopathy. *Gut* 57, 1156–1165.
- Herring, B.E., et al., 2013. Cornichon proteins determine the subunit composition of synaptic AMPA receptors. *Neuron* 77, 1083–1096.
- Jackson, A.C., Nicoll, R.A., 2011. The expanding social network of ionotropic glutamate receptors: TARPs and other transmembrane auxiliary subunits. *Neuron* 70, 178–199.
- Kaech, S., Banker, G., 2006. Culturing hippocampal neurons. *Nat. Protoc.* 1, 2406–2415.
- Kato, A.S., et al., 2010. TARPs differentially decorate AMPA receptors to specify neuropharmacology. *Trends Neurosci.* 33, 241–248.
- Kessels, H.W., Malinow, R., 2009. Synaptic AMPA receptor plasticity and behavior. *Neuron* 61, 340–350.
- Kratzer, I., et al., 2012. Complexity and developmental changes in the expression pattern of claudins at the blood-CSF barrier. *Histochem. Cell Biol.* 138, 861–879.
- Lee, H.K., Kirkwood, A., 2011. AMPA receptor regulation during synaptic plasticity in hippocampus and neocortex. *Semin. Cell Dev. Biol.* 22, 514–520.
- Lee, H., et al., 1998. NMDA induces long-term synaptic depression and dephosphorylation of the GluR1 subunit of AMPA receptors in hippocampus. *Neuron* 21, 1151–1162.
- Lu, W., et al., 2001. Activation of synaptic NMDA receptors induces membrane insertion of new AMPA receptors and LTP in cultured hippocampal neurons. *Neuron* 29, 243–254.
- Malenka, R.C., Bear, M.F., 2004. LTP and LTD: an embarrassment of riches. *Neuron* 44, 5–21.
- Malenka, R.C., Nicoll, R.A., 1999. Long-term potentiation—a decade of progress? *Science* 285, 1870–1874.
- Malinow, R., Malenka, R.C., 2002. AMPA receptor trafficking and synaptic plasticity. *Annu. Rev. Neurosci.* 25, 103–126.
- Mendez, M., et al., 2008. Spatial memory alterations in three models of hepatic encephalopathy. *Behav. Brain Res.* 188, 32–40.
- Mendez, M., et al., 2009. Associative learning deficit in two experimental models of hepatic encephalopathy. *Behav. Brain Res.* 198, 346–351.
- Mendez, M., et al., 2011. Portosystemic hepatic encephalopathy model shows reversal learning impairment and dysfunction of neural activity in the prefrontal cortex and regions involved in motivated behavior. *J. Clin. Neurosci.* 18, 690–694.
- Milstein, A.D., Nicoll, R.A., 2008. Regulation of AMPA receptor gating and pharmacology by TARP auxiliary subunits. *Trends Pharmacol. Sci.* 29, 333–339.
- Monyer, H., et al., 1991. Glutamate operated channels: developmentally early and mature forms arise by alternative splicing. *Neuron* 6, 799–810.
- Norenberg, M.D., et al., 2009. Signaling factors in the mechanism of ammonia neurotoxicity. *Metab. Brain Dis.* 24, 103–117.
- Opazo, P., et al., 2012. Regulation of AMPA receptor surface diffusion by PSD-95 slots. *Curr. Opin. Neurobiol.* 22, 453–460.
- Pfaffl, M.W., et al., 2002. Relative expression software tool (REST[®]) for group-wise comparison and statistical analysis of relative expression results in real-time PCR. *Nucleic Acids Res.* 30, e36.
- Rao, K.V., et al., 2005. Astrocytes protect neurons from ammonia toxicity. *Neurochem. Res.* 30, 1311–1318.
- Rose, C.F., 2012. Ammonia-lowering strategies for the treatment of hepatic encephalopathy. *Clin. Pharmacol. Ther.* 92, 321–331.
- Rouach, N., et al., 2005. TARP gamma-8 controls hippocampal AMPA receptor number, distribution and synaptic plasticity. *Nat. Neurosci.* 8, 1525–1533.
- Sainlos, M., et al., 2011. Biomimetic divalent ligands for the acute disruption of synaptic AMPAR stabilization. *Nat. Chem. Biol.* 7, 81–91.

- Schwenk, J., et al., 2009. Functional proteomics identify cornichon proteins as auxiliary subunits of AMPA receptors. *Science* 1313–1319.
- Schwenk, J., et al., 2012. High-resolution proteomics unravel architecture and molecular diversity of native AMPA receptor complexes. *Neuron* 74, 621–633.
- Selcher, J.C., et al., 2012. Glutamate receptor subunit GluA1 is necessary for long-term potentiation and synapse unsilencing, but not long-term depression in mouse hippocampus. *Brain Res.* 1435, 8–14.
- Shepherd, J.D., Huganir, R.L., 2007. The cell biology of synaptic plasticity: AMPA receptor trafficking. *Annu. Rev. Cell Dev. Biol.* 23, 613–643.
- Stein, E.L., Chetkovich, D.M., 2010. Regulation of stargazin synaptic trafficking by C-terminal PDZ ligand phosphorylation in bidirectional synaptic plasticity. *J. Neurochem.* 113, 42–53.
- Sumioka, A., et al., 2010. TARP phosphorylation regulates synaptic AMPA receptors through lipid bilayers. *Neuron* 66, 755–767.
- Sumioka, A., et al., 2011. PDZ binding of TARPGamma-8 controls synaptic transmission but not synaptic plasticity. *Nat. Neurosci.* 14, 1410–1412.
- Swain, M., et al., 1992. Ammonia and related amino acids in the pathogenesis of brain edema in acute ischemic liver failure in rats. *Hepatology* 15, 449–453.
- Tomita, S., et al., 2003. Functional studies and distribution define a family of transmembrane AMPA receptor regulatory proteins. *J. Cell Biol.* 161, 805–816.
- Tomita, S., et al., 2005. Bidirectional synaptic plasticity regulated by phosphorylation of stargazin-like TARPs. *Neuron* 45, 269–277.
- Wen, S., et al., 2013. Synaptic plasticity in hepatic encephalopathy – a molecular perspective. *Arch. Biochem. Biophys.* 536, 183–188.
- Wesierska, M., et al., 2006. Cognitive flexibility but not cognitive coordination is affected in rats with toxic liver failure. *Behav. Brain Res.* 171, 70–77.
- Zamanillo, D., et al., 1999. Importance of AMPA receptors for hippocampal synaptic plasticity but not for spatial learning. *Science* 284, 1805–1811.

3.3 “Heterogeneity of the Astrocytic AMPA-Receptor Transcriptome”

Andrea Mölders, Angela Koch, Raphael Menke, Nikolaj Klöcker

Glia, [Epub ahead of print] 28 October 2018

DOI: 10.1002/glia.23514

I established the workflow of isolating astrocytes from mouse tissue by employing the transgenic hGFAP-GFP mouse line. I developed, designed, performed, and analyzed all experiments except for the ones in *Xenopus laevis* oocytes. I designed and analyzed the *Xenopus laevis* oocyte experiments as well as the preparation of the corresponding figure (Fig. 6) together with Angela Koch. I drafted the first version of the manuscript and prepared the figures 1 - 5. I revised the manuscript and figures together with Nikolaj Klöcker and Angela Koch.

This publication is reprinted and reused with permission from John Wiley and Sons, © 2018

RESEARCH ARTICLE

Heterogeneity of the astrocytic AMPA-receptor transcriptome

Andrea Mölders | Angela Koch | Raphael Menke | Nikolaj Klöcker Institute of Neural and Sensory Physiology,
Medical Faculty, University of Düsseldorf,
Düsseldorf, Germany

Correspondence

Nikolaj Klöcker, Institute of Neural and
Sensory Physiology, Heinrich-Heine
Universität Düsseldorf, Universitätsstr. 1,
D-40225 Düsseldorf, Germany.
Email: nikolaj.kloecker@uni-duesseldorf.de

Funding information

Deutsche Forschungsgemeinschaft (DFG),
Grant/Award Number: KL 1168/7-1

Abstract

Astrocytes form the largest class of glial cells in the central nervous system. They serve plenty of diverse functions that range from supporting the formation and proper operation of synapses to controlling the blood–brain barrier. For many of them, the expression of ionotropic glutamate receptors of the AMPA subtype (AMPA receptors) in astrocytes is of key importance. AMPARs form as macromolecular protein complexes, whose composition of the pore-lining GluA subunits and of an extensive set of core and peripheral complex constituents defines both their trafficking and gating behavior. Although astrocytic AMPARs have been reported to exhibit heterogeneous properties, their molecular composition is largely unknown. In this study, we sought to quantify the astrocytic AMPAR transcriptome during brain development and with respect to selected brain regions. Whereas the early postnatal pattern of AMPAR mRNA expression showed minor variation over time, it did show significant heterogeneity in different brain regions. Cerebellar astrocytes express a combination of AMPAR complex constituents that is remarkably distinct from the one in neocortical or hippocampal astrocytes. Our study provides a workflow and a first reference for future investigations into the molecular and functional diversity of glial AMPARs.

KEYWORDS

AMPA, astrocytes, fluorescence activated cell sorting, heterogeneous composition, ionotropic glutamate receptors, quantitative real-time PCR

1 | INTRODUCTION

Astrocytes represent the largest class of glial cells in the mammalian central nervous system (CNS) and are distributed throughout the whole brain. They are crucial for CNS development including synaptogenesis, they control ion homeostasis and neurotransmitter uptake, and they are important regulators of the blood–brain barrier (Allaman, Bélanger, & Magistretti, 2011; Allen, 2014; Haim & Rowitch, 2016). Astrocytes have traditionally been viewed as a rather uniform subpopulation of glial cells. However, growing experimental evidence demonstrates that astrocytes are highly diverse, with respect to not only their morphology but also their physiology (Matyash & Kettenmann, 2010; Zhang & Barres, 2010). Recent whole transcriptome and proteome analyses provide an exciting insight into the developmental and regional heterogeneity of astrocytes (Chai et al., 2017; Zhang et al., 2014).

Astrocytes may express neurotransmitter receptors, among them ionotropic glutamate receptors of the α -amino-3-hydroxy-5-methyl-

4-isoxazolepropionic acid subtype (AMPA receptors), which enable them to sense and respond to neuronal signaling. Electrophysiological studies indicate substantial heterogeneity of astrocytic AMPAR properties between brain regions. Thus, cerebellar Bergmann glia cells express inwardly rectifying and calcium-permeable AMPARs, which have been demonstrated to be crucial for the formation and maintenance of synapses between climbing fibers and Purkinje cells. Their genetic deletion leads to impaired motor performance and changes in eyeblink conditioning (Saab et al., 2012). Also, in both neocortex and brainstem, astrocytes show pharmacologically identifiable AMPAR currents and/or AMPAR calcium responses, respectively (Lalo, Pankratov, Kirchhoff, North, & Verkhratsky, 2006; McDougal, Hermann, & Rogers, 2011). In addition to neuron–glia interaction, they might be involved in glia–vascular signaling and control vasodilation (Parfenova et al., 2012). Whereas in thalamic nuclei, a subpopulation of astrocytes do express functional AMPARs, hippocampal astrocytes have been reported to be devoid of them, underlining a concept of significant astrocytic heterogeneity even beyond brain regions but within

neuronal circuits (Chai et al., 2017; Israel, Schipke, Ohlemeyer, Theodosis, & Kettenmann, 2003; Matthias et al., 2003). Native AMPARs exist as macromolecular protein complexes. Their core is formed by tetrameric assembly of the pore-lining subunits GluA1–4 (Hollmann & Heinemann, 1994; Seeburg, 1993; Sobolevsky, Rosconi, & Gouaux, 2009) and members of the family of transmembrane AMPAR regulatory proteins (TARPs; Milstein, Zhou, Karimzadegan, Bredt, & Nicoll, 2007; Tomita et al., 2003), the cornichon homologs (CNIHs) 2 or 3 (Schwenk et al., 2009), and the germ cell-specific gene 1 like (GSG1L) protein (Schwenk et al., 2012; Shanks et al., 2012). Peripheral constituents of native AMPARs comprise the cysteine-knot AMPAR modulating proteins (CKAMPs) 44 and 52 (von Engelhardt et al., 2010), the soluble noelins (olfactomedins) 1–3, the proline-rich transmembrane proteins (PRRTs) 1 and 2 and Leucine-rich repeat transmembrane protein 4 (LRRTM4), and four isoforms of the membrane-associated guanylate kinase (MAGUK) family (Schwenk et al., 2012). Porcupine (PORCN) and ferric-chelate reductase 1-like protein (FRRS1L) seem to be rather transient complex constituents serving a role in subcellular processing of AMPARs along the secretory pathway (Brecht et al., 2017; Erlenhardt et al., 2016). The great number of complex constituents identified in previous comprehensive proteomic analyses strongly suggests an equally great molecular diversity of AMPARs in their regional, cellular, or even subcellular composition. Regional heterogeneity and developmental dynamics have recently been addressed in a high-resolution proteomic study of native AMPARs from brain (Schwenk et al., 2014). Due to methodological constraints, however, diverse cell types were sampled. Thus, the molecular composition of glial cell-specific AMPARs is still elusive.

Here, we sought to quantify the astrocytic AMPAR transcriptome during early postnatal brain development and with respect to selected brain regions. Our data will provide a first reference for future investigations into the molecular and functional diversity of glial AMPARs.

2 | MATERIALS AND METHODS

2.1 | Animals

For all experiments, hGFAP-GFP transgenic mice (FVB/N-Tg (GFAPGFP)14Mes/J, Jackson Lab) were used, in which the expression of GFP is controlled by the human GFAP (hGFAP) promoter. As a negative control for FACS experiments, FVB/N mice (Janvier Labs) were used. All experiments were in compliance with German law and were approved by the local authorities of the University of Düsseldorf.

2.2 | Fluorescence activated cell sorting (FACS)

Mice were anesthetized, decapitated, and the brains were rapidly removed. For tissue dissociation, the Neural Tissue Dissociation Kit (Miltenyi Biotec) was used according to the manufacturer's instructions. Dissociated cells were harvested by centrifugation and cells of 3–4 littermates were pooled for FACS. The cells were resuspended in Hank's BSS (HBSS) supplemented with 10 mM HEPES pH 7.4 and 5% fetal bovine serum (FBS Superior, Biochrome/Merck) to warrant

sufficient cell survival. Cells were then strained using a 40 μ m cell strainer directly before FACS to prevent clotting. FACS was performed on a BD FACS Arial (BD Biosciences) using a 70 μ m nozzle. Dead cells and debris were first gated out by forward and side scatter, and second by high propidium iodide (PI) staining. The fluorescence threshold for the GFP-positive (GFP+) cells was set using a non-fluorescent cell suspension derived from FVB/N mice. As control, GFP-negative (GFP-) cells were also collected using a second lower threshold, which was determined considering a Gaussian distribution of fluorescence populations (Figure 1a). After sorting, cells were centrifuged for 10 min at 300g and 4°C and stored at –80°C. For the preparation of crude membrane fractions (MF), pelleted cells were pooled from different FACS experiments, for all other experiments one cell pellet of each population was used.

2.3 | Quantitative real-time PCR (qPCR) and cluster analysis

For qPCR analysis of AMPAR constituent expression, sorted cells were split into different experimental groups. In one set of experiments, we compared AMPAR expression in cells sorted from whole brains of 7–9 days (p7–p9, week [w] 1) and 13–16 days old mice (p13–p16, week [w] 2). In another set of experiments, AMPAR expression was studied in three different brain regions, that are cerebellum, neocortex, and hippocampus of 13–16 days (week [w] 2) old mice. Total RNA was isolated from sorted GFP+ and GFP- cells using the RNeasy Micro kit (Qiagen). For every reverse transcription, the total RNA was first spiked with 150 pg of *E. coli* AraB RNA (Applied Microarray, Tempe) as an external standard. The RNA mixture was reverse-transcribed with the QuantiTect Reverse Transcription kit (Qiagen) including a genomic DNA elimination step. All kits were used according to the manufacturer's instructions. The external bacterial RNA spike was used for normalization of gene expression because several conventional house-keeping genes are differentially regulated under our experimental conditions as described before (Mauric et al., 2013; Schroeter et al., 2015). Quantitative real-time PCR was performed in an Applied Biosystems StepOne real time PCR System using SYBR green PCR Mastermix (Applied Biosystems/Thermo Fisher Scientific). Assays were run in triplicates with a total volume of 10 μ l containing 200 ng cDNA and forward and reverse primers at 100 nM each in 1 \times SYBR green PCR Master mix and MicroAmp optical 96-well reaction plates (Applied Biosystems/Thermo Fisher Scientific). Real-time PCR parameters were: 10 min at 95°C, 40 cycles of 15 s at 95°C, 30 s at 55°C, and 60 s at 60°C each. Melting-curve analysis was performed to verify the amplification of a single product with a specific melting temperature, and the specificity of all PCR amplifications was verified by sequencing. Standard curves with sequential dilutions up to 1:128 were used to determine the primer efficiency. Primer efficiency with linear regression coefficients >0.98 was found optimal. The relative expression levels were normalized to the C_t value of the bacterial AraB RNA spike (% of AraB), and for the calculation, the corresponding primer efficiencies were taken into account. For controlling the enrichment of astrocytes in the GFP+ cells, the relative expression ratios between GFP+ cells and GFP- cells (Fold Change, log scale) were calculated using the $\Delta\Delta C_t$ method considering the efficiencies.

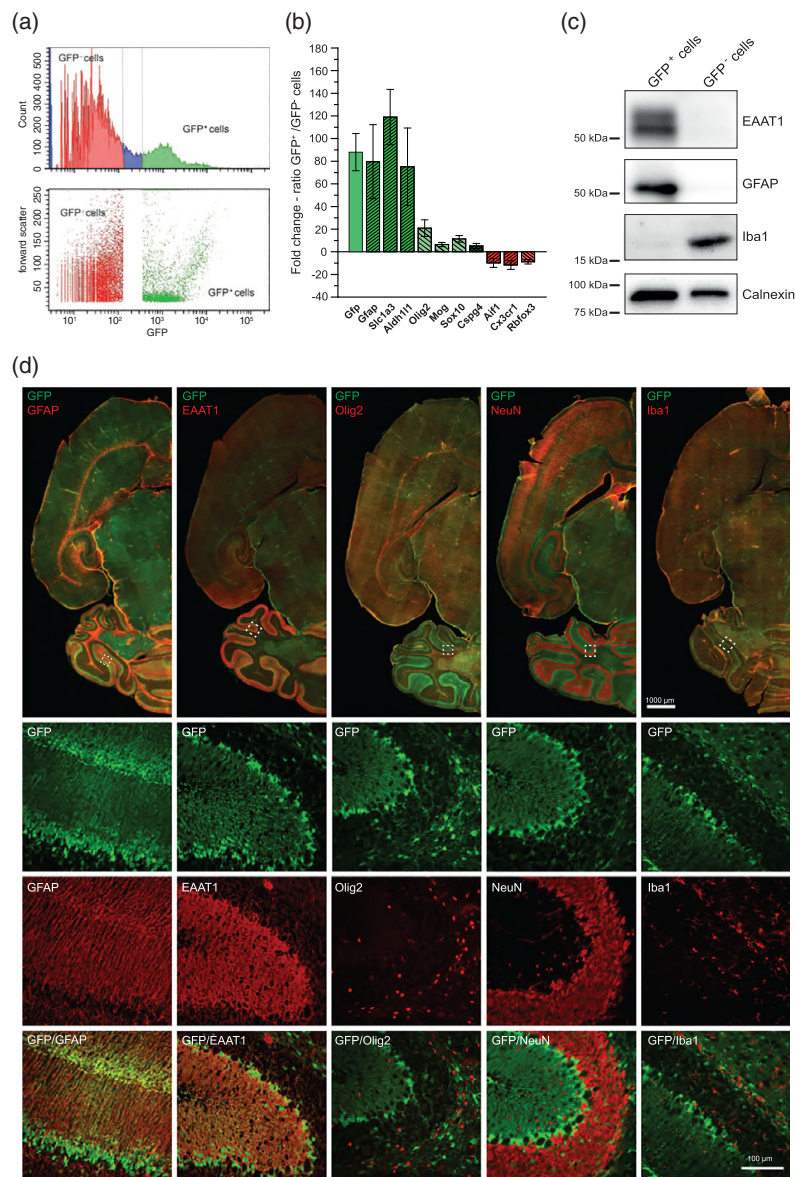


FIGURE 1 Isolation of astrocytes. (a) FACS histogram and plot depicting the distribution of dissociated GFP+ and GFP- cells prepared from hGFAP-GFP mouse brain tissue. Wild-type littermates were used for negative control, and the intermediate fraction was discarded. (b) Quantification of mRNA expression of indicated cell type markers in GFP+ and GFP- cells by qPCR (whole brain, postnatal week 2 (w2)). Expression levels were normalized to an external spike of AraB RNA. Data are given as fold change-ratios of relative expression levels in GFP+ and GFP- cells \pm SEM ($n = 3$). (c) Immunoblotting of whole-cell lysates from GFP+ and GFP- cells as indicated (whole brain, p12). Calnexin served as loading control. Both qPCR (b) and western blot analysis (c) show the enrichment of astrocytic markers in GFP+ cells and microglia markers in GFP- cells. (d) Immunohistochemical staining of horizontal hGFAP-GFP mouse brain slices (p15) for indicated marker proteins confirms the astrocytic origin of GFP+ cells. AxioScan images of horizontal sections (upper panels) with white boxes (broken lines), which indicate the region of confocal images in lower panels (zoom-in). Scale bars: upper panels, 1,000 μ m; lower panels, 100 μ m

Table 1 shows the primer pairs that were used (sequence in 5'-3' direction). Data are given as mean \pm standard error of the mean (SEM) unless otherwise stated. Statistical differences between expression values were assessed by two-way ANOVA with a Bonferroni's multiple comparisons test or Tukey's multiple comparisons test using GraphPad Software (GraphPad Software). Cluster analysis and

dendrogram calculation of normalized gene expression data was performed according to complete-linkage hierarchical clustering and using the Euclidean distance, as implemented in the heatmap.2 function of the gplots R package (version 3.3.1). Heatmap colors are based upon normalization across rows (row z-score), and scales represent standard deviations above or below mean.

TABLE 1 Primers used in qPCRs

Gene/protein	Primer sequence	Amplicon size (bp)	Efficiency
AraB/Ribulokinase (<i>E. coli</i>)	F: ATCCCCTGATCGGTAAAGCA R: ACGCCTGAAAGGGGTGATTA	126	1.93
Gria1/GluA1	F: GACCATAACCTTGGTCCGGG R: CTGGTTGTCTGGTCTCGTCC	258	2.00
Gria2/GluA2	F: GAGGACTACCCGAGAAGGAGTAGC R: TCGTACCACCATTGTTTTTCA	251	1.88
Gria3/GluA3	F: GCCAGGCGTCTTTTCATTCC R: TGCGCCAGAAAGTGATCTT	272	2.00
Gria4/GluA4	F: TCTTGGCAATGACACAGCAG R: TCGTCCCTTGCTCCATATT	220	1.99
Cnih2/CNIH2	F: TGGCACATCATAGCCTTTGA R: GGACGGTGAAGTACCTCC	150	1.97
Cnih3/CHNIH3	F: GAGGAACATCGAACGCATCT R: GGCATTATGACAACCTGGTG	214	2.00
Cacng2/TARP γ -2	F: GGCTGACACCGCAGAGTATT R: ACTTAGACCTGCAGACACGA	175	1.99
Cacng3/TARP γ -3	F: CCGCAGTAGGCACAGTGTTA R: AGGACCAGCCGTAGGAGTAG	152	1.93
Cacng4/TARP γ -4	F: TTTATTGTGGCGGAGACCGT R: CCTGTAACCTCGGCATCCTGG	138	1.86
Cacng5/TARP γ -5	F: GTGATGCCCATGAACTCCCA R: AAAGCCAGTATGGTCCGGTG	164	2.00
Cacng7/TARP γ -7	F: ACTACTCGGGCCAGTTTCTG R: AGGTGGTCCGGTACTTGAT	127	1.90
Cacng8/TARP γ -8	F: GCTGCCTGGAAGGGTTGAA R: TTTGTAGACGCGAGAGGCAG	188	1.89
Gsg11/GSG11	F: CATTACCTGCTGCATGGCGG R: GGAAGTATTTGATGGCCTCAGGA	147	1.97
Shisa9/CKAMP44	F: CACCAAGGACAAGACCAACC R: AGGTCTCTCCATGTGGTCA	192	1.95
Shisa6/CKAMP52	F: GCAGACTCCAGGTGATCGTC R: GTTCTGGTAAGAGCGCGAGA	145	2.00
Prrt1/PRRT1	F: ACACGACTACATGCCATCG R: CGATCTCGGCAGACACCAAA	131	1.91
Prrt2/PRRT2	F: GGTAGCCTAAGCCGTCATCC R: CCACAATGTTGACAGGCAC	139	1.86
Olfm1/Noelin-1	F: GGCCATGATCACAACTGGA R: CTGTACACCTGCCAGTCTC	147	1.92
Olfm2/Noelin-2	F: ATCTCCAGTATGTTCCGAGC R: GCTCTGCATCCTGCTCTTC	120	2.00
Olfm3/Noelin-3	F: CAAAACCGACGCAAGCTCA R: TTCATGCAGTCACGAAGCCT	156	2.00
Nrn1/Neuritin	F: CGGGTGCAAATAGCTTACC R: TGTTCTGCTTGTCTCCAGG	143	2.00
Frrs11/FRRS11	F: TACCTGTTTGCTTGGGTCC R: GAAGGTCAGGGCGACAATGA	180	1.92
Vwc2/Brorin	F: CCGATCTGCAAAAACGGTCC R: CGTTCAATTCTCCACGTGCC	128	1.92
Vwc2l/Brorin-2-like	F: AAGTTGCGCCTTTGCTTCAC R: CACAGTGTGCTACGGCAG	187	1.87
Lrrtm4/LRRTM4	F: AAACCGGATGCGATCCCG R: CGCTCCCTGCGATGATTTG	118	1.95
Porcn/PORCN	F: TCCTTCCACAGCTACCTACA R: CTCAGACAGAAAGCCACAA	300	1.87
Abhd6/ABHD6	F: GGATTCTCCGCACACAAGGA R: CTTGCCCACTATGGACAGG	139	2.00
Abhd12/ABHD12	F: GCGCTGGCAGACGAAA R: TCAGTTTGGCCTGTATCCAG	156	2.00
Gfp/GFP	F: GCGGATCTTGAAGTTCACCTTGATGCC R: GCACGACTTCTCAAGTCCGCCATGCC	280	1.65

(Continues)

TABLE 1 (Continued)

Gene/protein	Primer sequence	Amplicon size (bp)	Efficiency
Gfap/GFAP	F: ACCAGCTTACGGCCAACAGTG R: TGTCTATACGCAGCCAGGTTGTC	138	1.84
Slc1a3/EAAT1	F: AACAACTGTCCAGAGGCCAT R: ACGAAACCGAAGCACATGGA	125	1.87
Aldh1l1/ALDH1L1	F: GCCCAATGTCCCAGAGGTAG R: GGATGAAGTCCCCGAAGGTG	161	1.90
Olig2/OLIG2	F: ATCTTCCTCCAGCACCTCTCT R: GTTCGGGCTGTTGATCTTC	122	1.95
Mog/Mog	F: TCCCATCCGGCTTTAGTTG R: GGTGCTTGTCTGCATCTTG	159	1.96
Sox10/Sox10	F: TACAAGTACCAACCTCGGCG R: GACATGGGGGAGCCTTCTTC	161	1.90
Cspg4/NG2	F: ACCCAGGCTGAGGTAAATGC R: ACAGGCAGCATCGAAAGACA	162	1.98
Aif1/lba1	F: GCTTTTGGACTGCTGAAGGC R: GGGAAACCCCAAGTTTCTCCA	207	2.00
Cx3cr1/CX3CR1	F: CATGTGCAAGCTCAGACTG R: CCCAGAGCCCAGACTAATG	164	2.00
Rbfox3, Fox-3/NeuN	F: GGCTGGAAGCTAAACCCTGT R: ACACGACCGCTCCATAAGTT	196	1.90

2.4 | Heterologous expression in *Xenopus laevis* oocytes

The following cDNAs were used for in vitro transcription: Gria1 (M38060.1), Gria4 (M36421.1), Cacng5 (NM_001199301.1), and Shisa9 (NM_028277.2). A tandem FLAG-tag was inserted into the Shisa9 cDNA between codons 29 (CAC, histidine) and 30 (GGG, glycine) according to von Engelhardt et al. (2010), and a V5-tag was fused at the C-terminal end of Cacng5. cRNA was synthesized from 1 µg of linearized plasmid DNA (backbone pBF) using the mMESSAGE mMACHINE[®] SP6 in-vitro transcription kit (Thermo Fisher Scientific). *Xenopus laevis* oocytes were purchased from EcoCyte Bioscience (Germany). Within 24 hr after surgery, oocytes were injected with 2 ng Gria1 (GluA1) and 2 ng Gria4 (GluA4) cRNA (= 4 ng total Gria cRNA), 4 ng Shisa9 (CKAMP44) and 0.4 ng Cacng5 cRNA (TARP γ -5) per oocyte using a Micro4 nanoliter injector (World Precision Instruments).

2.5 | Cell lysis and preparation of membrane fractions

For cell lysis, pellets of GFP+ and GFP- cells (from p12 mice) were resuspended in cell homogenization buffer (20 mM Tris-HCl pH 7.4, 1 mM iodoacetamide, 1 mM EDTA, 150 mM NaCl, protease inhibitors: aprotinin, leupeptin, pepstatin A [at 1 µg/ml each], and 1 mM PMSF) supplemented with 1% dodecanoyl D-sucrose and incubated for 30 min on ice. After ultracentrifugation (131,000g, 25 min, 4°C) 5× modified Laemmli and 0.1 M DTT were added to the supernatant and incubated for 10 min at 37°C for SDS-Page. Crude membrane fractions were prepared from whole mouse brain and from pooled GFP+ cell pellets (from p7–14 old mice), respectively. Mouse brains were lysed with the gentleMACS Dissociator (Miltenyi Biotec), and the sorted GFP+ cells were lysed by sonication in homogenization buffer and then centrifuged at 1,000g for 5 min at 4°C. The supernatant was ultracentrifuged at 145,000g for 60 min at 4°C. Pellets

containing the crude membrane fraction were resuspended in homogenization buffer, and the final protein concentration was determined in a BCA Assay using bovine serum albumin as a standard (Pierce/Thermo Fisher Scientific). For SDS-PAGE, 5× modified Laemmli and 0.1 M DTT were added to 20 µg of protein from the sorted GFP+ cells and 7 µg of protein from whole brain MF fraction as a positive control and then incubated for 10 min at 37°C.

2.6 | Immunoprecipitation

2.6.1 | GFP+ cells

Crude membrane fractions of sorted cell pellets were solubilized in solubilization buffer (cell homogenization buffer supplemented with 1% dodecanoyl D-sucrose), incubated for 30 min on ice and cleared by ultracentrifugation for 25 min at 131,000g and 4°C. The supernatant was then incubated with respective immobilized antibodies for 2 hr at 4°C. A 1:10 ratio of immobilized antibodies to solubilized protein was used. For immunoprecipitation, rabbit anti-GluA1 (AB1504, Millipore) alone as well as in combination with mouse anti-GluA2 (75-002, NeuroMab) were coupled to Protein G Dynabeads[™] (Invitrogen/Thermo Fisher Scientific). After brief washing with solubilization buffer containing 0.1% dodecanoyl D-sucrose, bound proteins were eluted with 1× modified Laemmli buffer at 37°C for 10 min. 0.1 M DTT was added after elution.

2.6.2 | *Xenopus laevis* oocytes

Immunoprecipitations were performed 3 days after cRNA injection. After two washing steps with oocyte homogenization buffer (83 mM NaCl, 1.5 mM MgCl₂, 10 mM HEPES, 1 mM EGTA, pH 7.4, protease inhibitors: aprotinin, leupeptin, pepstatin A [at 1 µg/ml each], and 1 mM PMSF), the oocytes were homogenized in 20 µL buffer per oocyte. The homogenate was cleared by centrifugation, and the membranes were sedimented at 125,000g for 10 min at 4°C. Membranes were then solubilized at 4°C for 30 min in solubilization buffer

(20 mM Tris-HCl pH 7.4, 1 mM iodoacetamide, 1 mM EDTA, 150 mM NaCl, protease inhibitors: aprotinin, leupeptin, pepstatin A [at 1 µg/mL each], and 1 mM PMSF, 1% dodecanoyl D-sucrose). The solubilizate was cleared by ultracentrifugation at 125,000g for 5 min at 4°C and incubated with 5 µg Protein G Dynabead™-coupled mouse monoclonal anti-V5-antibody (Invitrogen/Thermo Fisher Scientific, R96025) per 10 oocytes for 2 hr at 4°C. The beads were washed twice with washing buffer (20 mM Tris-HCl pH 7.4, 1 mM EDTA, 150 mM NaCl, 1 mM IAA, 0.1% dodecanoyl D-sucrose) and bound proteins were eluted by heating the washed beads in 2 µl modified Laemmli buffer per oocyte for 10 min at 37°C. For SDS-PAGE, 0.1 M DTT was added, and the proteins were denatured for 10 min at 60°C.

2.7 | SDS-PAGE and immunoblotting

Protein samples were separated by 10% or 12% SDS-PAGE, electroblotted on PVDF membrane (Millipore/Merck, Germany), and detected by immunoblot analysis. If necessary, the blot membrane was cut horizontally at different molecular weight ranges. The membranes were blocked with 5% BSA in TBS-T (20 mM Tris, 140 mM NaCl, 0.1% Tween 20, pH 7.6) and incubated overnight at 4°C with the primary antibodies. After incubation with the secondary antibodies, the blots were developed using ECL plus reagent (GE Healthcare, UK) or Westar *nc* Ultra 2.0 reagent (Cyanagen).

The following antibodies were used for immunoblotting: mouse anti-GLAST (1:250, 130-095-822, Miltenyi BioTec), rabbit anti-GFAP (1:1000, Z0334, DAKO/Agilent technologies), rabbit anti-Iba1 (1:1000, 016-20001, Wako), rabbit anti-Calnexin (1:1000, ab13504, Abcam), rabbit anti-GluA1 (1:1000, AB1504, Millipore/Merck), mouse anti-GluA2 (1:1000, 75-002, UC Davis/NIH NeuroMab Facility), rabbit anti-GluA4 (1:1000, AB1508, Millipore/Merck), mouse anti-V5 (1:5000, R96025, Invitrogen/Thermo Fisher Scientific), mouse anti-FLAG M2 (1:2000, F3165, Sigma-Aldrich), and goat anti-rabbit and anti-mouse secondary antibodies conjugated to horseradish peroxidase (1:10,000–15,000, Santa Cruz Biotechnologies).

2.8 | Immunohistochemistry

Mice (p14–15 old mice) were anesthetized, decapitated, and the brains were rapidly removed. After brief washing with phosphate-buffered saline (PBS), the brain tissue was subjected to immersion fixation in 4% paraformaldehyde in PBS at 4°C for 2 days. The brains were cut at 35–40 µm thickness using a vibratome (Microm HM650V, Thermo Fisher Scientific). The brain slices were first permeabilized in 2% Triton X100/PBS, unspecific antibody binding was blocked by 10% normal goat serum (NGS) in PBS for 2 hr and then incubated overnight with the respective primary antibody in the staining solution (2% NGS, 0.1% Triton X100 in PBS) at room temperature (RT) or 4°C. After repeated washing with PBS, the slices were incubated with the secondary antibody in the staining solution for 2 hr at RT. Subsequently, the slices were thoroughly washed with PBS including nuclei staining with the NucBlue Fixed Cell Stain DAPI Solution (Molecular Probes Thermo Fisher Scientific). Brain slices were mounted and imaged using an AxioScan and a confocal LSM810 (Zeiss).

The following antibodies were used for immunohistochemistry: anti-GLAST (1:250, 130-095-822, Miltenyi BioTec), rabbit anti-GFAP (1:1000, Z0334, DAKO/Agilent technologies), rabbit anti-Olig2 (1:500, AB9610, Millipore/Merck), mouse anti-NeuN (1:100, MAB377, Millipore/Merck), rabbit anti-Iba1 (1:1000, 016-20001, Wako), chicken anti-GFP (1:500, ab13970, Abcam), and as secondary antibodies goat anti-rabbit conjugated Cy3 (1:500, A10520, Thermo Fisher Scientific), goat anti-mouse conjugated Cy3 (1:500, A10521, Thermo Fisher Scientific), and goat anti-chicken conjugated Alexa Fluor 488 (1:500, A11039, Thermo Fisher Scientific). Primary antibodies were omitted in negative controls.

2.9 | Recombinant electrophysiology in *Xenopus laevis* oocytes

AMPA current responses were detected by two-electrode voltage clamp recordings in oocytes 3–4 days after cRNA injection at –70 mV holding potential using a Turbo Tec-03X amplifier (npi electronic) controlled by Pulse software (HEKA). Electrodes were filled with 3 M KCl and had resistances of 0.5–1.5 MΩ. Oocytes were superfused with calcium-free Mg²⁺-Ringer's solution (in mM: 115 NaCl, 2.5 KCl, 1.8 MgCl₂, and 10 HEPES, pH 7.2) to prevent the activation of endogenous Ca²⁺-gated chloride channels. Agonists (300 µM glutamate (Glu) with and without 50 µM cyclothiazide (CTZ), 150 µM kainate (KA)) were applied for 20 s. Current–voltage relationships were determined by ramping the holding potential (V_h) from –140 mV to 50 mV corrected for background conductivities. Data are given as mean ± SEM. The rectification index (RI) was defined as the ratio of current response at $V_h = 50$ mV to the response at $V_h = -80$ mV (I_{50mV}/I_{-80mV}). Statistical differences were assessed by a one-way ANOVA with a Tukey's multiple comparisons test using GraphPad Software.

3 | RESULTS

3.1 | Isolation of astrocytes

First, we established a FACS protocol to isolate astrocytes from dissociated brain tissue of hGFAP/GFP transgenic mice (Zhuo et al., 1997). As plotted in Figure 1a, the chosen FACS gating parameters separated a GFP+ from a GFP– cell population. In GFP+ cells, mRNA expression of the astrocytic marker genes *Gfap*, *Slc1a3* (EAAT1), and *Aldh1l1* was enriched 75- to 120-fold compared to the GFP– cell population (Figure 1b). In good agreement, we were able to detect GFAP and EAAT1 protein expression only in GFP+ cells (Figure 1c). By contrast, expression of the microglial marker genes *Aif1* (*Iba1*) and *Cx3cr1*, and also of the neuronal marker gene *Rbfox3* was depleted from GFP+ cells. The enriched *Aif1* mRNA expression in GFP– cells was paralleled by selective *Iba1* protein detection in these cells (Figure 1b,c). We found little higher expression of *Olig2*, *Mog*, *Sox10*, and *Cspg4* mRNAs in GFP+ compared to GFP– cells, indicating limited contamination of the targeted astrocytes with cells of the oligodendrocyte lineage. Routine qPCR of marker mRNAs provided standard quality control in all FACS experiments (Supporting Information, Table S1).

To further ascertain the predominantly astrocytic origin of sorted GFP+ cells, we performed immunohistochemical analysis in hGFAP/GFP mice (Figure 1d). As exemplified in cerebellar stainings (insets), immunoreactivities of GFAP and EAAT1 were found to co-localize with GFP, particularly in Bergmann glia processes as expected (Sofroniew & Vinters, 2010), whereas the ones of oligodendrocytic Olig2, neuronal NeuN, and microglial Iba1 did not show any overlap with GFP localization. Respective immunostainings of hippocampus and neocortex at higher magnification are depicted in Supporting Information, Figure 1. In summary, the chosen experimental approach enabled us to isolate cells for mRNA and protein analysis, which are predominantly of astrocytic origin.

3.2 | AMPAR expression in astrocytes during early postnatal development

We next quantified mRNA expression of AMPARs in astrocytes sorted from whole brains. As astrocytogenesis and synaptic growth and maturation takes place within the first two postnatal weeks (Reemst, Noctor, Lucassen, & Hol, 2016; Wang & Bordey, 2008), the expression profiles of the pore-lining GluA subunits, Gria1–4, and other AMPAR constituents as defined in our previous proteomics study (Schwenk et al., 2012) were analyzed for this period of time. As depicted in Figure 2 (upper panels), a distinct mRNA expression pattern of the four Gria genes was observed, with Gria2 being the most abundant subunit and Gria1, 3, and 4 summing up to not even half of Gria2 expression (Supporting Information, Table S2). This differential pattern did not change within the first two postnatal weeks; however, overall expression of total Gria1–4 decreased by ~36% from w1 to w2. Similarly, we found rather moderate changes in the differential expression pattern of examined AMPAR constituents in whole brain astrocytes during the same period of development (Figure 2 lower panels and Supporting Information, Table S2). A total of 22 from 24 selected AMPAR constituent mRNAs could be detected; neither Cacng3 (TARP γ -3) nor Vwc2l (Brorin-2-like) expression was above background and hence excluded from further analysis. In the first postnatal week, Cacng4 mRNA (TARP γ -4) was the most abundant AMPAR constituent. Despite a strong decrease in expression by >75% during the second postnatal week, Cacng4 still remained the predominant TARP mRNA expressed in astrocytes. Surprisingly, we found appreciable expression of Shisa9 (CKAMP44), which had formerly been described as a neuronal auxiliary subunit (von Engelhardt et al., 2010). In parallel with the developmental reduction of mRNAs coding for the pore-lining GluA subunits, also the ones coding for other AMPAR constituents decreased in expression from w1 to w2. However, the reduction in mRNA expression of non-pore-lining AMPAR constituents was more pronounced amounting up to 59%.

3.3 | AMPAR expression in astrocytes from different brain regions

Functional properties of astrocytic AMPARs vary considerably between brain regions. Cerebellar Bergmann glia express Ca^{2+} -permeable and inwardly rectifying AMPARs (Burnashev et al., 1992; Müller, Möller, Berger, Schnitzer, & Kettenmann, 1992). In contrast,

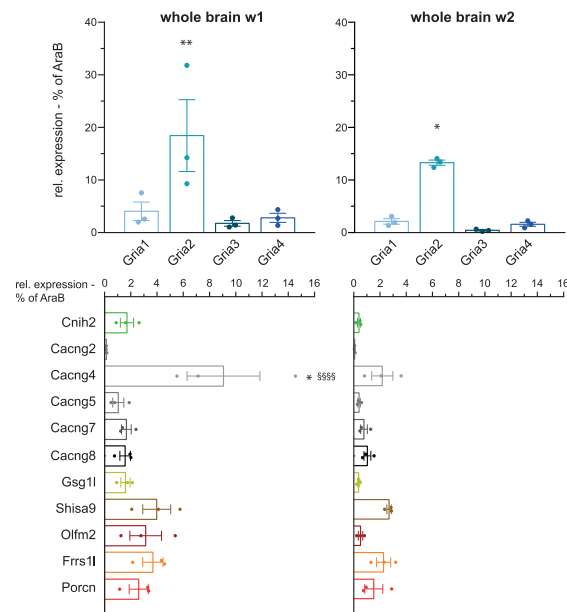


FIGURE 2 mRNA expression of AMPARs in astrocytes isolated during development. Quantification of mRNA expression of GluA1–4 (upper panel) and indicated AMPAR constituents (lower panel) in sorted astrocytes at postnatal week 1 (w1, left) and postnatal week 2 (w2, right), respectively. Expression levels were normalized to an external spike of AraB RNA. Data are given as mean relative expression (% of AraB) \pm SEM ($n = 3$). GluA2 is the predominantly expressed pore-lining subunit during development, whereas Cacng4 is the main TARP in these astrocytes. In general, AMPAR mRNA expression decreases during development. Asterisks indicate statistically significant differences in gene expression levels at a single developmental stage, whereas section signs indicate statistically significant differences in gene expression levels between developmental stages (* $/\$p < .05$; ** $/\$\$p < .01$; *** $/\$\$\$p < .001$; **** $/\$\$\$\$p < .0001$). Statistical differences in expression levels were analyzed by two-way ANOVA followed by Tukey's (asterisks) or Bonferroni's (section signs) multiple comparisons tests

hippocampal astrocytes exhibit no AMPAR currents at all, and astrocytes in the neocortex show only small AMPA-mediated currents (Lalo et al., 2006; Matthias et al., 2003). To address the question, whether the reported functional diversity is reflected by specific expression patterns of AMPAR constituents, we sorted astrocytes from cerebellum, neocortex, and hippocampus from the second postnatal week for further qPCR analysis. Indeed, we found distinct expression levels and patterns of AMPAR complex constituents in the selected brain regions (Figure 3). Whereas in astrocytes sorted from cerebellum, Gria1 and Gria4 represented the predominant pore-forming subunits ($17.8\% \pm 1.5\%$ and $13.5\% \pm 1\%$, respectively), Gria2 was the predominant one in neocortex ($13.5\% \pm 2.2\%$) and hippocampus ($8.4\% \pm 1.9\%$). In the latter two regions, the other Gria genes were barely expressed (Figure 3, upper panels). Brain region-specific differences were also found in the expression patterns of the other AMPAR complex constituents (Figure 3, lower panels). Astrocytes from cerebellum expressed strikingly high levels of mRNA coding for Frrs11 ($13.5\% \pm 1.0\%$) compared to neocortex ($1.1\% \pm 0.2\%$) or

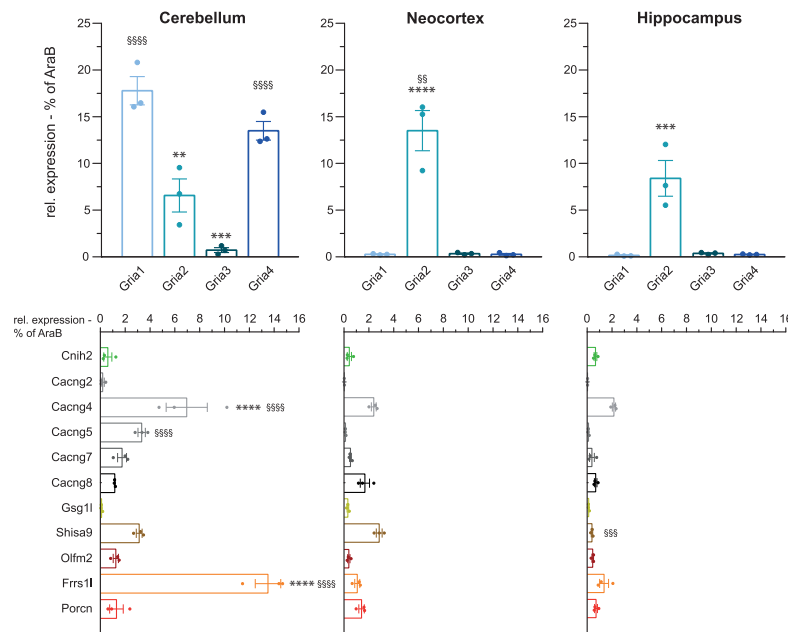


FIGURE 3 mRNA expression of AMPARs in astrocytes isolated from distinct brain regions. Quantification of mRNA expression of GluA1–4 (upper panel) and indicated AMPAR constituents (lower panel) in astrocytes sorted from cerebellum, neocortex, and hippocampus at postnatal week 2 (w2). Expression levels were normalized to an external spike of AraB RNA. Data are given as mean relative expression (% of AraB) \pm SEM ($n = 3$). The mRNA expression profile of cerebellar astrocytes showed prominent differences compared to neocortex and hippocampus. Asterisks indicate statistically significant differences in gene expression levels within a single brain region, whereas section signs indicate statistically significant differences in gene expression levels between brain regions (*/ $\$p < .05$; **/ $\$\$p < .01$; ***/ $\$\$\$p < .001$; ****/ $\$\$\$\$p < .0001$). Statistical differences in expression levels were analyzed by two-way ANOVA followed by Tukey's multiple comparisons test

hippocampus ($1.4\% \pm 0.4\%$). Among the TARPs, Cacng4 mRNA was predominant in astrocytes from all brain regions; Cacng5 and Cacng7 mRNAs were rather selectively expressed in cerebellum. In contrast, Shisa9 mRNA showed appreciable expression in both cerebellum and neocortex. In general, however, we observed that total mRNA expression levels of AMPARs in astrocytes sorted from neocortex and hippocampus were lower than in astrocytes from cerebellum. Overall, the observed regional AMPAR expression profiles showed prominent differences and more heterogeneity than the temporal AMPAR expression profiles within the first two postnatal weeks when averaged throughout whole brain.

3.4 | Hierarchical clustering of AMPAR expression levels reveals appreciable heterogeneity between brain regions

To assess the relationship between the mRNA expression profiles of the different brain regions, we performed hierarchical clustering analysis. As shown in Figure 4, the resulting heat map and dendrogram depicts unequivocal heterogeneity among cerebellar, neocortical, and hippocampal astrocytic AMPARs. Overall, AMPARs in cerebellar astrocytes are most distinct from neocortical and hippocampal ones with distances of 27.32 and 26.13, respectively, whereas AMPARs in neocortical and hippocampal astrocytes are much more alike with a distance of only 7.96. Exceptions exist at the level of specific genes, including Shisa and Abhd, for which astrocytic AMPARs from either

neocortex or hippocampus and cerebellum share more similarity, respectively.

In summary, our qPCR analysis of astrocytic AMPAR expression disclosed appreciable heterogeneity among brain regions, which may give rise to region-specific molecular compositions and hence the reported functional heterogeneity of glial AMPARs.

3.5 | Native AMPAR protein complexes in sorted astrocytes

To check whether mRNA expression translates into protein, immunoblot analysis was performed on crude membrane fractions of sorted GFP+ cells. As shown in Figure 5a, the expression of the pore-lining subunits GluA1, GluA2, and GluA4 could be confirmed. However, their level of expression was by far lower than in crude membrane fractions from whole brain containing neuronal AMPARs as well. We also sought to investigate whether intact native AMPAR complexes may be affinity-purified from sorted astrocytes. Figure 5b shows the isolation of native AMPAR pore-forming complexes. Affinity-purification of GluA1-containing complexes (IP GluA1) from whole brain astrocytic membrane fractions co-purified both GluA2 and GluA4. While GluA1 was depleted in these experiments, significant amounts of GluA2 and GluA4 remained unbound. Affinity-purifications virtually depleting GluA2 as well (IP GluA1/2) co-depleted GluA4. GluA3 was not further pursued because of negligible

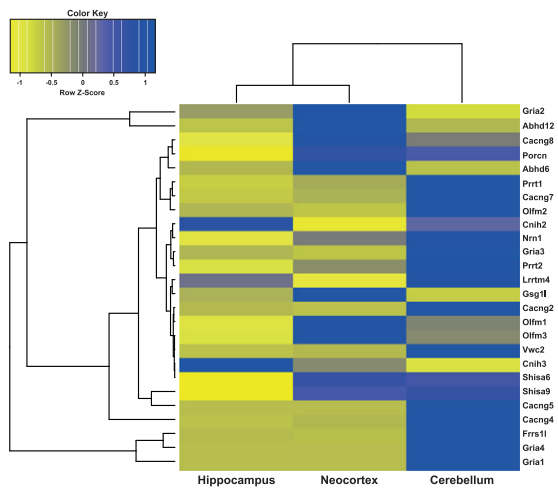


FIGURE 4 Heterogeneity of the AMPAR transcriptome between brain regions. Heat map and hierarchical clustering of selected astrocytic AMPAR constituents in indicated brain regions by normalized gene expression values (row z-score). Note that mRNA expression profiles of hippocampal and neocortical astrocytic AMPAR constituents are similar to each other, but clearly distinct from cerebellar astrocytes at postnatal week 2 (w2)

expression in astrocytes (Figures 2 and 3) and the lack of available antibodies specifically purifying native GluA3.

Given a preferential heteromeric assembly of the pore-lining AMPAR subunits (Greger, Watson, & Cull-Candy, 2017), we conclude that astrocytes express mainly GluA1/2, GluA1/4, and GluA2/4 heteromers.

3.6 | Functional reconstitution of selected astrocytic AMPARs

Intrigued by the novel finding of astrocytic Shisa9 expression, we sought to reconstitute AMPAR complexes, which are prototypic for cerebellar astrocytes. To this end, GluA1/4 heteromeric receptors were co-expressed in *Xenopus laevis* oocytes with CKAMP44 and TARP γ -5. Functional properties of resulting receptor complexes were

probed by two-electrode voltage-clamp (TEVC) bath-applying the ligands glutamate or kainate (Figure 6a).

As quantified in Figure 6b, GluA1/4 heteromers alone show a kainate/glutamate (KA/Glu) ratio of 1.60 ± 0.2 ($n = 12$) and strong desensitization, which is inhibited by application of cyclothiazide (CTZ). The current/voltage (I/V) relationship of GluA1/4 receptors is characterized by inward rectification typical of GluA2-lacking receptor complexes (Boulter et al., 1990; Bowie & Mayer, 1995; Figure 6c). Co-expression of CKAMP44 significantly reduced the KA/Glu ratio to 0.56 ± 0.05 ($n = 20$; $p < .0001$) and also receptor desensitization, which is reflected by a significantly smaller effect of CTZ. Rectification properties of GluA1/4 receptors did not change upon co-expression of CKAMP44. Co-expression of TARP γ -5 also reduced the KA/Glu ratio in GluA1/4 heteromers (1.15 ± 0.06 ; $n = 13$; $p = .03$), but to a significantly smaller extent than did CKAMP44 ($p = .0005$). Desensitization of GluA1/4 heteromers was not affected, nor was the strong effect of CTZ diminished. The rectification index (RI) showed only a tendency to increase upon co-expression of TARP γ -5, but did not significantly differ from GluA1/4 heteromers alone ($n = 11$; $p = .6642$). Co-expression of both CKAMP44 and TARP γ -5 resulted in receptors with functional properties predominantly determined by CKAMP44. Thus, the KA/Glu ratio decreased to 0.63 ± 0.1 ($n = 11$; $p < .0001$) and the effect of CTZ was significantly smaller than in GluA1/4 heteromers alone or upon co-expression of TARP γ -5 (3.60 ± 0.43 ($n = 11$; $p = .001$ vs GluA1/4), $p = .011$ vs GluA1/4 + γ -5)). Only the RI further increased, although still not significantly ($n = 11$; $p = .0681$). As TEVC recordings would not distinguish between receptor subpopulations, the virtual co-assembly of GluA1/4 with both CKAMP44 and TARP γ -5 was probed by immunoprecipitation experiments. As shown in Figure 6d, precipitating TARP γ -5 co-purified CKAMP44 in the presence of GluA1/4 heteromers. Thus, the heterologously expressed constituents integrate into common receptor complexes. Whether those complexes, however, may show different stoichiometries, remains elusive at this point.

4 | DISCUSSION

Here, we have quantified the astrocytic transcriptome of AMPARs in early postnatal development. Whereas the pattern of AMPAR mRNA

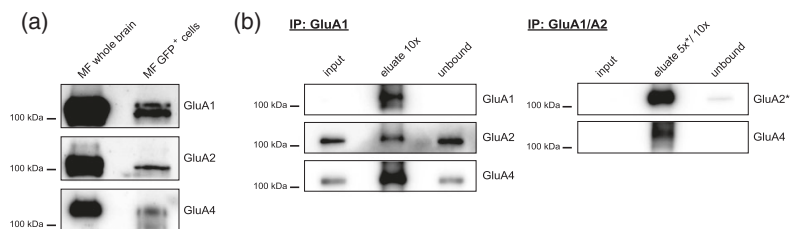


FIGURE 5 AMPAR protein expression and complex formation in astrocytes. (a) Immunoblot analysis of crude membrane fractions (MF) from mouse whole brain and sorted astrocytes. Protein expression of GluA1, GluA2, and GluA4 subunits may well be detected in sorted astrocytes but to a far smaller extent than in whole brain fractions (note the differences in loaded protein amounts: MF GFP+ cells: 20 μ g, MF whole brain: 7 μ g). (b) Immunoprecipitation of AMPARs from GFP+ cells using an anti-GluA1 antibody alone (left) or both anti-GluA1 and anti-GluA2 antibodies (right). Depleting immunoprecipitation of GluA1 co-purified a subpopulation of GluA2 and GluA4. Depleting immunoprecipitation of both GluA1 and GluA2 co-depleted GluA4

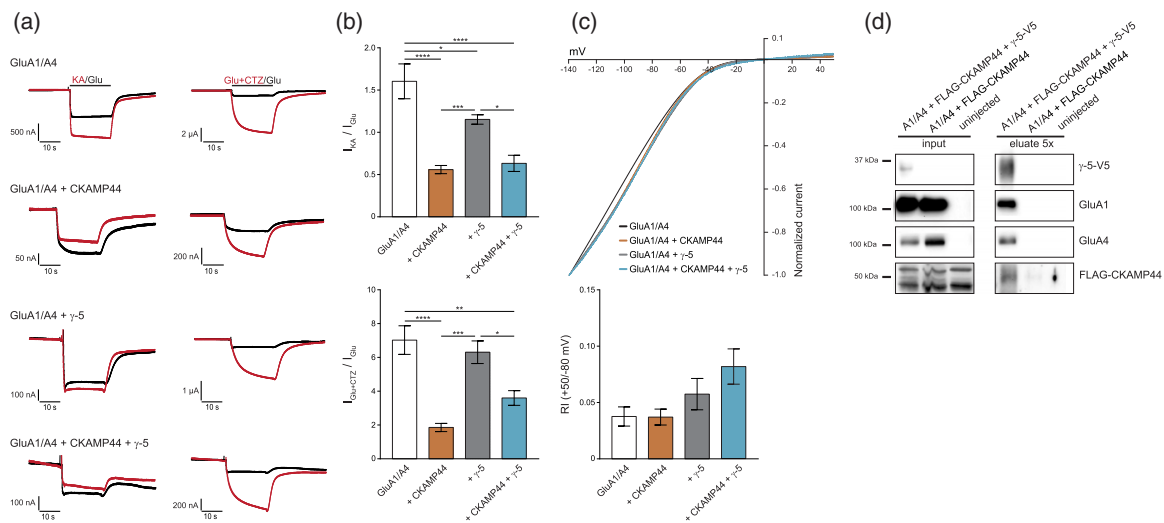


FIGURE 6 Functional reconstitution of AMPARs in *Xenopus laevis* oocytes using the main constituents detected in cerebellar astrocytes (a) Representative TEVC current traces recorded from oocytes expressing GluA1 and GluA4 alone or GluA1/4 with CKAMP44, with TARP γ -5, or with both CKAMP44 and TARP γ -5 upon agonist application (300 μ M Glu \pm 50 μ M CTZ, 150 μ M KA). (b) Kainate/glutamate ratio and Glu + CTZ/Glu ratio of evoked currents in indicated complex compositions. Data are given as mean steady-state currents \pm SEM for GluA1/4 ($n = 12$), GluA1/4 + CKAMP44 ($I_{KA}/I_{Glu} n = 20$; $I_{Glu} + CTZ/I_{Glu} n = 17$), GluA1/4 + TARP γ -5 ($n = 13$), and GluA1/4 + CKAMP44 + TARP γ -5 ($n = 11$). Asterisks indicate statistically significant differences (* $p < .05$; ** $p < .01$; *** $p < .001$; **** $p < .0001$). Co-expression of both CKAMP44 and TARP γ -5 resulted in GluA1/4 receptors with functional properties predominantly determined by CKAMP44. (c) Mean current–voltage (I/V) relationships and rectification indices (RI, at 50 mV/–80 mV) of GluA1/4 alone ($n = 11$), GluA1/4 with CKAMP44 ($n = 6$), GluA1/4 with TARP γ -5 ($n = 11$) or GluA1/4 with both CKAMP44 and TARP γ -5 ($n = 11$). Currents were activated by bath application of 300 μ M Glu. To facilitate comparison, all I/V curves were normalized to the maximum inward current at –140 mV. Co-expression of both CKAMP44 and TARP γ -5 with GluA1/4 heteromers tended to increase RI. (d) Immunoprecipitation of AMPAR complexes from oocytes using an anti-V5 antibody. Immunoprecipitation of γ -5-V5 co-purified GluA1, GluA4, and also CKAMP44 indicating all constituents being in the same complex

expression showed minor variation over time, it did exhibit significant heterogeneity with respect to different brain regions. Cerebellar astrocytes express a combination of AMPAR complex constituents that is remarkably distinct from the one in neocortical or hippocampal astrocytes. Altogether, we provide both a workflow and a first reference for future investigations into the molecular and functional diversity of astrocytic AMPARs.

4.1 | Experimental design

We used a transgenic mouse line expressing an optimized GFP variant (hGFP-S65T) under the human GFAP promoter to isolate astrocytes from brain tissue by FACS (Zhuo et al., 1997). GFAP was the first molecular marker used to designate astrocytic identity (Eng, Ghirnikar, & Lee, 2000). However, two observations advice caution: GFAP expression level varies among astrocytes from different brain regions (Sofroniew & Vinters, 2010) and GFAP may be expressed by other cell types than mature astrocytes, for example, progenitor cells affording constitutive neurogenesis in the adult CNS (García, Doan, Imura, Bush, & Sofroniew, 2004; Molofsky & Deneen, 2015; Platel, Gordon, Heintz, & Bordey, 2009). For routine quality control, we have therefore performed extensive characterization of GFP+ cells isolated in our experimental model. The enrichment of GFAP, Slc1a3 (EAAT1), and Aldh1l1 mRNAs by two orders of magnitude and the depletion of both microglial and neuronal marker genes, confirmed by immunoblot analysis, validated the predominantly astrocytic origin of sorted GFP+

cells. A limited contamination by cells of the oligodendrocytic lineage or by the above mentioned progenitor cells may be indicated by the elevated detection of Olig2, Mog, Sox10, and Cspg4. The qPCR and immunoblot results were finally confirmed by whole brain immunohistochemistry showing exclusive co-localization of GFP-immunoreactivity with astrocytic but neither with microglial nor with neuronal markers.

4.2 | Temporal profile of the early postnatal astrocytic AMPAR transcriptome

As a start, we quantified mRNA expression of AMPAR constituents in astrocytes isolated from whole brain after the first postnatal week (w1). At this developmental stage, astrocytes grow steadily and promote the formation of neuronal synapses. Among the pore-forming subunits, we found *Gria2* to be the predominant isoform. This observation is in good agreement with a recent proteomic analysis of rat whole brain membrane fractions, which identified GluA2-containing AMPAR complexes to be the most abundant ones from birth until adulthood (Schwenk et al., 2014). Among the inner core complex constituents, *Cacng4* (TARP γ -4) mRNA was most abundant of the *Cacng* (TARP) family, but also compared to *CNIH2* and *GSG11*. In line with these data, TARP γ -4 has been reported to be expressed in glial cells, particularly during embryonic and early postnatal development (Tomita et al., 2003). Also, proteomic analysis quantified TARP γ -4 as

the most abundant TARP assembling into native AMPARs isolated from whole brain tissue in early postnatal stages (Schwenk et al., 2014). The accordance of our results obtained from isolated astrocytes with the proteomic data from whole brain tissue sampling diverse cell types, including neurons and other glial cells, was somewhat unexpected. Astrocytic AMPARs may outnumber neuronal ones dominating the whole brain proteomic results; alternatively, the temporal profile of the early postnatal AMPAR composition may rather be independent of cell type. Of note were the significant amounts of Shisa9 (CKAMP44) mRNA detected in astrocytes, which had so far been reported as a neuronal AMPAR constituent (Khodosevich et al., 2014; von Engelhardt et al., 2010). In contrast to the high mRNA and protein levels of CNIH2 and its high abundance in whole brain AMPAR complexes, astrocytic CNIH2 mRNA expression was relatively low (Mauric et al., 2013; Schwenk et al., 2014). Interestingly, we observed also low levels of TARP γ -8 mRNA in astrocytes and no developmental increase, which somewhat contrasts proteomic data showing that both CNIH2 and TARP γ -8 compete for the most abundant inner core constituent of AMPARs during development (Schwenk et al., 2014; Tomita et al., 2003).

In all likelihood, however, the transcriptome will not be linearly translated into its proteome challenging more detailed quantitative comparisons. The pattern of astrocytic constituent expression remained basically constant during later postnatal development, confirming earlier microarray data, which claimed the genetic profile of p7 astrocytes to closely resemble already that of mature astrocytes (Cahoy et al., 2008). We noted, however, a marked decrease in overall mRNA levels of both pore-forming subunits and other complex constituents after the second postnatal week [w2]. Such distinct dip in AMPAR expression was similarly observed in the whole brain proteomic study around p14 (Schwenk et al., 2014). It may reflect maturation of glutamatergic neurotransmission in the developing rodent brain.

4.3 | Regional profile of the early postnatal astrocytic AMPAR transcriptome

In the next series of experiments, we quantified astrocytic AMPAR transcriptomes derived from cerebellum, neocortex, and hippocampus after the second postnatal week. The expression patterns of both pore-lining and other AMPAR constituents showed appreciable heterogeneity over brain region. Hierarchical clustering revealed cerebellar AMPARs most distant from neocortical and hippocampal ones. The predominant expression of Gria1 and Gria4 at the expense of Gria2 in cerebellum may well explain the prototypical Ca^{2+} -permeable inwardly rectifying AMPAR currents recorded from Bergmann glia (Burnashev et al., 1992; Muller et al., 1992), which represent most likely the largest population of GFAP expressing cells in the cerebellum. The far lower expression of the majority of AMPAR constituents except for Gria2 in neocortex and hippocampus compared to cerebellum may account for the rather small or nondetectable currents in neocortical and hippocampal astrocytes, respectively (Lalo et al., 2006; Matthias et al., 2003). RNA editing of Gria2, translated into GluA2, has been described as a crucial determinant of AMPAR pore assembly by regulating channel tetramerization and its export from the endoplasmic reticulum (ER) (Greger & Esteban, 2007). Thus, Q/R edited GluA2

does not homotetramerize but instead favors heteromerization with the other pore-lining subunits for efficient ER export (Greger, Khatri, Kong, & Ziff, 2003; Greger, Khatri, & Ziff, 2002). However, if expression levels of the latter are rather low as suggested by our qPCR data for neocortex and hippocampus, also low numbers of functional channels are expected on the cell surface, with most GluA2 being retained within the ER. Such discrepancy of AMPAR surface expression between brain regions may well be increased by another conspicuous finding of our qPCR analysis: contrasting neocortical and hippocampal astrocytes, cerebellar astrocytes express strikingly high levels of FRRS1, which has recently been reported as a priming catalyst for early AMPAR biogenesis in the ER (Brechet et al., 2017). High levels of FRRS1 may hence support efficient assembly and export of AMPARs from the ER, eventually resulting in robust surface expression and respective current amplitudes.

Deep sequencing of RNA (RNA-Seq) isolated from astrocytes has recently allowed establishing the first comprehensive databases of their transcriptome with respect to brain region and developmental stage (Chai et al., 2017; Srinivasan et al., 2016; Zhang et al., 2014). Our qPCR results on postnatal expression of AMPAR complex constituents in astrocytes, even though generated in independent sample preparations, may validate respective transcriptome databases. In good agreement with our study, RNA-Seq of p7 astrocytes from mouse neocortex as well as single cell expression data from neocortical astrocytes identified Gria2 as the by far predominant pore-lining subunit of AMPARs (Dzamba et al., 2015; Rusnakova et al., 2013; Zhang et al., 2014). During further development, the dominance in expression of Gria2 over the other three isoforms fades when averaged over whole brain; still, Gria2 exhibits highest transcript expression in (adult) neocortical and hippocampal astrocytes among the AMPAR pore-forming subunits (Chai et al., 2017; Rusnakova et al., 2013; Srinivasan et al., 2016; Zhang et al., 2014). For astrocytic mRNA expression of inner core constituents, we also find some discrepancies between our qPCR and published RNA-Seq datasets. While we find Cacng4 as the dominant TARP isoform in neocortical and hippocampal astrocytes after the second postnatal week, RNA-Seq data identified Cacng7 dominant in both p7 and adult astrocytes from the same brain regions (Chai et al., 2017; Srinivasan et al., 2016; Zhang et al., 2014). Such discrepancies, in general, might derive from heterogeneity among astrocytes from the same brain region but specializing within different neuronal circuits, and from different marker genes used in respective purification protocols (Chai et al., 2017; Zhang et al., 2014). However, fully consistent with our data are the similar levels of neocortical Cacng4 and Shisa9 expression throughout postnatal development (Chai et al., 2017; Srinivasan et al., 2016; Zhang et al., 2014).

4.4 | Limitations

Our study provides a reference for further investigations into the molecular and functional heterogeneity of astrocytic AMPARs. As demonstrated, the cell type-specific transcriptomic profiles may further be probed by cell type-specific analysis of protein expression or even protein assembly. Recombinant electrophysiology of reconstituted AMPARs may eventually guide experiments defining the molecular basis of AMPAR currents in native cells. Finally, the herein

presented experimental approach may be applied to other cell types provided the respective animal models for cell isolation.

However, certain limitations have to be taken into account when interpreting the data or seeking for further methodological improvement. Regional heterogeneity of a specific cell type is underestimated when sample preparation is solely based on anatomical borders without considering specific integration into neuronal circuitry. Functional testing prior to cell isolation and single cell profiling will help improve resolution (Chai et al., 2017; Dzamba et al., 2015; Rusnakova et al., 2013). Also, local mRNA expression might be underestimated, as cell processes will most likely be lost during cell sampling by FACS (Sakers et al., 2017). Finally, an unbiased analysis of glial AMPAR composition would require a cell type specific proteomic analysis (Schwenk et al., 2012). For making the claim of being comprehensive, such approach will always be limited by the amounts of surface membrane protein available for affinity purification of AMPARs, their enzymatic digest, and eventual high-resolution mass spectrometry.

ACKNOWLEDGMENTS

This study was supported by a grant from the Deutsche Forschungsgemeinschaft (DFG) to NK (KL 1168/7-1) within the Priority Program SPP1757. AM was an associated member of iBrain graduate program at Heinrich-Heine University of Düsseldorf. The authors would particularly like to thank Klaus Meyer (Institute of Functional Genome Research of Microorganisms, HHU Düsseldorf) for his help and support with FACS, Rafael Dellen (Center for Bioinformatics and Biostatistics, Biological Medical Research Center, HHU Düsseldorf) for support with the hierarchical clustering analysis, and René Hübbers (Cécile and Oskar Vogt Institute of Brain Research, HHU Düsseldorf) for his help with the AxioScan imaging.

ORCID

Nikolaj Klöcker  <http://orcid.org/0000-0002-7864-1348>

REFERENCES

- Allaman, I., Bélanger, M., & Magistretti, P. J. (2011). Astrocyte-neuron metabolic relationships: For better and for worse. *Trends in Neurosciences*, 34, 76–87. <https://doi.org/10.1016/j.tins.2010.12.001>
- Allen, N.J., 2014. Astrocyte regulation of synaptic behavior. *Annual Review of Cell and Developmental Biology* 30, 439–463. <https://doi.org/10.1146/annurev-cellbio-100913-013053>
- Boulter, J., Hollmann, M., O'Shea-Greenfield, A., Hartley, M., Deneris, E., Maron, C., Heinemann, S., 1990. Molecular cloning and functional expression of glutamate receptor subunit genes. *Science* 249, 1033–1037. <https://doi.org/10.1126/science.2168579>
- Bowie, D., Mayer, M.L., 1995. Inward rectification of both AMPA and kainate subtype glutamate receptors generated by polyamine-mediated ion channel block. *Neuron* [https://doi.org/10.1016/0896-6273\(95\)90049-7](https://doi.org/10.1016/0896-6273(95)90049-7), 15, 453, 462
- Brechet, A., Buchert, R., Schwenk, J., Boudkazi, S., Zolles, G., Siquier-Pernet, K., Schaber, I., Bildl, W., Saadi, A., Bole-Feysot, C., Nitschke, P., Reis, A., Sticht, H., Al-Sanna'a, N., Rolfs, A., Kulik, A., Schulte, U., Colleaux, L., Abou Jamra, R., Fakler, B., 2017. AMPA-receptor specific biogenesis complexes control synaptic transmission and intellectual ability. *Nature Communications* 8, 15910. <https://doi.org/10.1038/ncomms15910>
- Burnashev, N., Khodorova, A., Jonas, P., Helm, P., Wisden, W., Monyer, H., Seeburg, P., Sakmann, B., 1992. Calcium-permeable AMPA-kainate receptors in fusiform cerebellar glial cells. *Science* 256, 1566–1570. <https://doi.org/10.1126/science.1317970>
- Cahoy, J.D., Emery, B., Kaushal, A., Foo, L.C., Zamanian, J.L., Christopherson, K.S., Xing, Y., Lubischer, J.L., Krieg, P.A., Krupenko, S. A., Thompson, W.J., Barres, B.A., 2008. A transcriptome database for astrocytes, neurons, and oligodendrocytes: A new resource for understanding brain development and function. *The Journal of Neuroscience* 28, 264–278. <https://doi.org/10.1523/JNEUROSCI.4178-07.2008>
- Chai, H., Diaz-Castro, B., Shigetomi, E., Monte, E., Oceau, J.C., Yu, X., Cohn, W., Rajendran, P.S., Vondriska, T.M., Whitelegge, J.P., Coppola, G., Khakh, B.S., 2017. Neural circuit-specialized astrocytes: Transcriptomic, proteomic, morphological, and functional evidence. *Neuron* 95, 531–549.e9. <https://doi.org/10.1016/j.neuron.2017.06.029>
- Dzamba, D., Honsa, P., Valny, M., Kriska, J., Valhrach, L., Novosadova, V., Kubista, M., Anderova, M., 2015. Quantitative analysis of glutamate receptors in glial cells from the cortex of GFAP/EGFP mice following ischemic injury: Focus on NMDA receptors. *Cellular and Molecular Neurobiology* 35, 1187–1202. <https://doi.org/10.1007/s10571-015-0212-8>
- Eng, L.F., Ghimikar, R.S., Lee, Y.L., 2000. Glial fibrillary acidic protein : GFAP-thirty-one years (1969-2000). *Neurochemical Research* <https://doi.org/10.1023/A:1007677003387>, 25, 1439, 1451
- Erlenhardt, N., Yu, H., Abiraman, K., Yamasaki, T., Wadiche, J.I., Tomita, S., Bredt, D.S., 2016. Porcupine controls hippocampal AMPAR levels, composition, and synaptic transmission. *Cell Reports* 14, 782–794. <https://doi.org/10.1016/j.celrep.2015.12.078>
- Garcia, A.D.R., Doan, N.B., Imura, T., Bush, T.G., Sofroniew, M. V., 2004. GFAP-expressing progenitors are the principal source of constitutive neurogenesis in adult mouse forebrain. *Nature Neuroscience* <https://doi.org/10.1038/nn1340>, 7, 1233, 1241
- Greger, I.H., Esteban, J.A., 2007. AMPA receptor biogenesis and trafficking. *Current Opinion in Neurobiology* 17, 289–297. <https://doi.org/10.1016/j.conb.2007.04.007>
- Greger, I.H., Khatri, L., Kong, X., Ziff, E.B., 2003. AMPA receptor tetramerization is mediated by Q / R editing. *Neuron* 40, 763–774. [https://doi.org/10.1016/S0896-6273\(03\)00668-8](https://doi.org/10.1016/S0896-6273(03)00668-8)
- Greger, I.H., Khatri, L., Ziff, E.B., 2002. RNA editing at Arg607 controls AMPA receptor exit from the endoplasmic reticulum. *Neuron* 34, 759–772. [https://doi.org/10.1016/S0896-6273\(02\)00693-1](https://doi.org/10.1016/S0896-6273(02)00693-1)
- Greger, I.H., Watson, J.F., Cull-Candy, S.G., 2017. Structural and functional architecture of AMPA-type glutamate receptors and their auxiliary proteins. *Neuron* 94, 713–730. <https://doi.org/10.1016/j.neuron.2017.04.009>
- Haim, L. Ben, Rowitch, D., 2016. Functional diversity of astrocytes in neural circuit regulation. *Nature Reviews. Neuroscience* 18, 31–41. <https://doi.org/10.1038/nrn.2016.159>
- Hollmann, M., Heinemann, S., 1994. Cloned glutamate receptors. *Annual Review of Neuroscience* 17, 31–108. <https://doi.org/10.1146/annurev.ne.17.030194.000335>
- Israel, J.-M., Schipke, C.G., Ohlemeyer, C., Theodosis, D.T., Kettenmann, H., 2003. GABAA receptor-expressing astrocytes in the supraproctic nucleus lack glutamate uptake and receptor currents. *Glia* 44, 102–110. <https://doi.org/10.1002/glia.10272>
- Khodosevich, K., Jacobi, E., Farrow, P., Schulmann, A., Rusu, A., Zhang, L., Sprengel, R., Monyer, H., von Engelhardt, J., 2014. Coexpressed auxiliary subunits exhibit distinct modulatory profiles on AMPA receptor function. *Neuron* 83, 601–615. <https://doi.org/10.1016/j.neuron.2014.07.004>
- Lalo, U., Pankratov, Y., Kirchoff, F., North, R.A., Verkhratsky, A., 2006. NMDA receptors mediate neuron-to-glia signaling in mouse cortical astrocytes. *The Journal of Neuroscience* 26, 2673–83. <https://doi.org/10.1523/JNEUROSCI.4689-05.2006>
- Matthias, K., Kirchoff, F., Seifert, G., Hüttmann, K., Matyash, M., Kettenmann, H., & Steinhäuser, C. (2003). Segregated expression of AMPA-type glutamate receptors and glutamate transporters defines distinct astrocyte populations in the mouse hippocampus. *The Journal of Neuroscience*, 23, 1750–1758.
- Matyash, V., Kettenmann, H., 2010. Heterogeneity in astrocyte morphology and physiology. *Brain Research Reviews* 63, 2–10. <https://doi.org/10.1016/j.brainresrev.2009.12.001>

- Mauric, V., Mölders, A., Harmel, N., Heimrich, B., Sergeeva, O.A., Klöcker, N., 2013. Ontogeny repeats the phylogenetic recruitment of the cargo exporter cornichon into AMPA receptor signaling complexes. *Molecular and Cellular Neurosciences* 56, 10–17. <https://doi.org/10.1016/j.mcn.2013.02.001>
- McDougal, D.H., Hermann, G.E., Rogers, R.C., 2011. Vagal afferent stimulation activates astrocytes in the nucleus of the solitary tract via AMPA receptors: Evidence of an atypical neural-glia interaction in the brainstem. *The Journal of Neuroscience* 31, 14037–14045. <https://doi.org/10.1523/JNEUROSCI.2855-11.2011>
- Milstein, A.D., Zhou, W., Karimzadegan, S., Bredt, D.S., Nicoll, R.A., 2007. TARPs subtypes differentially and dose-dependently control synaptic AMPA receptor gating. *Neuron* 55, 905–918. <https://doi.org/10.1016/j.neuron.2007.08.022>
- Molofsky, A.V., Deneen, B., 2015. Astrocyte development: A guide for the perplexed. *Glia* 63, 1320–1329. <https://doi.org/10.1002/glia.22836>
- Muller, T., Möller, T., Berger, T., Schnitzer, J., Kettenmann, H., 1992. Calcium entry through kainate receptors and resulting potassium-channel blockade in Bergmann glial cells. *Science* 256, 1563–1566. <https://doi.org/10.1126/science.1317969>
- Parfenova, H., Tcheranova, D., Basuroy, S., Fedinec, A.L., Liu, J., Leffler, C.W., 2012. Functional role of astrocyte glutamate receptors and carbon monoxide in cerebral vasodilation response to glutamate. *American Journal of Physiology-Heart and Circulatory Physiology* 302, H2257–H2266. <https://doi.org/10.1152/ajpheart.01011.2011>
- Platel, J.C., Gordon, V., Heintz, T., Bordey, A., 2009. GFAP-GFP neural progenitors are antigenically homogeneous and anchored in their enclosed mosaic niche. *Glia* 57, 66–78. <https://doi.org/10.1002/glia.20735>
- Reemst, K., Noctor, S.C., Lucassen, P.J., Hol, E.M., 2016. The indispensable roles of microglia and astrocytes during brain development. *Frontiers in Human Neuroscience* 10, 1–28. <https://doi.org/10.3389/fnhum.2016.00566>
- Rusnakova, V., Honsa, P., Dzamba, D., Ståhlberg, A., Kubista, M., Anderova, M., 2013. Heterogeneity of astrocytes: From development to injury - single cell gene expression. *PLoS One* 8, e69734. <https://doi.org/10.1371/journal.pone.0069734>
- Saab, A.S., Neumeier, A., Jahn, H.M., Cupido, A., Šimek, A.A.M., Boele, H. J., Scheller, A., Le Meur, K., Götz, M., Monyer, H., Sprengel, R., Rubio, M.E., Deitmer, J.W., De Zeeuw, C.I., Kirchhoff, F., 2012. Bergmann glial AMPA receptors are required for fine motor coordination. *Science* 337, 749–753. <https://doi.org/10.1126/science.1221140>
- Sakers, K., Lake, A.M., Khazanchi, R., Ouwenga, R., Vasek, M.J., Dani, A., Dougherty, J.D., 2017. Astrocytes locally translate transcripts in their peripheral processes. *Proceedings of the National Academy of Sciences of the United States of America* 114, E3830–E3838. <https://doi.org/10.1073/pnas.1617782114>
- Schroeter, A., Wen, S., Mölders, A., Erlenhardt, N., Stein, V., Klöcker, N., 2015. Depletion of the AMPAR reserve pool impairs synaptic plasticity in a model of hepatic encephalopathy. *Molecular and Cellular Neurosciences* 68, 331–339. <https://doi.org/10.1016/j.mcn.2015.09.001>
- Schwenk, J., Baehrens, D., Haupt, A., Bildl, W., Boudkkazi, S., Roper, J., Fakler, B., Schulte, U., 2014. Regional diversity and developmental dynamics of the AMPA-receptor proteome in the mammalian brain. *Neuron* 84, 41–54. <https://doi.org/10.1016/j.neuron.2014.08.044>
- Schwenk, J., Harmel, N., Brechet, A., Zolles, G., Berkefeld, H., Müller, C.S., Bildl, W., Baehrens, D., Hüber, B., Kulik, A., Klöcker, N., Schulte, U., Fakler, B., 2012. High-resolution proteomics unravel architecture and molecular diversity of native AMPA receptor complexes. *Neuron* 74, 621–633. <https://doi.org/10.1016/j.neuron.2012.03.034>
- Schwenk, J., Harmel, N., Zolles, G., Bildl, W., Kulik, A., Heimrich, B., Chisaka, O., Jonas, P., Schulte, U., Fakler, B., Klockner, N., 2009. Functional proteomics identify cornichon proteins as auxiliary subunits of AMPA receptors. *Science* 323, 1313–1319. <https://doi.org/10.1126/science.1167852>
- Seeburg, P.H., 1993. The TIPS/TINS lecture: The molecular biology of mammalian glutamate receptor channels. *Trends in Pharmacological Sciences* 14, 297–303. [https://doi.org/10.1016/0165-6147\(93\)90047-N](https://doi.org/10.1016/0165-6147(93)90047-N)
- Shanks, N.F., Savas, J.N., Maruo, T., Cais, O., Hirao, A., Oe, S., Ghosh, A., Noda, Y., Greger, I.H., Yates, J.R., Nakagawa, T., 2012. Differences in AMPA and kainate receptor interactomes facilitate identification of AMPA receptor auxiliary subunit GSG1L. *Cell Reports* 1, 590–598. <https://doi.org/10.1016/j.celrep.2012.05.004>
- Sobolevsky, A.I., Rosconi, M.P., Gouaux, E., 2009. X-ray structure, symmetry and mechanism of an AMPA-subtype glutamate receptor. *Nature* 462, 745–756. <https://doi.org/10.1038/nature08624>
- Sofroniew, M. V., Vinters, H. V., 2010. Astrocytes: Biology and pathology. *Acta Neuropathologica* 119, 7–35. <https://doi.org/10.1007/s00401-009-0619-8>
- Srinivasan, R., Lu, T.Y., Chai, H., Xu, J., Huang, B.S., Golshani, P., Coppola, G., Khakh, B.S., 2016. New transgenic mouse lines for selectively targeting astrocytes and studying calcium signals in astrocyte processes in situ and in vivo. *Neuron* 92, 1181–1195. <https://doi.org/10.1016/j.neuron.2016.11.030>
- Tomita, S., Chen, L., Kawasaki, Y., Petralia, R.S., Wenthold, R.J., Nicoll, R.A., Bredt, D.S., 2003. Functional studies and distribution define a family of transmembrane AMPA receptor regulatory proteins. *The Journal of Cell Biology* 161, 805–816. <https://doi.org/10.1083/jcb.200212116>
- von Engelhardt, J., Mack, V., Sprengel, R., Kavenstock, N., Li, K.W., Stern-Bach, Y., Smit, A.B., Seeburg, P.H., Monyer, H., 2010. CKAMP44: A brain-specific protein attenuating short-term synaptic plasticity in the dentate Gyrus. *Science* 327, 1518–1522. <https://doi.org/10.1126/science.1184178>
- Wang, D.D., Bordey, A., 2008. The astrocyte odyssey. *Progress in Neurobiology* 86, 342–367. <https://doi.org/10.1016/j.pneurobio.2008.09.015>
- Zhang, Y., Barres, B.A., 2010. Astrocyte heterogeneity: An underappreciated topic in neurobiology. *Current Opinion in Neurobiology* 20, 588–594. <https://doi.org/10.1016/j.conb.2010.06.005>
- Zhang, Y., Chen, K., Sloan, S.A., Bennett, M.L., Scholze, A.R., O’Keeffe, S., Phatnani, H.P., Guarnieri, P., Caneda, C., Ruderisch, N., Deng, S., Liddelow, S.A., Zhang, C., Daneman, R., Maniatis, T., Barres, B.A., Wu, J.Q., 2014. An RNA-sequencing transcriptome and splicing database of glia, neurons, and vascular cells of the cerebral cortex. *The Journal of Neuroscience* 34, 11929–11947. <https://doi.org/10.1523/JNEUROSCI.1860-14.2014>
- Zhuo, L., Sun, B., Zhang, C.L., Fine, A., Chiu, S.Y., Messing, A., 1997. Live astrocytes visualized by green fluorescent protein in transgenic mice. *Developmental Biology* 187, 36–42. <https://doi.org/10.1006/dbio.1997.8601>

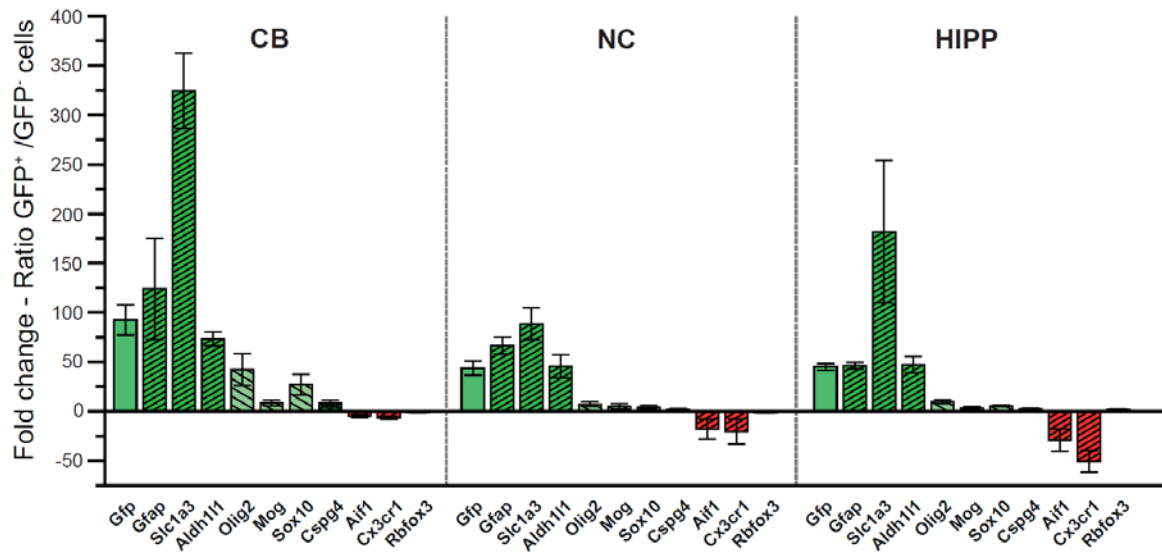
SUPPORTING INFORMATION

Additional supporting information may be found online in the Supporting Information section at the end of the article.

How to cite this article: Mölders A, Koch A, Menke R, Klöcker N. Heterogeneity of the astrocytic AMPA-receptor transcriptome. *Glia*. 2018;1–13. <https://doi.org/10.1002/glia.23514>

Supporting Information (Moelders et al., 2018)

A



B

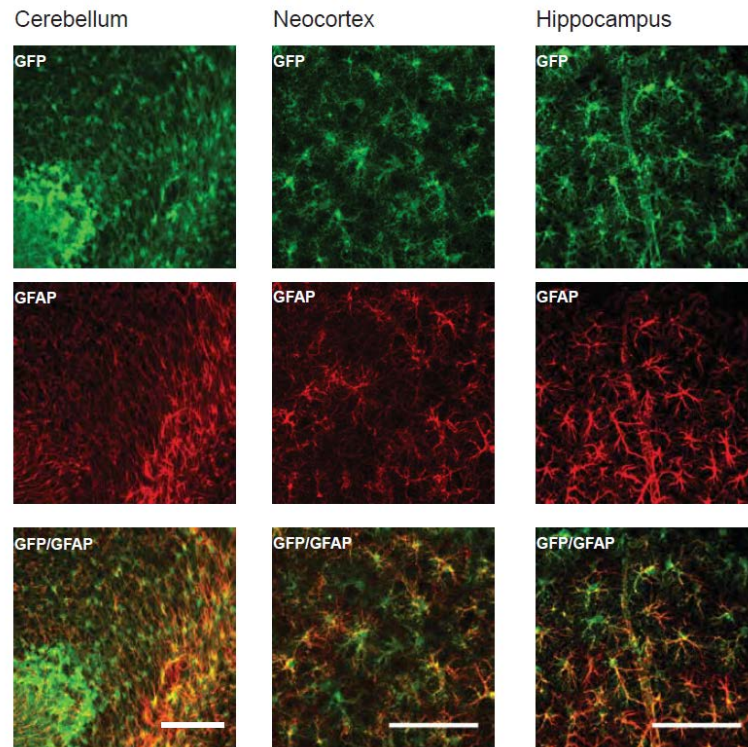


Figure S1. Astrocytic origin of GFP+ cells sorted from anatomical brain regions. (A) Quantification of mRNA expression of indicated cell type markers in GFP+ and GFP- cells in indicated brain regions by qPCR (CB: cerebellum, NC: neocortex, HIPP: hippocampus). Expression levels were normalized to an external spike of AraB RNA. Data are given as fold change – ratios of relative expression levels in GFP+ and GFP- cells \pm SEM ($n = 3$). **(B)** Immunohistochemical stainings of horizontal hGFAP-GFP mouse brain slices (p15) confirm the astrocytic origin of GFP+ cells in indicated brain regions. Confocal images of GFP (upper panels) and GFAP (middle panels) immunoreactivities and respective overlays (lower panels). Scale bars: 100 μ m

Table S1. Quantification of mRNA expression of indicated cell type markers in GFP+ and GFP- cells by qPCR. Expression levels were normalized to an external spike of AraB RNA. Data are given as fold change – ratios of relative expression levels in GFP+ and GFP- cells \pm SEM.

Gene	whole brain, postnatal week 1 (w1), n=2		whole brain, postnatal week 2 (w2), n=3		Cerebellum n=3		Neocortex n=3		Hippocampus n=3	
	Mean	\pm SEM	Mean	\pm SEM	Mean	\pm SEM	Mean	\pm SEM	Mean	\pm SEM
Gfp	59.36	11.80	88.02	16.41	92.56	15.22	43.93	7.22	44.95	3.29
Gfap	166.15	0.63	79.56	32.67	123.90	51.27	66.75	8.50	46.20	3.30
Eaat1	118.87	16.02	118.96	24.47	324.42	38.03	89.06	16.06	181.87	72.13
Aldh1l1	86.89	17.06	75.10	34.18	73.31	7.16	45.94	11.70	47.30	8.44
Olig2	20.17	8.00	20.90	7.33	42.25	16.20	7.64	2.38	9.84	1.92
Mog	1.57	1.35	6.42	1.83	8.57	2.91	5.23	2.56	3.24	1.43
Sox10	9.00	6.07	11.42	2.94	27.14	10.42	4.40	1.65	5.57	0.77
Cspg4	4.88	2.55	5.14	2.20	8.57	2.91	1.98	1.00	2.57	0.43
Iba1	-8.78	-4.06	-9.82	-3.89	-4.77	-1.60	-17.61	-9.80	-29.01	-11.17
Cx3cr1	-11.28	-5.87	-11.71	-3.86	-6.53	-1.89	-20.23	-12.64	-50.49	-11.00
Rbfox3	-9.84	-2.57	-8.79	-1.92	-1.46	-0.29	-1.44	-0.15	1.81	0.41

Table S2. Quantification of mRNA expression of Gria1-4 and indicated AMPAR constituents in sorted astrocytes. Expression levels were normalized to an external spike of AraB RNA. Data are given as mean relative expression (% of AraB) \pm SEM. Asterisks indicate statistically significant differences in expression levels at a single developmental stage or in a single anatomical brain region. Section signs indicate statistically significant differences in gene expression levels between developmental stages or brain regions (*/ \S $p < 0.05$; **/ $\S\S$ $p < 0.01$; ***/ $\S\S\S$ $p < 0.001$; ****/ $\S\S\S\S$ $p < 0.0001$). Statistically significant differences in expression levels were analyzed by Two-Way ANOVA followed by Tukey's (asterisks) or Bonferroni's (section signs) multiple comparisons tests. Numbers and letters indicate further details. **1:** significant (s.) against Gria1, Gria3, Gria4; **2:** s. against Gria2, Gria3; **3:** s. against Cacng2, Cacng5, Shisa9; **4:** s. against Cacng2, Cacng5; **a:** s. against cerebellum, **b:** s. against neocortex, **c:** s. against hippocampus. **5:** not significant (n.s.) against Cacng7, Shisa9, Olfm2, Porcn; **6:** n.s. against Cacng5, Olfm2, Porcn; **7:** n.s. against Cacng8, Frrs11, Porcn.

Gene	whole brain, postnatal week 1 (w1), n=3			whole brain, postnatal week 2 (w2), n=3			Cerebellum n=3			Neocortex n=3			Hippocampus n=3		
	Mean	\pm SEM		Mean	\pm SEM		Mean	\pm SEM		Mean	\pm SEM		Mean	\pm SEM	
Gria1	4.04	1.76		2.12	0.52		17.78	1.52	****2/ §§§§b,c	0.27	0.04		0.16	0.06	
Gria2	18.45	6.83	**1	13.30	0.49	*1	6.57	1.77	**1	13.52	2.15	****1/§§a,c	8.40	1.91	***1
Gria3	1.76	0.53		0.43	0.12		0.72	0.26	**1	0.34	0.07		0.37	0.06	
Gria4	2.81	0.87		1.58	0.38		13.51	1.00	***2/ §§§§b,c	0.27	0.09		0.25	0.03	
Cnih2	1.70	0.50		0.40	0.11		0.60	0.32		0.43	0.17		0.67	0.11	
Cnih3	0.15	0.09		0.03	0.02		0.00	0.00		0.01	0.00		0.03	0.01	
Cacng2	0.14	0.02		0.07	0.02		0.19	0.12		0.03	0.01		0.03	0.00	
Cacng4	9.07	2.78	*/§§§§	2.17	0.81		6.95	1.65	****/ §§§§b,c	2.40	0.20	*3	2.16	0.13	*4
Cacng5	1.07	0.42		0.40	0.09		3.33	0.30	*5/ §§§§b,c	0.12	0.02		0.11	0.03	
Cacng7	1.69	0.37		0.78	0.26		1.75	0.36	§c	0.52	0.08		0.39	0.19	
Cacng8	1.54	0.41		1.04	0.26		1.16	0.03		1.68	0.37		0.69	0.10	
Gsg11	1.60	0.35		0.37	0.08		0.10	0.05		0.31	0.07		0.13	0.03	
Shisa9	3.99	1.06		2.69	0.17		3.13	0.24	**6	2.83	0.23	*7	0.39	0.06	§§§c,b
Shisa6	0.01	0.01		0.00	0.00		0.00	0.00		0.00	0.00		0.00	0.00	
Prrt1	0.86	0.03		1.16	0.20		1.64	0.48		0.74	0.12		0.57	0.14	
Prrt2	1.09	0.17		0.69	0.12		0.76	0.23		0.41	0.08		0.22	0.07	
Olfm1	0.07	0.04		0.06	0.01		0.08	0.02		0.09	0.01		0.08	0.01	
Olfm2	3.12	1.21		0.52	0.17		1.25	0.21		0.39	0.09		0.45	0.07	
Olfm3	0.11	0.03		0.05	0.01		0.04	0.01		0.05	0.01		0.04	0.01	
Nrn1	0.58	0.16		0.71	0.28		0.54	0.40		0.48	0.12		0.41	0.10	
Frrs11	3.69	0.77		2.27	0.54		13.50	1.03	****/ §§§§b,c	1.06	0.21		1.37	0.36	
Vw2	0.23	0.16		0.03	0.01		0.06	0.02		0.01	0.00		0.01	0.00	
Lrrtm4	0.67	0.25		0.32	0.08		0.35	0.11		0.23	0.06		0.30	0.03	
Porcn	2.61	0.72		1.53	0.69		1.32	0.55		1.41	0.22		0.72	0.12	
Abhd6	1.84	0.61		0.98	0.18		0.63	0.09		1.79	0.33		0.68	0.06	
Abhd12	19.22	10.69		6.39	0.84		5.04	0.66		10.05	2.04		4.75	0.66	

4. Discussion and conclusion

Since it has been discovered that AMPARs are responsible for fast excitatory neurotransmission and play a crucial role in synaptic plasticity, their structure, composition, and function have been intensively studied. The research of the last decades revealed remarkable progress in understanding AMPAR function as well as the composition and structure of the complex. It turned out, that AMPARs are highly diverse and that their composition and function changes in development and with brain region. It is established that quite a number of AMPAR complex constituents exist, which influence their trafficking and fine-tune their properties. The present work addressed the molecular and functional diversity of AMPARs and investigated the diversity depending on different cell types, different developmental stages, and brain regions as well as in disease. In the first part of the thesis, the developmental expression of cornichon homologs (CNIHs) and their relation with the AMPAR pore composition was investigated. The second part of the thesis examined AMPAR function in the disease model of hepatic encephalopathy (HE). The last part of the thesis revealed the heterogeneity of AMPARs in astrocytes.

4.1 Analysis of developmental expression of CNIH2/3 and AMPARs and the consequence for the AMPA complex

The expression of the pore-lining subunits GluA1-4 is strictly regulated during development and there is only few information about the developmental regulation of the auxiliary subunits (Henley and Wilkinson, 2016; Pellegrini-Giampietro et al., 1991). Up to our study by Mauric et al., data on the expression and function of the auxiliary AMPA subunits CNIH2/3 originated only from studies in adult animals. In Mauric et al., we reported that also CNIH2 and CNIH3 are highly regulated during development, with CNIH2 being expressed at higher levels than CNIH3. The mRNA expression as well as the protein expression of CNIH2 and CNIH3 peaked within the first two postnatal weeks and then declined towards adulthood. In contrast, AMPAR and TARP expression increased continuously during development. Our data showed that the relative ratio of CNIH2/3 integrated into AMPARs did not change during development, whereas the absolute amount of CNIH2/3 integrated into AMPAR complexes did increase indicating that CNIHs gain importance for AMPARs in development.

First, the expression of CNIH2 was observed in brain regions with migrating and proliferating cells. Towards adulthood, it was strongest in regions with postmitotic and differentiated cells. Interestingly, GluA1 expression in the cerebellum exhibits an expression pattern similar to CNIH2 during development (Martin et al., 1998). Both GluA1 and CNIH2 are detectable transiently in granule cells of the internal layer and towards adult stages, the expression in granule cells vanishes. In adulthood, the granule cells express GluA2, Glu4, and TARP γ -2 (Bats et al., 2013; Martin et al., 1998; Schwenk et al., 2009). Also, in Purkinje cells, CNIH2 and GluA1 expression peaks during development and is lower again in adulthood. In contrast, CNIH2 and GluA1 are both present in Bergmann glia at adult stages (Martin et al., 1998; Schwenk et al., 2009). Interestingly, several studies indicate that CNIH2 prefer to interact with GluA1 and predominantly modulate the properties of GluA1 (Gill et al., 2011; Herring et al., 2013; Kato et al., 2010a). We found in compliance with several other studies, that within the whole brain mRNA and protein expression of all GluAs subunits increased during postnatal development and slightly decreased towards adulthood as already described (Blair et al., 2013; Luján et al., 2005; Martin et al., 1998, 1993, Pellegrini-Giampietro et al., 1992, 1991). For GluA1, the protein expression is detectable around E16 for the first time and it subsequently increases (Martin et al., 1998). Although for GluA4 a decrease in expression towards adulthood is known for the forebrain, the total GluA4 brain expression increases towards adulthood (Schwenk et al., 2014; Zhu et al., 2000). The observed increase in GluA4 whole brain expression could be due to its

high amount in the cerebellum, where GluA4 makes up two-thirds of the GluA subunits (Schwenk et al., 2014).

The diametral expression patterns of CNIHs and AMPARs might suggest different stoichiometry of CNIHs and GluA subunits during development. However, the co-immunoprecipitation experiments showed that the relative amount of CNIH2/3 co-purifying with AMPARs remained constant and the overall ratio of CNIH2/3 integrated into AMPARs did not change throughout development. The co-immunoprecipitation experiments have revealed that during development the AMPA-free amount of CNIH2/3 declined and the amount of integrated CNIH2/3 into the AMPAR complex increased. Since co-immunoprecipitation was performed with whole brain material, regional differences were not detectable because potential local differences might balance each other. Cell type specific changes and differences regarding the subcellular compartments were also not detectable as well as developmental changes between E18 and adulthood since only these two timepoints were examined. Indeed, Schwenk and colleagues showed that during development the abundance of CNIH2 in the AMPAR complex is changing (Schwenk et al., 2014). The CNIH2 abundance in the AMPA complex increased in the first postnatal week, then declined at p14 and rose again in adult animals (Schwenk et al., 2014). The observed increase in CNIH2 abundance until the second postnatal week is in line with the increasing CNIH2 expression at the same time.

This leads to the question what benefit and influence CNIHs might have on AMPARs during development? Several studies have described CNIHs as ER cargo exporters for soluble growth factors, like the members of the epidermal growth factor (EGF) family (Bökel, 2006; Castro et al., 2007; Hoshino et al., 2007; Roth et al., 1995). In connection with AMPARs, it is known that CNIHs also work as ER cargo exporter and enhance the export of AMPARs from ER and Golgi to the plasma membrane. Moreover, they modulate the electrophysiological properties of AMPARs at the synapse (Harmel et al., 2012; Herring et al., 2013; Kato et al., 2010a; Schwenk et al., 2009). It seems therefore likely that CNIH2/3 influence AMPAR complex surface expression and AMPAR currents during brain development. During early postnatal development, after neuronal differentiation, migration and axon guidance, neuronal activity is generated spontaneously within the network reflecting an immature activity pattern (reviewed by Kirkby et al., 2013). This early immature activity pattern, which includes synchronized oscillatory network activity or giant depolarization potentials, is supposed to sculpt, and refine the precise local circuits (fire to together, wire together). During later development, external patterns and sources influence the local network and replace the immature activity pattern with behaviorally relevant activities (Colonnese et al., 2010; Dehorter et al., 2012). In these phases, silent synapses transform into active synapses. Zhu and colleagues showed that spontaneous activity in the hippocampus in early postnatal development is sufficient to incorporate GluA4-containing AMPARs into silent synapses (Zhu et al., 2000). GluA4 expression at the synapse leads to strengthening of the synapse for several days, but for long-term maintenance of the synapse an exchange for GluA2-containing AMPARs is necessary (Zhu et al., 2000). The transport of AMPARs to the cell surface is essential for the switch of silent synapses into AMPAR containing synapses (Zhu et al., 2000). Furthermore, the already described switch of CP- to CI-AMPARs, where the edited GluA2 becomes the predominant subunit, is important for synapse maturation (Henley and Wilkinson, 2016; Kumar et al., 2002; Pickard et al., 2000). Edited GluA2 subunits are retained in the ER and need the co-assembly with other non-edited GluA subunits to be trafficked to the plasma membrane (Araki et al., 2010; Greger et al., 2017; Greger and Esteban, 2007). As CNIH2/3 enhances surface expression of AMPARs *in vitro* (Harmel et al., 2012; Schwenk et al., 2009) and a conditional knockout (KO) of CNIH2/3 in CA1 neurons has revealed that CNIH2/3 is also mandatory for the surface expression *in vivo* (Herring et al., 2013), CNIH2/3 expression in early development will most likely be very beneficial for AMPAR function at this timepoint. Indeed, the KO of CNIH2/3 has caused a loss of GluA1/2 heteromers leading to a reduction of synaptic transmission and impaired LTP as well as faster AMPAR kinetics (Herring et al., 2013). In addition, it has been shown that early postnatal

expression of AMPARs is an important determinant for activity-dependent dendritic growth in the neocortex although in a subunit dependent manner (Hamad et al., 2011) indicating broader functions of AMPARs during development. Hence, the presence of CNIHs in these AMPAR complexes could be also advantageous for the dendritic development. The function of an AMPAR modulating auxiliary subunit of CNIH2/3, which becomes more important during development, could be caused by the high affinity between GluAs and CNIHs (Harmel et al., 2012). Upon binding of GluAs, CNIHs exit the ER-to-Golgi cycle and guide AMPAR complexes to the plasma membrane, indicating a strong interaction between these proteins (Harmel et al., 2012).

Concluding, our data strongly support the assumption that CNIHs promote surface expression of AMPARs during development. Their additional function as an auxiliary subunit gains more and more importance during development and therefore CNIHs may play a crucial role in synapse maturation during brain development.

4.2 AMPAR function in the disease model of hepatic encephalopathy (HE)

Many neurological and neurodegenerative diseases involve malfunction of excitatory synapses, like abnormal AMPAR function and deficits in LTP and LDP, as well as altered synapse structures (Chang et al., 2012; Henley and Wilkinson, 2016). One of such disease states is hepatic encephalopathy (HE), which is a common neuropsychiatric complication of both acute liver failure or chronic liver disease. Patients suffering from HE show impaired cognitive function (Felipo, 2013). Also, animal models for both acute and chronic HE exhibit dysfunctions in learning, memory function as well as impaired LTP. Moreover, in animal models of acute HE, LTD is also affected (Chepkova et al., 2012, 2006; Monfort et al., 2007; Muñoz et al., 2000; Sergeeva et al., 2005). Furthermore, in neurological diseases not only neurons are affected, but also glial cells and an altered neuron-glia cell interaction might contribute to the pathophysiology (Häussinger and Schliess, 2008). In HE, astrocytes play an important part, because they detoxify ammonia in the brain (Rao et al., 2005). Therefore, we employed a co-culture model of neurons and astrocytes to mimic the interplay between neurons and astrocytes not only during the following ammonia treatment but also to model synaptic development and maturation before it (Kaeck and Banker, 2006). We found that chronic ammonia treatment caused a reduction of the neuronal AMPAR complex expression, mainly affecting the extrasynaptic complexes since normal glutamatergic neurotransmission was not affected but the induction of LTP was abolished.

Analysis of our *in vitro* model of HE showed that the chronic treatment with ammonia leads to a reduction of AMPAR expression in neurons. Particularly, the GluA1 and GluA2 subunits showed a dose-dependent decrease in both protein and mRNA expression with increasing ammonia levels, whereas the mRNA and protein expression of the GluA3 and GluA4 subunits were not altered. Furthermore, expression of CNIH2, CNIH3, as well as TARP γ -2 and γ -8 decreased in a dose-dependent manner. Altogether, chronic ammonia stress reduces the neuronal expression of AMPAR complexes.

Astrocytes play an important role in the pathophysiology of HE, as they provide the only mechanism in the brain to detoxified ammonia and thereby protect neurons against ammonia toxicity (Felipo, 2013; Rao et al., 2005). The detoxification process of ammonia by astrocytes is performed by the intake of ammonia from extracellular space into the cell. Subsequently, the enzyme glutamine synthetase (GS) catalyzes the condensation of ammonia to glutamate under ATP consumption resulting in glutamine. In general, ammonia is an unspecifically and broad acting pathogen, which negatively impacts a lot of various processes and pathways resulting in a variety of secondary effects in neurons and astrocytes (Felipo and Butterworth, 2002; Häussinger and Schliess, 2008; Norenberg et al., 2009). Furthermore, ammonia increases the

formation of reactive nitrogen and oxygen species (RNOS) and leads to more oxidative stress by an NMDAR and Ca^{2+} -dependent mechanism (Felipo and Butterworth, 2002; Görg et al., 2013, 2008). Görg and his colleagues showed in an animal model of HE that ammonia-induced RNA oxidation occurs predominantly in neurons rather than in astrocytes (Görg et al., 2008). RNA oxidation could affect gene expression and local protein synthesis as it might increase RNA degradation and impaired protein translation. Additionally, there is evidence that ammonia-induced oxidative stress activates mitogen-activated protein kinases (MAPKs) and thereby influences gene transcription (Norenberg et al., 2009). The mechanisms discussed here could also be involved in the observed reduction of mRNA and protein levels in our *in vitro* model.

Regarding the manifold effects of ammonia, there are indications that chronic hyperammonemia contributes to altered neurotransmission in HE and can affect every possible mechanistic step in the function of different neurotransmitter systems (Felipo, 2013). In HE, it has been observed, that an increase of inhibitory neurotransmission potentially caused by an increase of GABAergic tone or by a decrease of glutamatergic neurotransmission, led to an imbalance between inhibitory and excitatory neurotransmission (Cauli et al., 2009; Felipo, 2013). But the effect of hyperammonemia of the GABAergic or glutamatergic neurotransmission depends on the brain area and can be quite contradictory (Palomero-Gallagher et al., 2009; Wen et al., 2013). For this reason, several different studies have investigated the expression of neurotransmitter receptors and neurotransmitter concentrations. For glutamate, it seems that in HE the extracellular concentration increases throughout the entire brain, whereas for GABA it depends on the brain region (Felipo and Butterworth, 2002; Palomero-Gallagher et al., 2009). Also, for the expression of neurotransmitter receptors, the observed changes are highly variable and depend on the brain region as well as the species giving a rather inconsistent picture. The study from Palomero-Gallagher et al. (Palomero-Gallagher et al., 2009) analyzed different neurotransmitter receptor densities in brain tissue from patients suffering from HE and revealed a high inter-individual variability, which might explain the contradictory results.

Interestingly, we did not observe a change in the normal basal glutamatergic transmission despite the mentioned reduction in AMPAR expression. We only observed faster mEPSC decay times in ammonia-treated neurons, and this could be due to a different stoichiometry of the GluA subunits. In contrast to GluA1 and GluA2, the expression of the faster gating subunits GluA3 and GluA4 was unaffected in our model, which could lead to possible changes in stoichiometry. Recordings from somatic outside-out patches of neurons revealed an ammonia dose-dependent reduction of AMPAR currents. From these data, we have concluded that high ammonia concentrations led to a decrease of extrasynaptic AMPARs, which was represented by the somatic currents and that synaptic receptors were not affected. Furthermore, we found that under high ammonia concentrations an induction of LTP was not longer possible, while LTD could still be observed, indicating that NMDAR function was unaffected.

The reduction of extrasynaptic AMPARs has not affected basal glutamatergic transmission, yet it prevented an increase in synaptic strength at the glutamatergic synapse. Several studies showed that extrasynaptic receptors play an important role in the mechanism of LTP and that the trafficking between and within the synaptic and extrasynaptic compartment is a key point for LTP (Choquet and Triller, 2013; Czöndör et al., 2012; Granger et al., 2013; Opazo and Choquet, 2011). During LTP, an increasing anchoring of AMPARs from the extrasynaptic compartment by lateral diffusing into PSD can be observed. The anchoring of AMPARs at the active zone of the PSD immobilizes the receptors and therefore is an essential prerequisite for LTP (Opazo and Choquet, 2011). A recent model suggests that AMPARs are organized in nanodomains in the postsynapse and that these nanodomains are at optimal distance to the presynaptic release site for receptor activation (Compans et al., 2016). While AMPARs within the nanodomains are immobilized, AMPARs outside the nanodomain are mobile and diffuse. Compans and his colleagues suggest the hypothesis that new immobilization slots for AMPAR are created during LTP induction mediated either by an increase in the number of nanodomains or an increase in the number of receptors in nanodomains (Compans et al., 2016). The severe loss of the

extrasynaptic AMPARs in our model of HE might lead to an end of the replenishment of synaptic AMPARs and thereby prevents the induction of LTP. The observed reduced extrasynaptic pool possible disturbs the recycling and trafficking cycle within the dendritic spine, whereas under normal conditions new generated AMPARs would be incorporated via exocytosis and increase the pool of extrasynaptic and perisynaptic AMPARs. When replenishment of synaptic AMPARs by extrasynaptic AMPARs is no longer possible, this could lead to a longer dwell time in the synapse and to higher immobilization of existing AMPARs at the synapse, to maintain the normal basal glutamatergic transmission. Stronger immobilization of AMPARs could be achieved by enhanced trapping of AMPARs at PSD. The interaction of TARPs with MAKUGs is crucial for trapping AMPARs in the synapse and phosphorylation of the cytoplasmic tail of TARPs increases the interaction with PSD-95, which immobilizes AMPARs (Henley and Wilkinson, 2016; Jackson and Nicoll, 2011). A study examining proteomes of HE animal models found indeed changes in the phospho-proteome (Brunelli et al., 2012). Increasing phosphorylation of TARPs could be a possible protective mechanism counteracting the reduced AMPAR expression.

Since ammonia is such a broadly acting pathogen, which impacts a lot of various processes, it is possible that hyperammonemia might also change the morphology of the synapse. The organization of synapses with their different nano- and microdomains within the PSD as well as the peri- and extrasynaptic space also influence the synaptic strength (Compans et al., 2016; Freche et al., 2011). Therefore, the geometry of the synapse and the size of the domains as well as the amount of available scaffolding proteins for clustering modulate the synaptic response. We cannot exclude these potential effects on the synaptic morphology in our model of HE. Hence, it is possible that a more efficient synapse organization such as an improved alignment between the release site and nanodomains is present in our model, which in turn contributes to maintaining the basal transmission. On the other hand, it is also possible that high ammonia concentrations impair the synapse structure and thereby contributes to the loss of LTP.

In summary, chronic exposure to ammonia leads to a reduction of the neuronal AMPAR complexes resulting in a decreased pool of the extrasynaptic AMPARs and therefore thus prevents the induction of LTP. This result supports the previous finding that LTP requires a reserve pool of glutamate receptors independent of subunit type (Granger et al., 2013). Only if an adequate reserve pool of glutamate receptors was absent a decreased LTP was observed indicating that an extrasynaptic pool is a prerequisite for LTP (Granger et al., 2013). Our study revealed the first pathophysiological setting, which supports this hypothesis and where this alteration in AMPA function seems to be a crucial part of the etiopathology.

4.3 AMPA Receptor heterogeneity in astrocytes

The previous parts of the discussion exemplified functional diversity of AMPARs in development and disease. In both parts, AMPARs and their function were analyzed in neurons, because AMPARs play a crucial role in fast excitatory neurotransmission. However, AMPARs are not exclusively neuronal receptors; different glia cell types including astrocytes also express AMPARs. While most studies have focused on neuronal AMPARs, their complex composition and functional role in glial cells have remained elusive. Here, we used a transgenic mouse line, in which green fluorescent protein (GFP) expression is driven by the human glial fibrillary acidic protein promoter (hGFAP promoter), and we developed a protocol to isolate green fluorescent astrocytes from mouse tissue to examine the astrocytic AMPAR composition. The native AMPAR complex in astrocytes was analyzed by real time PCR or Western blot analysis. The established experimental workflow enabled us to investigate specifically astrocytic AMPARs at different developmental stages and in different brain regions. Our data revealed that the mRNA

expression pattern of AMPAR constituents in astrocytes isolated from whole brain did not differ between the first two weeks of development, unlike during neuronal development. Instead, the mRNA expression levels and pattern of AMPAR constituents varied highly between astrocytes from different brain regions, i.e. from cerebellum, neocortex, and from hippocampus. Indeed, hierarchical clustering analysis identified significant heterogeneity in the expression of AMPAR constituents in astrocytes with respect to brain region. Our study provides a first insight into the molecular diversity of astrocytic AMPARs. The established workflow may serve as a reference for further experiments that examine the function of AMPARs *in vitro* and *in vivo*.

In our study, we combined successfully transgenic lineage tracing using the hGFAP-GFP mice with fluorescence-activated cell sorting (FACS) to enrich astrocytes. Real time PCR (qPCR), Western blot analysis and immunohistochemistry of GFP+ and GFP- cells validated the astrocytic origin of GFP+ cells. Immunohistochemistry also revealed co-localization of GFP-immunoreactivity only with astrocytic but neither with microglial, oligodendrocytic nor with neuronal markers. Since the protein GFAP was the first marker used for identification of astrocytes, GFAP+ astrocytes have been the most extensively studied astrocytes (Reemst et al., 2016; Sofroniew and Vinters, 2010). However, in the adult brain, not all astrocytes express GFAP, and the astrocytic GFAP expression pattern exhibits a regional and spatial variability in the brain. Finally, also other cell types like radial glia (RG), progenitor cells, ependymal cells, and adult neural stem cells express GFAP (Khakh and Sofroniew, 2015; Reemst et al., 2016; Sofroniew and Vinters, 2010). In recent years, additional astrocytes specific proteins have been discovered and used as markers like EAAT1 and Aldh1L1. Due to distinct expression patterns, a single astrocyte marker is not sufficient to label all types of astrocytes. Indeed, the isolated GFP+ cells were positive for the other prototypical astrocyte markers EAAT1 and Aldh1L1, indicating a strong astrocytic origin of the cells studied.

The minor expression of markers from the oligodendrocytic lineage detected in the GFP+ cells could be due to limited contamination with these cells. In the case of Olig2, the expression could additionally be caused by progenitor cells that are positive for GFAP and Olig2 (Meijer et al., 2012; Nishiyama et al., 2016). During cortical development, Olig2 is transiently expressed in immature developing astrocytes at neonatal stages and is progressively downregulated in astrocytes at late postnatal stages (Cai et al., 2007). Furthermore, Cahoy et al. observed that a small percentage (~3%) of cells in the adult mouse brain that were positive for Aldh1L1 also expressed Olig2 (Cahoy et al., 2008).

The qPCR analysis of the pore-lining subunits Gria1-4 in isolated total brain astrocytes revealed general expression of all subunits during the first two postnatal weeks with Gria2 as the predominant subunit. This result is congruent with the fact that GluA2 is the most abundant isoform in the brain from birth until adulthood (Sans et al., 2003; Schwenk et al., 2014, 2012). In general, the expression profile of the AMPAR complex components remained basically constant during the first two weeks of postnatal development. We observed a general decrease of mRNA expression of AMPAR complex components in the second postnatal week, but the proportions of the subunits to each other remained the same. This result is in line with the study from Cahoy et al., (Cahoy et al., 2008), who observed that the gene expression profiles of p7 astrocytes closely resembled that of mature astrocytes. Interestingly, in a developmental total brain proteomic study, some AMPAR constituents showed a transient decrease in abundance with lowest levels at p14 (Schwenk et al., 2014). This decrease in abundance, as well as our observed decrease in AMPAR expression, could reflect a general feature of maturation of glutamatergic neurotransmission in the developing rodent brain. Notably, in astrocytes, there was no change in the expression pattern of the GluA subunits during development, unlike during neuronal development where GluA4 expression is downregulated and GluA2 expression increases leading to a switch of CP-AMPARs to CI-AMPARs (Henley and Wilkinson, 2016; Kumar et al., 2002; Schwenk et al., 2014; Zhu et al., 2000).

Furthermore, the observed expression profiles of AMPAR pore-lining subunits and constituents is in some respects consistent with protein data from total brain tissue, but it also suggests that astrocytes may have a different complex composition than neurons.

Among the complex constituents, the TARPs and CNIHs belong to the predominant auxiliary subunits and they have a considerable impact in promoting AMPAR surface transport and in slowing the receptors' gating properties. Together with CKAMPs and GSG1L, which also modify the gating kinetics of AMPAs, they belong to the *bona fide* auxiliary AMPA subunits.

For TARP γ -4 it is known that it is expressed by glial cells and that the highest expression and abundance is found in early development, whereas expression is down-regulated towards adulthood (Fukaya et al., 2005; Schwenk et al., 2014; Tomita et al., 2003). We found the auxiliary subunit Cacng4 (TARP γ -4) was the predominantly expressed constituent in astrocytes, not only of all TARPs but also in comparison with the constituents CNIH2 und GSG1L. In line with the literature, we also observed a downregulation of the expression in the second postnatal week. TARP γ -2 seems to be expressed by nearly every type of neuron through the brain and TARP γ -8 is the predominant subunit in hippocampus and cortex, whereas, in contrast, they were expressed at much lower levels in astrocytes. Additionally, for TARP γ -8 a developmental increase in expression and abundance has been described, which we could not detect in the astrocytes (Fukaya et al., 2005; Schwenk et al., 2014, 2012; Tomita et al., 2003). Furthermore, in the first part of this work, high mRNA and protein levels of CNIH2 were described in early postnatal development but here the astrocytic CNIH2 mRNA expression was relatively low. Interestingly, proteomic data showed that CNIH2 and TARP γ -8 compete for being the most abundant inner core constituent of AMPARs during development, whereas in astrocytes other candidates may take over (Schwenk et al., 2012). We also detected significant amounts of Shisa9 (CKAMP44) mRNA in astrocytes, which has so far only been described as a neuronal AMPAR constituent (von Engelhardt et al., 2010).

As already mentioned, we found a downregulation of mRNA expression during development. Some studies reported an increase in olfactomedin 2 expression and abundance in the AMPAR complex in the first postnatal week, followed by a reduction in expression from the second postnatal week towards adulthood (Schwenk et al., 2014; Sultana et al., 2011). We also observed a downregulation over six times for olfactomedin 2 mRNA during postnatal development. For Vwc2 (Brorin), we detected even a downregulation by more than ten times. Both, olfactomedin 2 and Vwc2 are secretory proteins and they seem to play a role in synapse-related functions during development and neurogenesis (Anholt, 2014; Koike et al., 2007; Sultana et al., 2014, 2011). It is possible that astrocytes secrete proteins such as olfactomedin 2 and Brorin that influence astrocytic as well as neuronal AMPAR signaling.

However, when comparing qPCR data with brain protein data, it has to be considered that it is not possible to distinguish between different cell types in brain protein data. Astrocytic AMPARs may represent a large proportion of the cells giving rise to the protein data, which could explain the basic consistency in both data sets. On the other hand, the basic temporal profile of the early postnatal AMPAR composition may also be independent of the cell type. Furthermore, the transcriptome is certainly not translated linearly into its proteome, which renders more detailed quantitative comparisons more difficult.

Although the AMPAR expression pattern of total brain astrocytes was homogenous in the first two weeks of postnatal development, we observed significant heterogeneity regarding the AMPAR transcriptome of two-week-old astrocytes from the brain regions cerebellum, neocortex, and hippocampus. The hierarchical clustering showed a clear heterogeneity of the AMPAR transcriptome in the examined brain regions and revealed cerebellar AMPARs remarkably more distant from neocortical and hippocampal ones. Cerebellar astrocytes predominantly expressed the pore-lining subunits Gria1 (GluA1) and Gria4 (GluA4), which are probably translated at the protein level to CP-AMPARs. They most probably reflect the cerebellar Bergmann glia with their well-described Ca^{2+} -permeable inwardly rectifying AMPAR currents (Burnashev et al., 1992a; Muller et al., 1992). It is well known that in Bergmann glia, AMPARs consist of the subunits

GluA1 and GluA4 as well as that they express TARP γ -4, γ -5, γ -7 (Bergles et al., 1997; Burnashev et al., 1992a; Fukaya et al., 2005; Iino et al., 2001; Yamazaki et al., 2010). Indeed, we detected the TARPs γ -4, γ -5, γ -7 in cerebellar astrocytes and the expression was stronger than in the two other brain regions. This finding indicates that the Bergmann glia represents the largest population of GFAP expressing cells in the cerebellar astrocytic fraction.

Moreover, by far the most abundant pore-lining subunit in neocortex and hippocampus was Gria2 (GluA2) whereas other pore-lining subunits and constituents were expressed at lower levels in these two brain regions compared to the cerebellum. In accordance with our data, RNA-Seq data from cortical and hippocampal astrocytes showed that GluA2 is the predominant subunit (Chai et al., 2017; Srinivasan et al., 2016; Zhang et al., 2014). As already described in the first part of the discussion, RNA editing of GluA2 slows down the ER export and leads to a preferred heterodimeric assembly of AMPARs in the ER. Under normal physiological conditions, the AMPAR currents in neocortical and hippocampal astrocytes are rather small or even non-detectable (Lalo et al., 2006; Matthias et al., 2003). This observation might be due to the high expression of Gria2 and the lack of the other pore-lining subunits probably resulting in low receptor numbers, non-functional receptors, or intracellularly located receptors in the neocortex and hippocampus.

The most striking observation among the expression patterns of the constituents was the high expression level of FRRS1I in the cerebellum and the rather low levels of FRRS1I in hippocampus and neocortex. FRRS1I was initially found as an AMPAR constituent in whole brain proteomics studies (Schwenk et al., 2012). The recent study from Brechet and colleagues reveals that FRRS1I exclusively localizes with AMPARs in the ER and that FRRS1I operates as a classical catalyst driving the assembly of GluA subunits with TARPs or CNIHs crucial for further biogenesis of AMPARs (Brechet et al., 2017). The KO of FRRS1I has caused a dramatic decrease of EPSC amplitudes and has reduced surface expression on synaptic and extrasynaptic sites, which may be explained by decreased receptor assembly in the ER (Brechet et al., 2017). Additionally, a number of loss-of-function mutations of FRRS1I in patients were described in the context of Epileptic-Dyskinetic Encephalopathy and intellectual disability (Brechet et al., 2017; Madeo et al., 2016; Shaheen et al., 2016). The mutations lead to a disturbed interaction with GluA subunits or failed to interact with AMPARs (Brechet et al., 2017). The fact that FRRS1I abundance in the AMPAR complex increases during development, which correlates with the time frame of synapse maturation, underline the crucial role of FRRS1I in AMPAR biogenesis (Schwenk et al., 2014). Therefore, the lack of FRRS1I in the neocortex and hippocampus may be an additional reason for the missing AMPA currents in these regions.

Although RNA-Seq data from Aldh1L1-GFP mice identified Cacng7 (TARP γ -7) as dominant isoform in both young and adult cortical astrocytes as well as in hippocampal astrocytes, we observed Cacng4 (TARP γ -4) as dominant TARP isoform cerebellum, neocortex, and hippocampus in the second postnatal week (Chai et al., 2017; Srinivasan et al., 2016; Zhang et al., 2014). On the other hand, the RNA-Seq data confirm the similar expression levels of Cacng4 and Shias9 (CKAMP44) in cortical astrocytes. Furthermore, we found in all three brain regions that Abhd12 was highly more expressed than Abhd6 and Porcn, whereas Abhd6 and Porcn were expressed on a similar level, which is in line with the RNA-Seq Data from cortical and hippocampal astrocytes (Chai et al., 2017; Srinivasan et al., 2016; Zhang et al., 2014). The contradictory findings in comparison with the RNA-Seq Data might be caused by the heterogeneity of astrocytes within the same brain region, which are specialized in different neuronal circuits as well as the different transgenic mouse lines used in respective purification protocols.

Our Protein data from total brain astrocytes confirmed the qPCR results and demonstrated that AMPARs also exist at the protein level and form functional receptors although their expression level was lower than in total brain material. Furthermore, we derived from the affinity-purifications that astrocytes express mainly GluA1/2, GluA1/4, and GluA2/4 heteromers, whereby the GluA1/4 subunits combination is probably most present in Bergmann glia. In

contrast, in the CNS and neurons, the combinations of the subunits GluA1/GluA2 and GluA2/GluA3 are the most common heterotetramers (Lu et al., 2009; Sans et al., 2003; Wenthold et al., 1996). Also, our results showed that it is possible to isolate intact AMPAR complexes from sorted astrocytes and therefore the here developed approach is suitable to investigate native receptor complex composition in a cell specific manner. Furthermore, this approach is applicable for further experiments to investigate the molecular basis of AMPAR currents in native cells as the heterologous electrophysiology analysis of GluA1/4 + TARP γ -5 and CKAMP44 revealed. But it is also suitable for developing new experiments, to translate the findings into an *in vivo* setting and study their physiological impact.

Altogether, we provide both a workflow and a first reference for future investigations into the molecular and functional diversity of astrocytic AMPARs. In summary, the study has revealed that the mRNA expression pattern of AMPAR complex constituents in isolated whole brain astrocytes does not differ between the first two weeks of development, but shows remarkable regional heterogeneity in astrocytes from cerebellum, neocortex, and hippocampus. Cerebellar astrocytes expressed a combination of AMPAR complex constituents that is clearly distinct from the one in neocortical or hippocampal astrocytes. Further experiments will now have to clarify in detail how the molecular heterogeneity in AMPAR expression is translated into physiological functions of astrocytes. Several studies indicate substantial heterogeneity of astrocytic AMPAR properties between brain regions. As mentioned above, Bergmann glia display inwardly rectifying and calcium-permeable AMPAR currents, but also in both neocortex, and brainstem astrocytes such currents are observed in response to glutamate (Lalo et al., 2006; McDougal et al., 2011). In the thalamic nuclei, only a subpopulation of astrocytes expresses functional AMPARs, whereas for hippocampal astrocytes no functional AMPARs are observed at all (Chai et al., 2017; Matthias et al., 2003; Matyash and Kettenmann, 2010). AMPARs in Bergmann glia, in cortical- and brainstem astrocytes are related to neuron-glia interaction and seem to be active participants in various brain functions like synapse formation and maintenance as well as glia-vascular signaling or regulation of autonomic reflexes, respectively. However, with the presented experimental approach it is not possible to analyze regional heterogeneity within the same brain regions, which is based on neuronal circuit specialization. Only a combination with functional experiments can address this. To analyze the native receptor complex composition of glia cells, an unbiased cell type specific proteomic analysis would be necessary. Such approach would have certain methodological limitations: the amounts of surface membrane protein available for affinity purification of AMPARs, their enzymatic digest, and eventual high-resolution mass spectrometry. In any case, the advantage of the presented experimental approach can be easily adapted for other cell types by using the respective animal models for cell isolation.

4.4 Conclusions and Outlook

The data presented in this thesis illustrates the molecular and functional diversity of AMPARs with respect to developmental stages, health and disease, and different brain regions as well as cell types. Since the identification of quite a number of AMPAR complex constituents, it seems for AMPARs a highly modular system exists resulting in diverse AMPAR complex composition and AMPAR function.

The analysis of the developmental expression of CNIH2/3 showed that CNIH2/3 gain importance for AMPARs in development. This study analyzed total brain material and there are hints that CNIHs play an important role in general AMPA function. Differences between brain regions and cell types were not detectable in this experimental setting. Indeed, we found CNIHs less expressed astrocytes demonstrating cell specific diversity of CNIHs expression.

Furthermore, the study from Schwenk et al. revealed CNIH expression in most of the brain regions, but there were regional differences (Schwenk et al., 2014).

Instead, the study of AMPARs in the *in vitro* model of HE focused only on the neuronal function and compared it between health and disease state. The study demonstrated subcellular AMPAR expression changes in the disease state and the change in subcellular expression affected different AMPAR functions. This finding underlines the importance of examining AMPARs in terms of their specific function and functional circuit in the future. The heterogeneity of AMPA mRNA expression in astrocytes from different brain regions emphasized the concept of cell specific AMPA expression and the need for cell specific analysis. For neurons, it is already known that they express different AMPAR types and therefore fulfilling different functions, but this paradigm also seems true for glia cell, like astrocytes.

The data from this thesis underlines the diversity of AMPARs in relation to brain regions and cell types as well as developmental, health and disease stages. It has shown that AMPAR complexes are highly diverse and that there is not “one AMPAR” complex in the brain. The modular system of AMPARs with all the constituents enables the cells to build different AMPARs depending on their task. But regarding the possible diversity of AMPARs in the brain, research has so far only touched the surface. The extent of the molecular heterogeneity and how this is translated into functional heterogeneity is still elusive. For a better understanding of the function of the diverse AMPARs, it is important to analyze AMPARs at least at the regional level, better at the cellular level or even within their functional circuit. For future investigations, the link between molecular data and physiological *in vivo* experiments are key to decode AMPAR functions, analog to the study from Chai and colleagues (Chai et al., 2017). Furthermore, the knowledge of their function in the health state can contribute to unravel pathophysiological mechanisms in neurological diseases. For example, in patients suffering from Schizophrenia CNIHs expression was found upregulated (Drummond et al., 2012). Like in our HE study, many neurological and neurodegenerative diseases show an excitatory synaptic malfunction including changes in LTP and LTD. A further prominent example with disturbed LTP is Alzheimer’s disease (AD). In addition, changes in the neuronal expression of CP-AMPARs and CI-AMPARs seem to play a role in ischemia and traumatic brain injury (Chang et al., 2012; Henley and Wilkinson, 2016; Spaethling et al., 2008). Interestingly, for both ischemic injury or epilepsy, astrocytic AMPAR function seems to be altered or to play an important role (Bedner et al., 2015; Dzamba et al., 2015). For the changes in disease state, it often remains unclear what is cause or consequence of the pathophysiological event. In case of pathophysiological events cells possibly react with changes in the AMPA function to maintain their task or the synaptic homeostasis or to counteract negative effects.

Overall, this thesis intends to shed further light on the diversity of AMPARs with respect to their different appearance in the brain. The presented results can serve as a stepping stone for future research of AMPARs in health and disease.

Bibliography

- Allaman, I., Bélanger, M., Magistretti, P.J., 2011. Astrocyte-neuron metabolic relationships: For better and for worse. *Trends Neurosci.* 34, 76–87. <https://doi.org/10.1016/j.tins.2010.12.001>
- Allen, N.J., 2014. Astrocyte Regulation of Synaptic Behavior. *Annu. Rev. Cell Dev. Biol.* 30, 439–463. <https://doi.org/10.1146/annurev-cellbio-100913-013053>
- Anholt, R.R.H., 2014. Olfactomedin proteins: central players in development and disease. *Front. Cell Dev. Biol.* 2, 489–511. <https://doi.org/10.3389/fcell.2014.00006>
- Araki, Y., Lin, D.-T., Haganir, R.L., 2010. Plasma membrane insertion of the AMPA receptor GluA2 subunit is regulated by NSF binding and Q/R editing of the ion pore. *Proc. Natl. Acad. Sci.* 107, 11080–11085. <https://doi.org/10.1073/pnas.1006584107>
- Armstrong, N., Gouaux, E., 2000. Mechanisms for Activation and Antagonism of an AMPA-Sensitive Glutamate Receptor: Crystal Structures of the GluR2 Ligand Binding Core. *Neuron* 28, 165–181. [https://doi.org/10.1016/S0896-6273\(00\)00094-5](https://doi.org/10.1016/S0896-6273(00)00094-5)
- Armstrong, N., Sun, Y., Chen, G.-Q., Gouaux, E., 1998. Structure of a glutamate-receptor ligand-binding core in complex with kainate. *Nature* 395, 913–917. <https://doi.org/10.1038/27692>
- Bats, C., Farrant, M., Cull-Candy, S.G., 2013. A role of TARPs in the expression and plasticity of calcium-permeable AMPARs: Evidence from cerebellar neurons and glia. *Neuropharmacology* 74, 76–85. <https://doi.org/10.1016/j.neuropharm.2013.03.037>
- Bayraktar, O.A., Fuentealba, L.C., Alvarez-buylla, A., Rowitch, D.H., 2015. Astrocyte Development and Heterogeneity. *Cold Spring Harb. Perspect.* 7, 1–16. <https://doi.org/10.1101/cshperspect.a020362>
- Bedner, P., Dupper, A., Hüttmann, K., Müller, J., Herde, M.K., Dublin, P., Deshpande, T., Schramm, J., Häussler, U., Haas, C.A., Henneberger, C., Theis, M., Steinhäuser, C., 2015. Astrocyte uncoupling as a cause of human temporal lobe epilepsy. *Brain* 138, 1208–1222. <https://doi.org/10.1093/brain/awv067>
- Bergles, D.E., Dzubay, J.A., Jahr, C.E., 1997. Glutamate transporter currents in Bergmann glial cells follow the time course of extrasynaptic glutamate. *Proc. Natl. Acad. Sci.* 94, 14821–14825. <https://doi.org/10.1073/pnas.94.26.14821>
- Blair, M.G., Nguyen, N.N.-Q., Albani, S.H., L'Etoile, M.M., Andrawis, M.M., Owen, L.M., Oliveira, R.F., Johnson, M.W., Purvis, D.L., Sanders, E.M., Stoneham, E.T., Xu, H., Dumas, T.C., 2013. Developmental Changes in Structural and Functional Properties of Hippocampal AMPARs Parallels the Emergence of Deliberative Spatial Navigation in Juvenile Rats. *J. Neurosci.* 33, 12218–12228. <https://doi.org/10.1523/JNEUROSCI.4827-12.2013>
- Bökel, C., 2006. *Drosophila* Cornichon acts as cargo receptor for ER export of the TGF-like growth factor Gurken. *Development* 133, 459–470. <https://doi.org/10.1242/dev.02219>
- Boudkkazi, S., Brechet, A., Schwenk, J., Fakler, B., 2014. Cornichon2 Dictates the Time Course of Excitatory Transmission at Individual Hippocampal Synapses. *Neuron* 82, 848–858. <https://doi.org/10.1016/j.neuron.2014.03.031>
- Boulter, J., Hollmann, M., O'Shea-Greenfield, A., Hartley, M., Deneris, E., Maron, C., Heinemann, S., 1990. Molecular cloning and functional expression of glutamate receptor subunit genes. *Science* 249, 1033–1037. <https://doi.org/10.1126/science.2168579>
- Brechet, A., Buchert, R., Schwenk, J., Boudkkazi, S., Zolles, G., Siquier-Pernet, K., Schaber, I., Bildl, W., Saadi, A., Bole-Feysot, C., Nitschke, P., Reis, A., Sticht, H., Al-Sanna'a, N., Rolfs, A., Kulik, A., Schulte, U., Colleaux, L., Abou Jamra, R., Fakler, B., 2017. AMPA-receptor specific biogenesis complexes control synaptic transmission and intellectual ability. *Nat. Commun.* 8, 15910. <https://doi.org/10.1038/ncomms15910>
- Brunelli, L., Campagna, R., Airolidi, L., Cauli, O., Llansola, M., Boix, J., Felipo, V., Pastorelli, R., 2012. Exploratory investigation on nitro- and phospho-proteome cerebellum changes in hyperammonemia and hepatic encephalopathy rat models. *Metab. Brain Dis.* 27, 37–49. <https://doi.org/10.1007/s11011-011-9268-4>
- Buffo, A., Rossi, F., 2013. Origin, lineage and function of cerebellar glia. *Prog. Neurobiol.* 109, 42–63. <https://doi.org/10.1016/j.pneurobio.2013.08.001>
- Burnashev, N., Khodorova, A., Jonas, P., Helm, P., Wisden, W., Monyer, H., Seeburg, P., Sakmann, B., 1992a. Calcium-permeable AMPA-kainate receptors in fusiform cerebellar glial cells. *Science* 256, 1566–1570. <https://doi.org/10.1126/science.1317970>
- Burnashev, N., Monyer, H., Seeburg, P.H., Sakmann, B., 1992b. Divalent ion permeability of AMPA receptor channels is dominated by the edited form of a single subunit. *Neuron* 8, 189–198. [https://doi.org/https://doi.org/10.1016/0896-6273\(92\)90120-3](https://doi.org/https://doi.org/10.1016/0896-6273(92)90120-3)

- Cahoy, J.D., Emery, B., Kaushal, A., Foo, L.C., Zamanian, J.L., Christopherson, K.S., Xing, Y., Lubischer, J.L., Krieg, P.A., Krupenko, S.A., Thompson, W.J., Barres, B.A., 2008. A Transcriptome Database for Astrocytes, Neurons, and Oligodendrocytes: A New Resource for Understanding Brain Development and Function. *J. Neurosci.* 28, 264–278. <https://doi.org/10.1523/JNEUROSCI.4178-07.2008>
- Cai, J., Chen, Y., Cai, W.-H., Hurlock, E.C., Wu, H., Kernie, S.G., Parada, L.F., Lu, Q.R., 2007. A crucial role for Olig2 in white matter astrocyte development. *Development* 134, 1887–1899. <https://doi.org/10.1242/dev.02847>
- Castro, C.P., Piscopo, D., Nakagawa, T., Derynck, R., 2007. Cornichon regulates transport and secretion of TGF- β -related proteins in metazoan cells. *J. Cell Sci.* 120, 2454–2466. <https://doi.org/10.1242/jcs.004200>
- Cauli, O., Rodrigo, R., Llansola, M., Montoliu, C., Monfort, P., Piedrafita, B., el Mili, N., Boix, J., Agustí, A., Felipo, V., 2009. Glutamatergic and gabaergic neurotransmission and neuronal circuits in hepatic encephalopathy. *Metab. Brain Dis.* 24, 69–80. <https://doi.org/10.1007/s11011-008-9115-4>
- Chai, H., Diaz-Castro, B., Shigetomi, E., Monte, E., Oceau, J.C., Yu, X., Cohn, W., Rajendran, P.S., Vondriska, T.M., Whitelegge, J.P., Coppola, G., Khakh, B.S., 2017. Neural Circuit-Specialized Astrocytes: Transcriptomic, Proteomic, Morphological, and Functional Evidence. *Neuron* 95, 531–549.e9. <https://doi.org/10.1016/j.neuron.2017.06.029>
- Chang, P.K.Y., Verbich, D., McKinney, R.A., 2012. AMPA receptors as drug targets in neurological disease - advantages, caveats, and future outlook. *Eur. J. Neurosci.* 35, 1908–1916. <https://doi.org/10.1111/j.1460-9568.2012.08165.x>
- Chepkova, A.N., Selbach, O., Haas, H.L., Sergeeva, O.A., 2012. Ammonia-induced deficit in corticostriatal long-term depression and its amelioration by zaprinast. *J. Neurochem.* 122, 545–556. <https://doi.org/10.1111/j.1471-4159.2012.07806.x>
- Chepkova, A.N., Sergeeva, O.A., Haas, H.L., 2006. Taurine rescues hippocampal long-term potentiation from ammonia-induced impairment. *Neurobiol. Dis.* 23, 512–521. <https://doi.org/10.1016/j.nbd.2006.04.006>
- Choquet, D., Triller, A., 2013. The Dynamic Synapse. *Neuron* 80, 691–703. <https://doi.org/10.1016/J.NEURON.2013.10.013>
- Chung, W.-S., Welsh, C.A., Barres, B.A., Stevens, B., 2015. Do glia drive synaptic and cognitive impairment in disease? *Nat. Neurosci.* 18, 1539–1545. <https://doi.org/10.1038/nn.4142>
- Colonnese, M.T., Kaminska, A., Minlebaev, M., Milh, M., Bloem, B., Lescure, S., Moriette, G., Chiron, C., Ben-Ari, Y., Khazipov, R., 2010. A Conserved Switch in Sensory Processing Prepares Developing Neocortex for Vision. *Neuron* 67, 480–498. <https://doi.org/10.1016/j.neuron.2010.07.015>
- Compans, B., Choquet, D., Hossy, E., 2016. Review on the role of AMPA receptor nano-organization and dynamic in the properties of synaptic transmission. *Neurophotonics* 3, 041811. <https://doi.org/10.1117/1.NPh.3.4.041811>
- Coombs, I.D., Soto, D., Zonouzi, M., Renzi, M., Shelley, C., Farrant, M., Cull-Candy, S.G., 2012. Cornichons modify channel properties of recombinant and glial AMPA receptors. *J. Neurosci.* 32, 9796–804. <https://doi.org/10.1523/JNEUROSCI.0345-12.2012>
- Croft, W., Dobson, K.L., Bellamy, T.C., 2015. Plasticity of Neuron-Glia Transmission: Equipping Glia for Long-Term Integration of Network Activity. *Neural Plast.* 2015, 1–11. <https://doi.org/10.1155/2015/765792>
- Czöndör, K., Mondin, M., Garcia, M., Heine, M., Frischknecht, R., Choquet, D., Sibarita, J.-B., Thoumine, O.R., 2012. Unified quantitative model of AMPA receptor trafficking at synapses. *Proc. Natl. Acad. Sci.* 109, 3522–3527. <https://doi.org/10.1073/pnas.1109818109>
- De Carlos, J.A., Borrell, J., 2007. A historical reflection of the contributions of Cajal and Golgi to the foundations of neuroscience. *Brain Res. Rev.* 55, 8–16. <https://doi.org/10.1016/j.brainresrev.2007.03.010>
- Dehorter, N., Vinay, L., Hammond, C., Ben-Ari, Y., 2012. Timing of developmental sequences in different brain structures: Physiological and pathological implications. *Eur. J. Neurosci.* 35, 1846–1856. <https://doi.org/10.1111/j.1460-9568.2012.08152.x>
- Drummond, J.B., Simmons, M., Haroutunian, V., Meador-Woodruff, J.H., 2012. Upregulation of cornichon transcripts in the dorsolateral prefrontal cortex in schizophrenia. *Neuroreport* 23, 1031–1034. <https://doi.org/10.1097/WNR.0b013e32835ad229>
- Dzamba, D., Honsa, P., Valny, M., Kriska, J., Valihrach, L., Novosadova, V., Kubista, M., Anderova, M., 2015. Quantitative Analysis of Glutamate Receptors in Glial Cells from the Cortex of GFAP/EGFP Mice Following Ischemic Injury: Focus on NMDA Receptors. *Cell. Mol. Neurobiol.* 35, 1187–1202. <https://doi.org/10.1007/s10571-015-0212-8>

- Erlenhardt, N., Yu, H., Abiraman, K., Yamasaki, T., Wadiche, J.I., Tomita, S., Brecht, D.S., 2016. Porcupine Controls Hippocampal AMPAR Levels, Composition, and Synaptic Transmission. *Cell Rep.* 14, 782–794. <https://doi.org/10.1016/j.celrep.2015.12.078>
- Farrow, P., Khodosevich, K., Sapir, Y., Anton Schulmann, M.A., Stern-Bach, Y., Monyer, H., Engelhardt, J. von, 2015. Auxiliary subunits of the CKAMP family differentially modulate AMPA receptor properties. *Elife* 10.7554, 1–16. <https://doi.org/http://dx.doi.org/10.7554/eLife.09693>
- Felipo, V., 2013. Hepatic encephalopathy: Effects of liver failure on brain function. *Nat. Rev. Neurosci.* 14, 851–858. <https://doi.org/10.1038/nrn3587>
- Felipo, V., Butterworth, R.F., 2002. Neurobiology of ammonia. *Prog. Neurobiol.* 67, 259–279. [https://doi.org/10.1016/S0301-0082\(02\)00019-9](https://doi.org/10.1016/S0301-0082(02)00019-9)
- Freche, D., Pannasch, U., Rouach, N., Holcman, D., 2011. Synapse Geometry and Receptor Dynamics Modulate Synaptic Strength. *PLoS One* 6, e25122. <https://doi.org/10.1371/journal.pone.0025122>
- Freeman, M.R., Rowitch, D.H., 2013. Evolving concepts of gliogenesis: A look way back and ahead to the next 25 years. *Neuron* 80, 613–623. <https://doi.org/10.1016/j.neuron.2013.10.034>
- Fuchs, E.C., Zivkovic, A.R., Cunningham, M.O., Middleton, S., LeBeau, F.E.N., Bannerman, D.M., Rozov, A., Whittington, M.A., Traub, R.D., Rawlins, J.N.P., Monyer, H., 2007. Recruitment of Parvalbumin-Positive Interneurons Determines Hippocampal Function and Associated Behavior. *Neuron* 53, 591–604. <https://doi.org/10.1016/j.neuron.2007.01.031>
- Fukaya, M., Yamazaki, M., Sakimura, K., Watanabe, M., 2005. Spatial diversity in gene expression for VDCCγ subunit family in developing and adult mouse brains. *Neurosci. Res.* 53, 376–383. <https://doi.org/10.1016/j.neures.2005.08.009>
- Ge, W.P., Jia, J.M., 2016. Local production of astrocytes in the cerebral cortex. *Neuroscience*. <https://doi.org/10.1016/j.neuroscience.2015.08.057>
- Gill, M.B., Kato, A.S., Roberts, M.F., Yu, H., Wang, H., Tomita, S., Brecht, D.S., 2011. Cornichon-2 Modulates AMPA Receptor-Transmembrane AMPA Receptor Regulatory Protein Assembly to Dictate Gating and Pharmacology. *J. Neurosci.* 31, 6928–6938. <https://doi.org/10.1523/JNEUROSCI.6271-10.2011>
- Glaum, S.R., Holzwarth, J.A., Miller, R.J., 1990. Glutamate receptors activate Ca²⁺ mobilization and Ca²⁺ influx into astrocytes. *Proc. Natl. Acad. Sci. U. S. A.* 87, 3454–8. <https://doi.org/10.1073/pnas.87.9.3454>
- Görg, B., Qvarckhava, N., Keitel, V., Bidmon, H.J., Selbach, O., Schliess, F., Häussinger, D., 2008. Ammonia induces RNA oxidation in cultured astrocytes and brain in vivo. *Hepatology* 48, 567–579. <https://doi.org/10.1002/hep.22345>
- Görg, B., Schliess, F., Häussinger, D., 2013. Osmotic and oxidative/nitrosative stress in ammonia toxicity and hepatic encephalopathy. *Arch. Biochem. Biophys.* 536, 158–163. <https://doi.org/10.1016/j.abb.2013.03.010>
- Granger, A.J., Nicoll, R.A., 2014. LTD expression is independent of glutamate receptor subtype. *Front. Synaptic Neurosci.* 6, 1–5. <https://doi.org/10.3389/fnsyn.2014.00015>
- Granger, A.J., Shi, Y., Lu, W., Cerpas, M., Nicoll, R.A., 2013. LTP requires a reserve pool of glutamate receptors independent of subunit type. *Nature* 493, 495–500. <https://doi.org/10.1038/nature11775>
- Greger, I.H., Esteban, J.A., 2007. AMPA receptor biogenesis and trafficking. *Curr. Opin. Neurobiol.* 17, 289–297. <https://doi.org/10.1016/j.conb.2007.04.007>
- Greger, I.H., Watson, J.F., Cull-Candy, S.G., 2017. Structural and Functional Architecture of AMPA-Type Glutamate Receptors and Their Auxiliary Proteins. *Neuron* 94, 713–730. <https://doi.org/10.1016/j.neuron.2017.04.009>
- Gu, X., Mao, X., Lussier, M.P., Hutchison, M.A., Zhou, L., Hamra, F.K., Roche, K.W., Lu, W., 2016. GSG1L suppresses AMPA receptor-mediated synaptic transmission and uniquely modulates AMPA receptor kinetics in hippocampal neurons. *Nat. Commun.* 7, 10873. <https://doi.org/10.1038/ncomms10873>
- Haering, S., Tapken, D., Pahl, S., Hollmann, M., 2014. Auxiliary Subunits: Shepherding AMPA Receptors to the Plasma Membrane. *Membranes (Basel)*. 4, 469–490. <https://doi.org/10.3390/membranes4030469>
- Haim, L. Ben, Rowitch, D., 2016. Functional diversity of astrocytes in neural circuit regulation. *Nat. Rev. Neurosci.* 18, 31–41. <https://doi.org/10.1038/nrn.2016.159>
- Hamad, M.I.K., Ma-Hogemeier, Z.-L., Riedel, C., Conrads, C., Veitinger, T., Habijan, T., Schulz, J.-N., Krause, M., Wirth, M.J., Hollmann, M., Wahle, P., 2011. Cell class-specific regulation of neocortical dendrite and spine growth by AMPA receptor splice and editing variants. *Development* 138, 4301–4313. <https://doi.org/10.1242/dev.071076>

- Hansen, K.B., Naur, P., Kurtkaya, N.L., Kristensen, A.S., Gajhede, M., Kastrup, J.S., Traynelis, S.F., 2009. Modulation of the dimer interface at ionotropic glutamate-like receptor delta2 by D-serine and extracellular calcium. *J. Neurosci.* 29, 907–917. <https://doi.org/10.1523/jneurosci.4081-08.2009>
- Harmel, N., Cokic, B., Zolles, G., Berkefeld, H., Mauric, V., Fakler, B., Stein, V., Klöcker, N., 2012. AMPA receptors commandeered an ancient cargo exporter for use as an auxiliary subunit for signaling. *PLoS One* 7, e30681. <https://doi.org/10.1371/journal.pone.0030681>
- Häussinger, D., Schliess, F., 2008. Pathogenetic mechanisms of hepatic encephalopathy. *Gut* 57, 1156–1165. <https://doi.org/10.1136/gut.2007.122176>
- Hayashi, Y., Shi, S.H., Esteban, J.A., Piccini, A., Poncer, J.C., Malinow, R., 2000. Driving AMPA receptors into synapses by LTP and CaMKII: Requirement for GluR1 and PDZ domain interaction. *Science* 287, 2262–2267. <https://doi.org/10.1126/science.287.5461.2262>
- Henley, J.M., Wilkinson, K.A., 2016. Synaptic AMPA receptor composition in development, plasticity and disease. *Nat. Rev. Neurosci.* advance on, 337–350. <https://doi.org/10.1038/nrn.2016.37>
- Herring, B.E., Shi, Y., Suh, Y.H., Zheng, C.Y., Blankenship, S.M., Roche, K.W., Nicoll, R.A., 2013. Cornichon Proteins Determine the Subunit Composition of Synaptic AMPA Receptors. *Neuron* 77, 1083–1096. <https://doi.org/10.1016/j.neuron.2013.01.017>
- Hollmann, M., Heinemann, S., 1994. Cloned Glutamate Receptors. *Annu. Rev. Neurosci.* 17, 31–108. <https://doi.org/10.1146/annurev.ne.17.030194.000335>
- Hollmann, M., O’Shea-Greenfield, A., Rogers, S.W., Heinemann, S., 1989. Cloning by functional expression of a member of the glutamate receptor family. *Nature* 342, 643–648. <https://doi.org/10.1038/342643a0>
- Hoshino, H., Uchida, T., Otsuki, T., Kawamoto, S., Okubo, K., Takeichi, M., Chisaka, O., 2007. Cornichon-like protein facilitates secretion of HB-EGF and regulates proper development of cranial nerves. *Mol. Biol. Cell* 18, 1143–52. <https://doi.org/10.1091/mbc.E06-08-0733>
- Iino, M., Goto, K., Kakegawa, W., Okado, H., Sudo, M., Ishiuchi, S., Miwa, A., Takayasu, Y., Saito, I., Tsuzuki, K., Ozawa, S., 2001. Glia-synapse interaction through Ca²⁺-permeable AMPA receptors in Bergmann glia. *Science* 292, 926–929. <https://doi.org/10.1126/science.1058827>
- Jackson, A.C., Nicoll, R.A., 2011. The Expanding Social Network of Ionotropic Glutamate Receptors: TARPs and Other Transmembrane Auxiliary Subunits. *Neuron* 70, 178–199. <https://doi.org/10.1016/j.neuron.2011.04.007>
- Jacobi, E., von Engelhardt, J., 2017. Diversity in AMPAR complexes in the brain. *Curr. Opin. Neurobiol.* 45, 32–38. <https://doi.org/10.1016/j.conb.2017.03.001>
- Jacobs, M.M., Fogg, R.L., Emeson, R.B., Stanwood, G.D., 2009. ADAR1 and ADAR2 expression and editing activity during forebrain development. *Dev. Neurosci.* 31, 223–37. <https://doi.org/10.1159/000210185>
- Jang, S.S., Chung, H.J., 2016. Emerging link between Alzheimer’s disease and homeostatic synaptic plasticity. *Neural Plast.* <https://doi.org/10.1155/2016/7969272>
- Jansson, L.C., Akerman, K.E., 2014. The role of glutamate and its receptors in the proliferation, migration, differentiation and survival of neural progenitor cells. *J. Neural Transm.* 121, 819–836. <https://doi.org/10.1007/s00702-014-1174-6>
- Kaech, S., Banker, G., 2006. Culturing hippocampal neurons. *Nat. Protoc.* 1, 2406–2415. <https://doi.org/10.1038/nprot.2006.356>
- Kakegawa, W., Miyoshi, Y., Hamase, K., Matsuda, S., Matsuda, K., Kohda, K., Emi, K., Motohashi, J., Konno, R., Zaitzu, K., Yuzaki, M., 2011. D-Serine regulates cerebellar LTD and motor coordination through the $\delta 2$ glutamate receptor. *Nat. Neurosci.* 14, 603–611. <https://doi.org/10.1038/nn.2791>
- Karataeva, A.R., Klaassen, R. V., Ströder, J., Ruiperez-Alonso, M., Hjorth, J.J.J., van Nierop, P., Spijker, S., Mansvelter, H.D., Smit, A.B., 2014. C-Terminal Interactors of the AMPA Receptor Auxiliary Subunit Shisa9. *PLoS One* 9, e87360. <https://doi.org/10.1371/journal.pone.0087360>
- Kato, A.S., Gill, M.B., Ho, M.T., Yu, H., Tu, Y., Siuda, E.R., Wang, H., Qian, Y.-W., Nisenbaum, E.S., Tomita, S., Bredt, D.S., 2010a. Hippocampal AMPA receptor gating controlled by both TARP and cornichon proteins. *Neuron* 68, 1082–96. <https://doi.org/10.1016/j.neuron.2010.11.026>
- Kato, A.S., Gill, M.B., Yu, H., Nisenbaum, E.S., Bredt, D.S., 2010b. TARPs differentially decorate AMPA receptors to specify neuropharmacology. *Trends Neurosci.* 33, 241–248. <https://doi.org/10.1016/j.tins.2010.02.004>
- Kato, A.S., Siuda, E.R., Nisenbaum, E.S., Bredt, D.S., 2008. AMPA Receptor Subunit-Specific Regulation by a Distinct Family of Type II TARPs. *Neuron* 59, 986–996. <https://doi.org/10.1016/j.neuron.2008.07.034>

- Kato, A.S., Zhou, W., Milstein, A.D., Knierman, M.D., Siuda, E.R., Dotzlaw, J.E., Yu, H., Hale, J.E., Nisenbaum, E.S., Nicoll, R.A., Bredt, D.S., 2007. New Transmembrane AMPA Receptor Regulatory Protein Isoform, -7, Differentially Regulates AMPA Receptors. *J. Neurosci.* 27, 4969–4977. <https://doi.org/10.1523/JNEUROSCI.5561-06.2007>
- Khakh, B.S., Sofroniew, M. V., 2015. Diversity of astrocyte functions and phenotypes in neural circuits. *Nat. Neurosci.* 18, 942–952. <https://doi.org/10.1038/nn.4043>
- Khodosevich, K., Jacobi, E., Farrow, P., Schulmann, A., Rusu, A., Zhang, L., Sprengel, R., Monyer, H., von Engelhardt, J., 2014. Coexpressed Auxiliary Subunits Exhibit Distinct Modulatory Profiles on AMPA Receptor Function. *Neuron* 83, 601–615. <https://doi.org/10.1016/j.neuron.2014.07.004>
- Kirkby, L.A., Sack, G.S., Firl, A., Feller, M.B., 2013. A role for correlated spontaneous activity in the assembly of neural circuits. *Neuron* 80, 1129–1144. <https://doi.org/10.1016/j.neuron.2013.10.030>
- Klaassen, R. V., Stroeder, J., Coussen, F., Hafner, A.-S., Petersen, J.D., Renancio, C., Schmitz, L.J.M., Normand, E., Lodder, J.C., Rotaru, D.C., Rao-Ruiz, P., Spijker, S., Mansvelter, H.D., Choquet, D., Smit, A.B., 2016. Shisa6 traps AMPA receptors at postsynaptic sites and prevents their desensitization during synaptic activity. *Nat. Commun.* 7, 10682. <https://doi.org/10.1038/ncomms10682>
- Koike, N., Kassai, Y., Kouta, Y., Miwa, H., Konishi, M., Itoh, N., 2007. Brorin, a novel secreted bone morphogenetic protein antagonist, promotes neurogenesis in mouse neural precursor cells. *J. Biol. Chem.* 282, 15843–15850. <https://doi.org/10.1074/jbc.M701570200>
- Kumar, S.S., Bacci, A., Kharazia, V., Huguenard, J.R., 2002. A developmental switch of AMPA receptor subunits in neocortical pyramidal neurons. *J. Neurosci.* 22, 3005–3015. <https://doi.org/20026285>
- Kuner, T., Beck, C., Sakmann, B., Seeburg, P.H., 2001. Channel-Lining Residues of the AMPA Receptor M2 Segment: Structural Environment of the Q/R Site and Identification of the Selectivity Filter. *J. Neurosci.* 21, 4162–4172. <https://doi.org/10.1523/JNEUROSCI.21-12-04162.2001>
- Lalo, U., Pankratov, Y., Kirchhoff, F., North, R.A., Verkhratsky, A., 2006. NMDA receptors mediate neuron-to-glia signaling in mouse cortical astrocytes. *J. Neurosci.* 26, 2673–83. <https://doi.org/10.1523/JNEUROSCI.4689-05.2006>
- Lee, H.-K., Takamiya, K., Han, J.-S., Man, H., Kim, C.-H., Rumbaugh, G., Yu, S., Ding, L., He, C., Petralia, R.S., Wenthold, R.J., Gallagher, M., Huganir, R.L., 2003. Phosphorylation of the AMPA Receptor GluR1 Subunit Is Required for Synaptic Plasticity and Retention of Spatial Memory. *Cell* 112, 631–643. [https://doi.org/https://doi.org/10.1016/S0092-8674\(03\)00122-3](https://doi.org/https://doi.org/10.1016/S0092-8674(03)00122-3)
- Lein, E.S., Hawrylycz, M.J., Ao, N., Ayres, M., Bensinger, A., Bernard, A., Boe, A.F., Boguski, M.S., Brockway, K.S., Byrnes, E.J., Chen, L., Chen, L., Chen, T.-M., Chi Chin, M., Chong, J., Crook, B.E., Czaplinska, A., Dang, C.N., Datta, S., Dee, N.R., Desaki, A.L., Desta, T., Diep, E., Dolbeare, T.A., Donelan, M.J., Dong, H.-W., Dougherty, J.G., Duncan, B.J., Ebbert, A.J., Eichele, G., Estin, L.K., Faber, C., Facer, B.A., Fields, R., Fischer, S.R., Fliss, T.P., Frensley, C., Gates, S.N., Glattfelder, K.J., Halverson, K.R., Hart, M.R., Hohmann, J.G., Howell, M.P., Jeung, D.P., Johnson, R.A., Karr, P.T., Kawal, R., Kidney, J.M., Knapik, R.H., Kuan, C.L., Lake, J.H., Laramie, A.R., Larsen, K.D., Lau, C., Lemon, T.A., Liang, A.J., Liu, Y., Luong, L.T., Michaels, J., Morgan, J.J., Morgan, R.J., Mortrud, M.T., Mosqueda, N.F., Ng, L.L., Ng, R., Orta, G.J., Overly, C.C., Pak, T.H., Parry, S.E., Pathak, S.D., Pearson, O.C., Puchalski, R.B., Riley, Z.L., Rockett, H.R., Rowland, S.A., Royall, J.J., Ruiz, M.J., Sarno, N.R., Schaffnit, K., Shapovalova, N. V., Sivasay, T., Slaughterbeck, C.R., Smith, S.C., Smith, K.A., Smith, B.I., Sodt, A.J., Stewart, N.N., Stumpf, K.-R., Sunkin, S.M., Sutram, M., Tam, A., Teemer, C.D., Thaller, C., Thompson, C.L., Varnam, L.R., Visel, A., Whitlock, R.M., Wohnoutka, P.E., Wolkey, C.K., Wong, V.Y., Wood, M., Yaylaoglu, M.B., Young, R.C., Youngstrom, B.L., Feng Yuan, X., Zhang, B., Zwingman, T.A., Jones, A.R., 2007. Genome-wide atlas of gene expression in the adult mouse brain. *Nature* 445, 168–176. <https://doi.org/10.1038/nature05453>
- Letts, V.A., 2005. Stargazer-A Mouse to Seize! *Epilepsy Curr.* 5, 161–165. <https://doi.org/10.1111/j.1535-7511.2005.00051.x>
- Letts, V.A., Felix, R., Biddlecome, G.H., Arikath, J., Mahaffey, C.L., Valenzuela, A., Bartlett, F.S., Mori, Y., Campbell, K.P., Frankel, W.N., 1998. The mouse stargazer gene encodes a neuronal Ca²⁺-channel γ subunit. *Nat. Genet.* 19, 340–347. <https://doi.org/10.1038/1228>
- Liao, D., Miller, E.C., Teravskis, P.J., 2014. Tau acts as a mediator for Alzheimer's disease-related synaptic deficits. *Eur. J. Neurosci.* 39, 1202–1213. <https://doi.org/10.1111/ejn.12504>

- Liu, S.-Q.Q., Cull-Candy, S.G., 2000. Synaptic activity at calcium-permeable AMPA receptors induces a switch in receptor subtype. *Nature* 405, 454–8. <https://doi.org/10.1038/35013064>
- Liu, X., Bolteus, A.J., Balkin, D.M., Henschel, O., Bordey, A., 2006. GFAP-expressing cells in the postnatal subventricular zone display a unique glial phenotype intermediate between radial glia and astrocytes. *Glia* 54, 394–410. <https://doi.org/10.1002/glia.20392>
- Lu, W., Shi, Y., Jackson, A.C., Bjorgan, K., Doring, M.J., Sprengel, R., Seeburg, P.H., Nicoll, R.A., 2009. Subunit Composition of Synaptic AMPA Receptors Revealed by a Single-Cell Genetic Approach. *Neuron* 62, 254–268. <https://doi.org/10.1016/j.neuron.2009.02.027>
- Luján, R., Shigemoto, R., López-Bendito, G., 2005. Glutamate and GABA receptor signalling in the developing brain. *Neuroscience* 130, 567–580. <https://doi.org/10.1016/j.neuroscience.2004.09.042>
- Madeo, M., Stewart, M., Sun, Y., Sahir, N., Wiethoff, S., Chandrasekar, I., Yarrow, A., Rosenfeld, J.A., Yang, Y., Cordeiro, D., McCormick, E.M., Muraresku, C.C., Jepperson, T.N., McBeth, L.J., Seidahmed, M.Z., El Khashab, H.Y., Hamad, M., Azzedine, H., Clark, K., Corrochano, S., Wells, S., Elting, M.W., Weiss, M.M., Burn, S., Myers, A., Landsverk, M., Croftwell, P.L., Waisfisz, Q., Wolf, N.I., Nolan, P.M., Padilla-Lopez, S., Houlden, H., Lifton, R., Mane, S., Singh, B.B., Falk, M.J., Mercimek-Mahmutoglu, S., Bilguvar, K., Salih, M.A., Acevedo-Arozena, A., Kruer, M.C., 2016. Loss-of-Function Mutations in FRRS1L Lead to an Epileptic-Dyskinetic Encephalopathy. *Am. J. Hum. Genet.* 98, 1249–1255. <https://doi.org/10.1016/j.ajhg.2016.04.008>
- Makino, H., Malinow, R., 2009. AMPA Receptor Incorporation into Synapses during LTP: The Role of Lateral Movement and Exocytosis. *Neuron* 64, 381–390. <https://doi.org/https://doi.org/10.1016/j.neuron.2009.08.035>
- Mao, X., Gu, X., Lu, W., 2017. GSG1L regulates the strength of AMPA receptor-mediated synaptic transmission but not AMPA receptor kinetics in hippocampal dentate granule neurons. *J. Neurophysiol.* 117, 28–35. <https://doi.org/10.1152/jn.00307.2016>
- Martin, L.J., Blackstone, C.D., Levey, A.I., Haganir, R.L., Price, D.L., 1993. AMPA glutamate receptor subunits are differentially distributed in rat brain. *Neuroscience* 53, 327–358. [https://doi.org/10.1016/0306-4522\(93\)90199-P](https://doi.org/10.1016/0306-4522(93)90199-P)
- Martin, L.J., Furuta, A., Blackstone, C.D., 1998. AMPA receptor protein in developing rat brain: Glutamate receptor-1 expression and localization change at regional, cellular, and subcellular levels with maturation. *Neuroscience* 83, 917–928. [https://doi.org/10.1016/S0306-4522\(97\)00411-9](https://doi.org/10.1016/S0306-4522(97)00411-9)
- Matsui, K., 2005. High-Concentration Rapid Transients of Glutamate Mediate Neural-Glial Communication via Ectopic Release. *J. Neurosci.* 25, 7538–7547. <https://doi.org/10.1523/JNEUROSCI.1927-05.2005>
- Matthias, K., Kirchhoff, F., Seifert, G., Hüttmann, K., Matyash, M., Kettenmann, H., Steinhäuser, C., 2003. Segregated Expression of AMPA-Type Glutamate Receptors and Glutamate Transporters Defines Distinct Astrocyte Populations in the Mouse Hippocampus. *J. Neurosci.* 23, 1750–1758. <https://doi.org/10.1523/JNEUROSCI.23-05-01750.2003>
- Matyash, V., Kettenmann, H., 2010. Heterogeneity in astrocyte morphology and physiology. *Brain Res. Rev.* 63, 2–10. <https://doi.org/10.1016/j.brainresrev.2009.12.001>
- McDougal, D.H., Hermann, G.E., Rogers, R.C., 2011. Vagal Afferent Stimulation Activates Astrocytes in the Nucleus of the Solitary Tract Via AMPA Receptors: Evidence of an Atypical Neural-Glial Interaction in the Brainstem. *J. Neurosci.* 31, 14037–14045. <https://doi.org/10.1523/JNEUROSCI.2855-11.2011>
- McGee, T.P., Bats, C., Farrant, M., Cull-Candy, S.G., 2015. Auxiliary Subunit GSG1L Acts to Suppress Calcium-Permeable AMPA Receptor Function. *J. Neurosci.* 35, 16171–16179. <https://doi.org/10.1523/JNEUROSCI.2152-15.2015>
- Meijer, D.H., Kane, M.F., Mehta, S., Liu, H., Harrington, E., Taylor, C.M., Stiles, C.D., Rowitch, D.H., 2012. Separated at birth? The functional and molecular divergence of OLIG1 and OLIG2. *Nat. Rev. Neurosci.* 13, 819–831. <https://doi.org/10.1038/nrn3386>
- Menuz, K., Kerchner, G.A., O'Brien, J.L., Nicoll, R.A., 2009. Critical role for TARPs in early development despite broad functional redundancy. *Neuropharmacology* 56, 22–29. <https://doi.org/10.1016/j.neuropharm.2008.06.037>
- Menuz, K., O'Brien, J.L., Karmizadegan, S., Brecht, D.S., Nicoll, R.A., 2008. TARP Redundancy Is Critical for Maintaining AMPA Receptor Function. *J. Neurosci.* 28, 8740–8746. <https://doi.org/10.1523/JNEUROSCI.1319-08.2008>
- Milstein, A.D., Zhou, W., Karimzadegan, S., Brecht, D.S., Nicoll, R.A., 2007. TARP Subtypes Differentially and Dose-Dependently Control Synaptic AMPA Receptor Gating. *Neuron* 55, 905–918. <https://doi.org/10.1016/j.neuron.2007.08.022>

- Molofsky, A.V., Deneen, B., 2015. Astrocyte development: A Guide for the Perplexed. *Glia* 63, 1320–1329. <https://doi.org/10.1002/glia.22836>
- Monfort, P., Erceg, S., Piedrafita, B., Llansola, M., Felipo, V., 2007. Chronic liver failure in rats impairs glutamatergic synaptic transmission and long-term potentiation in hippocampus and learning ability. *Eur. J. Neurosci.* 25, 2103–2111. <https://doi.org/10.1111/j.1460-9568.2007.05444.x>
- Muller, T., Möller, T., Berger, T., Schnitzer, J., Kettenmann, H., 1992. Calcium entry through kainate receptors and resulting potassium-channel blockade in Bergmann glial cells. *Science* 256, 1563–1566. <https://doi.org/10.1126/science.1317969>
- Muñoz, M.-D., Monfort, P., Gaztelu, J.-M., Felipo, V., 2000. Hyperammonemia Impairs NMDA Receptor-Dependent Long-Term Potentiation in the CA1 of Rat Hippocampus In Vitro. *Neurochem. Res.* 25, 437–441. <https://doi.org/10.1023/A:1007547622844>
- Naur, P., Hansen, K.B., Kristensen, A.S., Dravid, S.M., Pickering, D.S., Olsen, L., Vestergaard, B., Egebjerg, J., Gajhede, M., Traynelis, S.F., Kastrop, J.S., 2007. Ionotropic glutamate-like receptor $\delta 2$ binds D-serine and glycine. *Proc. Natl. Acad. Sci.* 104, 14116–14121. <https://doi.org/10.1073/pnas.0703718104>
- Nicholls, J.G., 2011. From neuron to brain, Fifth Edit. ed. Sinauer Associates,.
- Nishiyama, A., Boshans, L., Goncalves, C.M., Wegrzyn, J., Patel, K.D., 2016. Lineage, fate, and fate potential of NG2-glia. *Brain Res.* 1638, 116–128. <https://doi.org/10.1016/j.brainres.2015.08.013>
- Norenberg, M.D., Rama Rao, K. V., Jayakumar, A.R., 2009. Signaling factors in the mechanism of ammonia neurotoxicity. *Metab. Brain Dis.* 24, 103–117. <https://doi.org/10.1007/s11011-008-9113-6>
- Opazo, P., Choquet, D., 2011. A three-step model for the synaptic recruitment of AMPA receptors. *Mol. Cell. Neurosci.* 46, 1–8. <https://doi.org/10.1016/j.mcn.2010.08.014>
- Pachernegg, S., Münster, Y., Muth-Köhne, E., Fuhrmann, G., Hollmann, M., 2015. GluA2 is rapidly edited at the Q/R site during neural differentiation in vitro. *Front. Cell. Neurosci.* 9, 69. <https://doi.org/10.3389/fncel.2015.00069>
- Palomero-Gallagher, N., Bidmon, H.J., Cremer, M., Schleicher, A., Kircheis, G., Reifenberger, G., Kostopoulos, G., Haussinger, D., Zilles, K., 2009. Neurotransmitter receptor imbalances in motor cortex and basal ganglia in hepatic encephalopathy. *Cell Physiol Biochem* 24, 291–306. <https://doi.org/000233254> [pii]r10.1159/000233254
- Parfenova, H., Tcheranova, D., Basuroy, S., Fedinec, A.L., Liu, J., Leffler, C.W., 2012. Functional role of astrocyte glutamate receptors and carbon monoxide in cerebral vasodilation response to glutamate. *Am. J. Physiol. Circ. Physiol.* 302, H2257–H2266. <https://doi.org/10.1152/ajpheart.01011.2011>
- Pei, J., Grishin, N. V., 2012. Unexpected diversity in Shisa-like proteins suggests the importance of their roles as transmembrane adaptors. *Cell. Signal.* 24, 758–769. <https://doi.org/10.1016/j.cellsig.2011.11.011>
- Pelkey, K.A., Barksdale, E., Craig, M.T., Yuan, X., Sukumaran, M., Vargish, G.A., Mitchell, R.M., Wyeth, M.S., Petralia, R.S., Chittajallu, R., Karlsson, R.M., Cameron, H.A., Murata, Y., Colonnese, M.T., Worley, P.F., McBain, C.J., 2015. Pentraxins coordinate excitatory synapse maturation and circuit integration of parvalbumin interneurons. *Neuron* 85, 1257–1272. <https://doi.org/10.1016/j.neuron.2015.02.020>
- Pellegrini-Giampietro, D.E., Bennett, M.V.L., Zukin, R.S., 1992. Are Ca²⁺-permeable kainate/AMPA receptors more abundant in immature brain? *Neurosci. Lett.* 144, 65–69. [https://doi.org/10.1016/0304-3940\(92\)90717-L](https://doi.org/10.1016/0304-3940(92)90717-L)
- Pellegrini-Giampietro, D.E., Bennett, M. V., Zukin, R.S., 1991. Differential expression of three glutamate receptor genes in developing rat brain: an in situ hybridization study. *Proc. Natl. Acad. Sci.* 88, 4157–4161. <https://doi.org/10.1073/pnas.88.10.4157>
- Pickard, L., Noël, J., Henley, J.M., Collingridge, G.L., Molnar, E., 2000. Developmental Changes in Synaptic AMPA and NMDA Receptor Distribution and AMPA Receptor Subunit Composition in Living Hippocampal Neurons. *J. Neurosci.* 20, 7922–7931. <https://doi.org/10.1523/JNEUROSCI.20-21-07922.2000>
- Platel, J.C., Lacar, B., Bordey, A., 2007. GABA and glutamate signaling: Homeostatic control of adult forebrain neurogenesis. *J. Mol. Histol.* 38, 303–311. <https://doi.org/10.1007/s10735-007-9103-8>
- Rao, K.V.R., Panickar, K.S., Jayakumar, A.R., Norenberg, M.D., 2005. Astrocytes Protect Neurons from Ammonia Toxicity. *Neurochem. Res.* 30, 1311–1318. <https://doi.org/10.1007/s11064-005-8803-2>

- Reemst, K., Noctor, S.C., Lucassen, P.J., Hol, E.M., 2016. The Indispensable Roles of Microglia and Astrocytes during Brain Development. *Front. Hum. Neurosci.* 10, 1–28. <https://doi.org/10.3389/fnhum.2016.00566>
- Roth, S., Shira Neuman-Silberberg, F., Barcelo, G., Schüpbach, T., 1995. *cornichon* and the EGF receptor signaling process are necessary for both anterior-posterior and dorsal-ventral pattern formation in *Drosophila*. *Cell* 81, 967–978. [https://doi.org/10.1016/0092-8674\(95\)90016-0](https://doi.org/10.1016/0092-8674(95)90016-0)
- Rusnakova, V., Honsa, P., Dzamba, D., Ståhlberg, A., Kubista, M., Anderova, M., 2013. Heterogeneity of astrocytes: from development to injury - single cell gene expression. *PLoS One* 8, e69734. <https://doi.org/10.1371/journal.pone.0069734>
- Saab, A.S., Neumeyer, A., Jahn, H.M., Cupido, A., Šimek, A.A.M., Boele, H.J., Scheller, A., Le Meur, K., Götz, M., Monyer, H., Sprengel, R., Rubio, M.E., Deitmer, J.W., De Zeeuw, C.I., Kirchhoff, F., 2012. Bergmann glial AMPA receptors are required for fine motor coordination. *Science* 337, 749–753. <https://doi.org/10.1126/science.1221140>
- Sans, N., Vissel, B., Petralia, R.S., Wang, Y.-X., Chang, K., Royle, G.A., Wang, C.-Y., O’Gorman, S., Heinemann, S.F., Wenthold, R.J., 2003. Aberrant Formation of Glutamate Receptor Complexes in Hippocampal Neurons of Mice Lacking the GluR2 AMPA Receptor Subunit. *J. Neurosci.* 23, 9367–9373.
- Schwenk, J., Baehrens, D., Haupt, A., Bildl, W., Boudkkazi, S., Roeper, J., Fakler, B., Schulte, U., 2014. Regional Diversity and Developmental Dynamics of the AMPA-Receptor Proteome in the Mammalian Brain. *Neuron* 84, 41–54. <https://doi.org/10.1016/j.neuron.2014.08.044>
- Schwenk, J., Harmel, N., Brechet, A., Zolles, G., Berkefeld, H., Müller, C.S., Bildl, W., Baehrens, D., Hüber, B., Kulik, A., Klöcker, N., Schulte, U., Fakler, B., 2012. High-Resolution Proteomics Unravel Architecture and Molecular Diversity of Native AMPA Receptor Complexes. *Neuron* 74, 621–633. <https://doi.org/10.1016/j.neuron.2012.03.034>
- Schwenk, J., Harmel, N., Zolles, G., Bildl, W., Kulik, A., Heimrich, B., Chisaka, O., Jonas, P., Schulte, U., Fakler, B., Klockner, N., 2009. Functional Proteomics Identify Cornichon Proteins as Auxiliary Subunits of AMPA Receptors. *Science* 323, 1313–1319. <https://doi.org/10.1126/science.1167852>
- Sergeeva, O.A., Schulz, D., Doreulee, N., Ponomarenko, A.A., Selbach, O., Borsch, E., Kircheis, G., Huston, J.P., Häussinger, D., Haas, H.L., 2005. Deficits in cortico-striatal synaptic plasticity and behavioral habituation in rats with portacaval anastomosis. *Neuroscience* 134, 1091–1098. <https://doi.org/10.1016/J.NEUROSCIENCE.2005.05.031>
- Shaheen, R., Al Tala, S., Ewida, N., Abouelhoda, M., Alkuraya, F.S., 2016. Epileptic encephalopathy with continuous spike-and-wave during sleep maps to a homozygous truncating mutation in AMPA receptor component FRRS1L. *Clin. Genet.* 90, 282–283. <https://doi.org/10.1111/cge.12796>
- Shankar, G.M., Li, S., Mehta, T.H., Garcia-Munoz, A., Shepardson, N.E., Smith, I., Brett, F.M., Farrell, M.A., Rowan, M.J., Lemere, C.A., Regan, C.M., Walsh, D.M., Sabatini, B.L., Selkoe, D.J., 2008. Amyloid- β protein dimers isolated directly from Alzheimer’s brains impair synaptic plasticity and memory. *Nat. Med.* 14, 837–842. <https://doi.org/10.1038/nm1782>
- Shanks, N.F., Savas, J.N., Maruo, T., Cais, O., Hirao, A., Oe, S., Ghosh, A., Noda, Y., Greger, I.H., Yates, J.R., Nakagawa, T., 2012. Differences in AMPA and Kainate Receptor Interactomes Facilitate Identification of AMPA Receptor Auxiliary Subunit GSG1L. *Cell Rep.* 1, 590–598. <https://doi.org/10.1016/j.celrep.2012.05.004>
- Shepherd, J.D., Huganir, R.L., 2007. The Cell Biology of Synaptic Plasticity: AMPA Receptor Trafficking. *Annu. Rev. Cell Dev. Biol.* 23, 613–643. <https://doi.org/10.1146/annurev.cellbio.23.090506.123516>
- Shi, Y., Suh, Y.H., Milstein, A.D., Isozaki, K., Schmid, S.M., Roche, K.W., Nicoll, R.A., 2010. Functional comparison of the effects of TARPs and cornichons on AMPA receptor trafficking and gating. *Proc. Natl. Acad. Sci.* 107, 16315–16319. <https://doi.org/10.1073/pnas.1011706107>
- Sobolevsky, A.I., Rosconi, M.P., Gouaux, E., 2009. X-ray structure, symmetry and mechanism of an AMPA-subtype glutamate receptor. *Nature* 462, 745–756. <https://doi.org/10.1038/nature08624>
- Sofroniew, M. V., Vinters, H. V., 2010. Astrocytes: Biology and pathology. *Acta Neuropathol.* 119, 7–35. <https://doi.org/10.1007/s00401-009-0619-8>
- Soto, D., Coombs, I.D., Renzi, M., Zonouzi, M., Farrant, M., Cull-Candy, S.G., 2009. Selective regulation of long-form calcium-permeable AMPA receptors by an atypical TARP, gamma-5. *Nat. Neurosci.* 12, 277–285. <https://doi.org/10.1038/nn0609-808c>
- Spaethling, J.M., Klein, D.M., Singh, P., Meaney, D.F., 2008. Calcium-Permeable AMPA Receptors Appear in Cortical Neurons after Traumatic Mechanical Injury and Contribute to Neuronal Fate. *J. Neurotrauma* 25, 1207–1216. <https://doi.org/10.1089/neu.2008.0532>

- Srinivasan, R., Lu, T.Y., Chai, H., Xu, J., Huang, B.S., Golshani, P., Coppola, G., Khakh, B.S., 2016. New Transgenic Mouse Lines for Selectively Targeting Astrocytes and Studying Calcium Signals in Astrocyte Processes In Situ and In Vivo. *Neuron* 92, 1181–1195. <https://doi.org/10.1016/j.neuron.2016.11.030>
- Studniarczyk, D., Coombs, I.D., Cull-Candy, S.G., Farrant, M., 2013. TARP γ -7 selectively enhances synaptic expression of calcium-permeable AMPARs. *Nat. Neurosci.* 16, 1266–74. <https://doi.org/10.1038/nn.3473>
- Sultana, A., Nakaya, N., Dong, L., Abu-Asab, M., Qian, H., Tomarev, S.I., 2014. Deletion of olfactomedin 2 induces changes in the AMPA receptor complex and impairs visual, olfactory, and motor functions in mice. *Exp. Neurol.* 261, 802–811. <https://doi.org/10.1016/j.expneurol.2014.09.002>
- Sultana, A., Nakaya, N., Senatorov, V. V., Tomarev, S.I., 2011. Olfactomedin 2: Expression in the eye and interaction with other olfactomedin domain-containing proteins. *Investig. Ophthalmol. Vis. Sci.* 52, 2584–2592. <https://doi.org/10.1167/iovs.10-6356>
- Tomita, S., Chen, L., Kawasaki, Y., Petralia, R.S., Wenthold, R.J., Nicoll, R.A., Brecht, D.S., 2003. Functional studies and distribution define a family of transmembrane AMPA receptor regulatory proteins. *J. Cell Biol.* 161, 805–816. <https://doi.org/10.1083/jcb.200212116>
- Traynelis, S.F., Wollmuth, L.P., McBain, C.J., Menniti, F.S., Vance, K.M., Ogden, K.K., Hansen, K.B., Yuan, H., Myers, S.J., Dingledine, R., 2010. Glutamate Receptor Ion Channels: Structure, Regulation, and Function. *Pharmacol. Rev.* 62, 405–496. <https://doi.org/10.1124/pr.109.002451>
- Twomey, E.C., Yelshanskaya, M. V., Grassucci, R.A., Frank, J., Sobolevsky, A.I., 2016. Elucidation of AMPA receptor-stargazin complexes by cryo-electron microscopy. *Science* 353, 83–86. <https://doi.org/10.1126/science.aaf8411>
- von Engelhardt, J., Mack, V., Sprengel, R., Kavenstock, N., Li, K.W., Stern-Bach, Y., Smit, A.B., Seeburg, P.H., Monyer, H., 2010. CKAMP44: A Brain-Specific Protein Attenuating Short-Term Synaptic Plasticity in the Dentate Gyrus. *Science* 327, 1518–1522. <https://doi.org/10.1126/science.1184178>
- Wahlstedt, H., Daniel, C., Enstero, M., Ohman, M., 2009. Large-scale mRNA sequencing determines global regulation of RNA editing during brain development. *Genome Res.* 19, 978–986. <https://doi.org/10.1101/gr.089409.108>
- Wen, S., Schroeter, A., Klöcker, N., 2013. Synaptic plasticity in hepatic encephalopathy – A molecular perspective. *Arch. Biochem. Biophys.* 536, 183–188. <https://doi.org/10.1016/j.abb.2013.04.008>
- Wenthold, R., Petralia, R., Blahos J, I., Niedzielski, A., 1996. Evidence for multiple AMPA receptor complexes in hippocampal CA1/CA2 neurons. *J. Neurosci.* 16, 1982–1989. <https://doi.org/10.1523/JNEUROSCI.16-06-01982.1996>
- Yamazaki, M., Fukaya, M., Hashimoto, K., Yamasaki, M., Tsujita, M., Itakura, M., Abe, M., Natsume, R., Takahashi, M., Kano, M., Sakimura, K., Watanabe, M., 2010. TARPs γ -2 and γ -7 are essential for AMPA receptor expression in the cerebellum. *Eur. J. Neurosci.* 31, 2204–2220. <https://doi.org/10.1111/j.1460-9568.2010.07254.x>
- Zamanillo, D., Sprengel, R., Hvalby, Ø., Jensen, V., Burnashev, N., Rozov, A., Kaiser, K.M.M., Köster, H.J., Borchardt, T., Worley, P., Lübke, J., Frotscher, M., Kelly, P.H., Sommer, B., Andersen, P., Seeburg, P.H., Sakmann, B., 1999. Importance of AMPA receptors for hippocampal synaptic plasticity but not for spatial learning. *Science* 284, 1805–1811. <https://doi.org/10.1126/science.284.5421.1805>
- Zhang, Y., Chen, K., Sloan, S.A., Bennett, M.L., Scholze, A.R., O’Keefe, S., Phatnani, H.P., Guarnieri, P., Caneda, C., Ruderisch, N., Deng, S., Liddelow, S.A., Zhang, C., Daneman, R., Maniatis, T., Barres, B.A., Wu, J.Q., 2014. An RNA-Sequencing Transcriptome and Splicing Database of Glia, Neurons, and Vascular Cells of the Cerebral Cortex. *J. Neurosci.* 34, 11929–11947. <https://doi.org/10.1523/JNEUROSCI.1860-14.2014>
- Zhu, J.J., Esteban, J.A., Hayashi, Y., Malinow, R., 2000. Postnatal synaptic potentiation: Delivery of GluR4-containing AMPA receptors by spontaneous activity. *Nat. Neurosci.* 3, 1098–1106. <https://doi.org/10.1038/80614>

Danksagung

Hier möchte ich allen Personen danken, welche mich bei meinem Werdegang und vor allem bei der Anfertigung dieser Doktorarbeit unterstützt haben.

Zuallererst möchte ich mich bei Herrn Prof. Nikolaj Klöcker für die gute Betreuung sowie die Möglichkeit, an diesem herausfordernden Projekt zu arbeiten, bedanken. Danke für das Vertrauen, dass Sie mir im Rahmen des Projekts entgegengebracht haben. Ein Projekt, in dem viele Prozesse neu etabliert und Hindernisse überwunden werden mussten. Vielen Dank für die Gespräche und die dazugehörigen Diskussionen. Ich habe sehr viel gelernt und mich weiterentwickelt, wissenschaftlich und persönlich.

Für die Übernahme des Korreferats und die Möglichkeit das Vibratom zum Herstellen von Hirnschnitten mit zu benutzen, danke ich Frau Prof. Dr. Christine R. Rose.

Frau Prof. Dr. Olga Sergeeva danke ich für die hGFAP-GFP Mauslinie und für den wissenschaftlichen Austausch rund um die real time PCR.

Klaus von der FACS Facility des Institutes Funktionelle Genomforschung der Mikroorganismen danke ich für den fachlichen und technischen Support beim FACS, aber auch für die vielen Diskussionen und Gespräche aller Art, während wir gemeinsam beim FACS saßen.

Ich möchte mich bei der „iBrain - interdisciplinary graduate school for brain research and translational neuroscience“, der „iGRAD“ und dem SelmaMeyerMentoring für die wissenschaftliche Förderung und für die Fortbildungsmöglichkeiten bedanken.

Allen aktuellen und ehemaligen Mitarbeitern des Institutes für Neuro- und Sinnesphysiologie möchte ich für die nette Arbeitsatmosphäre, die fruchtbaren Diskussionen, nicht nur wissenschaftlicher Natur, und eure Unterstützung bei meiner Doktorarbeit danken.

Veronika Mauric, Annett Schroeter und Shuping Wen für die gute Zusammenarbeit im „CNIH-Projekt“ bzw. „HE Projekt“. Angela und Raphael für die fruchtbare Mitarbeit am „Astrozyten AMPAR Projekt“ und die vielen dazugehörigen Diskussionen. Den Postdocs Angela, Babara, Ehsan, Nadine, Nicole, Steffi und Timm für Ihre Hilfe und Diskussionen in fachlichen und methodischen Dingen, für die netten Gespräche und Mittagsessen, aber auch für die aufmunternden Worte und der moralischen Unterstützung, wenn es mal nicht so lief. Außerdem möchte ich Angela für die gute Organisation und Vorbereitung der Praktika danken, wodurch das Betreuen der Praktika sehr angenehm war und vor allem Spaß gemacht hat.

Claudia, Esin und Julia für die Unterstützung bei den Bestellungen und administrativen Dingen, den Genotypisierungen, der Zellkultur und im Molbiolabor sowie in der Proteinbiochemie.

Vor allem möchte ich auch allen jetzigen und ehemaligen „Mitbewohnern“ des Doktorandenzimmers aka „Kinderzimmers“ danken! Vielen Dank natürlich für die ganzen wissenschaftlichen Diskussionen in unserem Büro als auch für das Teilen der Freude und des Leides! Aber vor allem Danke, dass ich mein „Nerdtum“ ausleben und nicht nur in Form von Memes mit euch teilen durfte. Vor allem sei da Harry Potter erwähnt. Dass ihr Gespräche über Star Wars & Co., Sharknado, Lego, Dinosaurier/Jurassic Park, die drei Fragezeichen im speziellen und Hörspielen im Allgemeinen u.v.m. erduldet habt. Aber auch für den sich-immer-nachfüllenden-Süßigkeitsvorrat im Büro. Danke, danke und nochmals danke, dass ihr meine vielen Selbstgespräche ertragen habt. Danke Kira und Franz!

Kira, Steffi, Franziska Wohlfahrt für die „Nach-der-Arbeit-Jogging-Runden“ im Südpark und das gemeinsame Motivieren für die Winterlaufserien in Duisburg.

Meinen Freunden danke ich für stete Unterstützung aller Art während all der Zeit. Danke, dass ihr mich von Zeit zu Zeit aus meiner „Uni-Filterblase“ herausgeholt habt und für Abwechslung gesorgt habt. In der letzten Zeit war das leider nicht ganz so oft, aber das wird jetzt wieder besser! Besonders danke an Kathi für einfach alles! Danke dafür! Aber auch für das, später leider viel zu wenig, regelmäßige therapeutische Kaffee-Trinken der „zwei Fragzeichen“ Doktoranden. Danke dir und Fabian für die Sharknado-SchleFaZ-PS4-Analog-Spiele-Abende, sowie für die Geburtstags-Feiern im Café Knülle! Dank geht hier auch an Merle und Niklas. Danke an meine Freunde aus Rheurdt und Umgebung, vor allem Kerstin und Christian. Für die vielen gemeinsamen Aktivitäten, das zusammen Sportmachen und für das einander da sein. Vielen Dank auch an meine „Bochumer Unimädels“, Anja, Annika, Imke und Katharina für eure moralische Unterstützung und das, wenn wir uns wieder treffen, immer so ist als wäre es gestern gewesen.

Meiner Familie: Mama, Papa, meiner Schwester Uli und Daniel! Für ihre unendliche Unterstützung schon während des gesamten Studiums und während meiner Doktorarbeit. Aber auch für ihre Hilfe abseits von universitären Dingen. Und darauf, dass ich immer und überall auf euch zählen kann und ihr immer für mich da wart.

Meinem Freund Basti kann ich nicht genug danken! Mir ist es schon schwer gefallen den Dank an alle anderen in Worte zu fassen und für dich jetzt passende Worte zu finden ist schwer. Und da du für das Verfassen von Hörspieltexten zuständig bist und ich der Science Nerd von uns beiden bin, ist es wie immer, ich schreibe „Klugscheißer-Science-Sachen“. Danke, dass du meine extrazelluläre Matrix warst, an der Halt finden und wachsen konnte. Danke, dass du mein passendes Connexon warst, wir damit wie Gap Junctions zusammengehalten haben und zur funktionellen Einheit wurden. Danke, dass du die Kraft warst die mein Drehmoment erhalten hat, wenn ich drohte zu straucheln oder hinzufallen. Danke, dass du meine Astrozyte warst, die mich nicht nur Nährstoffen versorgt hat (vor allem fürs Kochen!), sondern auch mich unterstützt hat meine Funktion zu erhalten. Danke für dein Verständnis, deine Rücksichtnahme und dein Glaube an mich, ohne all das hätte ich diese Arbeit und vieles mehr nie geschafft!

Declaration

I, Andrea Mölders declare that I wrote my dissertation “Cell specific analysis of AMPA receptor complexes in development and disease” independently and any undue assistance by third parties under compliance with the “Principles for the Safeguarding of Good Scientific Practice at Heinrich Heine University Düsseldorf”.

This dissertation has not been submitted in its present or a similar form in any other institution. I have not made any successful or unsuccessful attempt to obtain a doctorate before.

Düsseldorf,

Andrea Mölders

Eidesstattliche Erklärung

Ich, Andrea Mölders, versichere an Eides statt, dass die vorliegende Dissertation “Cell specific analysis of AMPA receptor complexes in development and disease” von mir selbstständig und ohne unzulässige fremde Hilfe unter Beachtung der „Grundsätze zur Sicherung guter wissenschaftlicher Praxis an der Heinrich-Heine-Universität Düsseldorf“ erstellt worden ist.

Diese Arbeit wurde weder vollständig noch in Teilen einem anderen Prüfungsamt zur Erlangung eines akademischen Grades vorgelegt.

Düsseldorf,

Andrea Mölders